

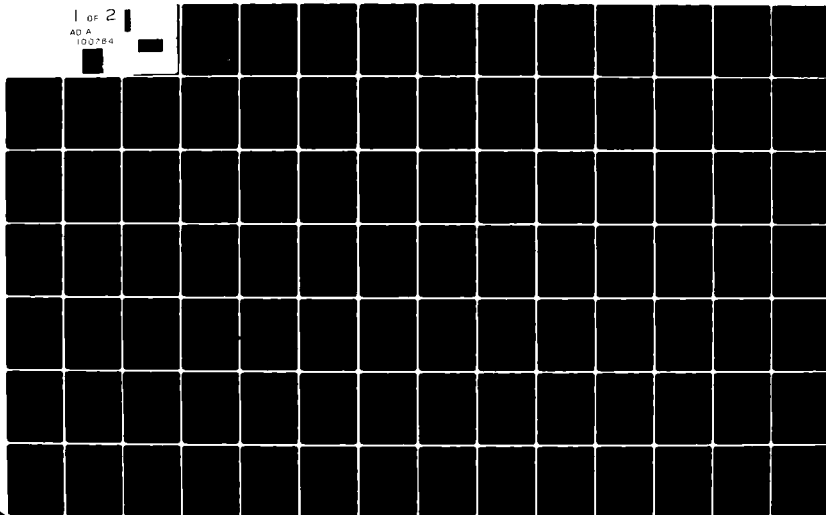
AD-A100 764

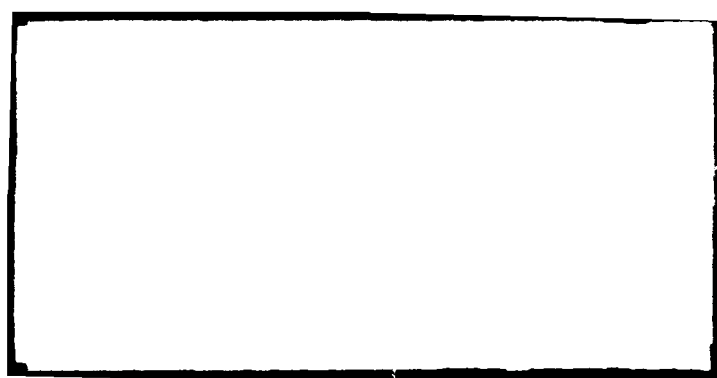
AIR FORCE INST OF TECH WRIGHT-PATTERSON AFB OH SCH00--ETC F/G 20/3
FREQUENCY DOMAIN MEASUREMENTS OF MICROWAVE ABSORBER DESIGN MATE--ETC(U)
DEC 80 D 6 AGUIRRE
AFIT/GE/EE/800-8

UNCLASSIFIED

NL

1 OF 2
AD A
100784





(14)

AFIT/GE/IE/80D-8

D-4

(12) 165

(6)

FREQUENCY DOMAIN MEASUREMENTS
OF

MICROWAVE ABSORBER DESIGN MATERIALS

THESIS

AFIT/GE/IE/80D-8

(19)

Donald G. Aguirre
CAPT USAF

DTIC
ELECTE
JUL 1 1981
S F D

Approved for Public Release; Distribution Unlimited.

C12225

FREQUENCY DOMAIN MEASUREMENTS OF MICROWAVE ABSORBER DESIGN MATERIALS

Presented to the Faculty of the School of Engineering
of the Air Force Institute of Technology
Air University
in Partial Fulfillment of the
Requirements for the Degree of
Master of Science

Donald G. Aguirre, B.S.
Capt USAF

December 1980

Approved for Public Release; Distribution Unlimited.

Preface

Measurements of the intrinsic properties, complex permittivity and permeability of radar absorber design materials whose properties change relatively slowly with frequency can presently be made over two or even three decades of frequency using a time domain system. Such a system was developed for the Air Force Avionics Laboratory by the Sperry Corporate Research Center. However, this time domain technique is limited to frequency measurements below 16 gigahertz (GHz).

This thesis is the documentation of a final automated experimental setup for measurement in the Ku band (12.4 - 18 GHz) used to demonstrate the feasibility of a possible frequency domain measurement technique to extend intrinsic property measurements up to 100 GHz.

The prospect of experimental work in the Air Force Avionics Laboratory, coupled with a project in the area of electromagnetics, presented a thesis topic ideally suited to my desires. The application of Maxwell's equations to the study of microwave absorber materials used to reduce the radar cross section of aircraft is a logical extension of my education in electronic warfare.

Acknowledgments

I wish to express my appreciation to all of the kind and helpful personnel at the Air Force Avionics Laboratory in the Passive Electronic Countermeasures Branch. In particular, I owe a special debt of gratitude to Dr. Pelton and Dr. Mentzer. Also, I wish to express thanks to my thesis advisor, Dr. Rustan, and to my readers, Dr. Fontana and Dr. Golden. Their positive feedback and words of encouragement provided the impetus for my work.

Finally, I would like to thank my lovely wife, Cathy, and my daughters, Ami and Heather, for their encouragement and understanding when I really needed it.

Donald G. Aguirre

(This thesis was typed by Sharon A. Gabriel)

TABLE OF CONTENTS

	Page
Preface	ii
Acknowledgments	iii
List of Figures	vi
List of Tables	viii
Notation	ix
Abstract	xi
I. Introduction	1
Background	1
Problem and Scope	3
Assumptions	4
General Approach	6
Sequence of Presentation	7
II. Theory	8
Dielectric Materials and Permittivity	8
Magnetic Materials and Permeability	9
Theoretical Development	10
III. Equipment	32
Frequency Synthesizer	32
Network Analyzer	33
Horn Assembly	34
21 MX Computer	37
Measurement System	37
IV. Procedure	40
V. Results	47
Expected Results	47
Fiberglass Sample	48
First Plexiglas Sample	48
Second Plexiglas Sample	57
Repeatability	57
Teflon Sample	68
FGM-40 Absorber Sample	68
VI. Conclusions and Recommendations	82
Conclusions	82
Recommendations	83

Bibliography	85
Appendix A: Control Software	86
Appendix B: First Test Setup of Frequency Domain Measurement System	130
Vita	149

List of Figures

<u>Figure</u>	<u>Page</u>
1 Frequency Domain Measurement System	5
2 Plane Wave at Sample.	11
3 Signal Flow Graph for Sample	20
4 Sectoral Horn and Cylindrical Coordinate System	29
5 Sectoral Horns and Sample Holder	36
6A Frequency Domain (Real) Characteristics of Mu and Epsilon	43
6B Frequency Domain (Imaginary) Characteristics of Mu and Epsilon	44
7A Time Domain (Real) Data for 134.5 mil Fiberglass Sample	49
7B Time Domain (Imaginary) Data for 134.5 mil Fiberglass Sample	50
8A Frequency Domain (Real) Data for 135 mil Fiberglass Sample	51
8B Frequency Domain (Imaginary) Data for 135 mil Fiberglass Sample	52
9A Time Domain (Real) Data for 64.5 mil Plexiglas Sample	55
9B Time Domain (Imaginary) Data for 64.5 mil Plexiglas Sample	56
10A Frequency Domain (Real) Data for 65.5 mil Plexiglas Sample	58
10B Frequency Domain (Imaginary) Data for 65.5 mil Plexiglas Sample	59
11A Time Domain (Real) Data for 174 mil Plexiglas Sample	62
11B Time Domain (Imaginary) Data for 174 mil Plexiglas Sample	63
12A Frequency Domain (Real) Data for 174 mil Plexiglas Sample	64

12B	Frequency Domain (Imaginary) Data for 174 mil Plexiglas Sample	65
13A	Time Domain (Real) Data for 181 mil Teflon Sample	69
13B	Time Domain (Imaginary) Data for 181 mil Teflon Sample	70
14A	Frequency Domain (Real) Data for 180 mil Teflon Sample	71
14B	Frequency Domain (Imaginary) Data for 180 mil Teflon Sample	72
15A	Time Domain (Real) Data for 37 mil FGM-40 Sample	75
15B	Time Domain (Imaginary) Data for 37 mil FGM-40 Sample	76
16A	Frequency Domain (Real) Data for 38.5 mil FGM-40 Sample	77
16B	Frequency Domain (Imaginary) Data for 38.5 mil FGM-40 Sample	78
17	Software Control Diagram	86
18	Frequency Domain Measurement Test Setup	131
19	Anechoic Chamber Used in Frequency Domain Measurement Test Setup	134
20	Modified H-Plane Sectoral Horn	136
21A	Frequency Domain (Real) Data for 142 mil Fiberglass Sample	140
21B	Frequency Domain (Imaginary) Data for 142 mil Fiberglass Sample	141
22A	Frequency Domain (Real) Data for 64 mil Plexiglas Sample	143
22B	Frequency Domain (Imaginary) Data for 64 mil Plexiglas Sample	144
23A	Frequency Domain (Real) Data for 172 mil Plexiglas Sample	146
23B	Frequency Domain (Imaginary) Data for 172 mil Plexiglas Sample	147

List of Tables

Table		Page
I	Fiberglass Frequency Domain Data	53
II	Fiberglass Time Domain/Frequency Domain Data	54
III	Plexiglas Frequency Domain Data.	60
IV	Plexiglas Time Domain/Frequency Domain Data (64.5/65.5 mil)	61
V	Plexiglas Frequency Domain Data	66
VI	Plexiglas Time Domain/Frequency Domain Data (174/174 mil)	67
VII	Teflon Frequency Domain Data	73
VIII	Teflon Time Domain/Frequency Domain Data (181/180 mil)	74
IX	FGM-40 Absorber Frequency Domain Data	79
X	FGM-40 Absorber Time Domain/Frequency Domain Data (37/38.5 mil)	80
XI	Fiberglass Time Domain/Frequency Domain Data (134.5/142 mils)	142
XII	Plexiglas Time Domain/Frequency Domain Data (64.5/64 mil)	145
XIII	Plexiglas Time Domain/Frequency Domain Data (174/172 mil)	148

Notation

Roman Letter Symbols

\bar{B}	Magnetic flux density (webers/m ²)
c	Velocity of light in vacuum (3×10^8 m/sec)
\bar{D}	Electric flux density (coulombs/m ²)
d	Distance (mils)
\bar{E}	Electric field (volts/m)
\bar{H}	Magnetic field (amp/m)
\bar{J}	Current density (amp/m ²)
K_{mv}	Hankel function
S_{11}	Reflection scattering coefficient
S_{21}	Transmission scattering coefficient
V_A^-	Reflected wave
V_A^+	Transmitted wave at interface
V_{inc}^+	Incident wave at interface
V_B	Transmitted wave through sample
Z_0	Characteristic impedance of free space (ohms)
Z	Impedance of medium (ohms)
z	A transmission coefficient ($\exp(\gamma d)$)

Greek Letter Symbols

α	Attenuation constant
β	Phase constant
ϵ_0	Permittivity for vacuum
ϵ_r	Relative permittivity
γ	Complex propagation constant

Γ Reflection coefficient
 λ Wavelength
 μ_0 Permeability for vacuum
 μ_r Relative permeability
 ρ Reflection coefficient
 τ Transmission coefficient
 ω Angular frequency

Abstract

Using frequency domain techniques, a system was developed to measure the complex permittivity and permeability of different materials in the Ku band (12.4 to 18 GHz). A sample of fiberglass, teflon, FOM-40, and two different plexiglas configurations were chosen for this experiment. The newly developed measuring system consisted of a two horizontal-plane sectoral horn and a sample holder assembly. A 9.5 x 0.8 cm piece of the sample material was cut and fitted into the sample holder assembly. The reflection and transmission coefficients for the sample were measured, using a network analyzer and frequency synthesizer as the swept frequency signal source. A dedicated computer calculated the complex permittivity and permeability and plotted the output data. The measurements were performed automatically by having the computer control the frequency synthesizer while running the experiment.

The two configurations of plexiglas and the fiberglass sample were tested ten times to obtain a statistical representation of the results. In all cases good repeatability was obtained. The standard deviation of the real part of the permittivity and permeability for the two cases of plexiglas was within $\pm 4\%$ of the mean. The fiberglass had a typical standard deviation within $\pm 7\%$ of the mean for the real part of the permittivity and permeability.

The permittivity and permeability obtained for the selected samples using the frequency domain measurement technique were compared with the results obtained in a previously developed system which used time domain techniques. The data comparison between the two systems was good for teflon, plexiglas, and fiberglass in the frequency range from 12.4 to \rightarrow

-16 GHz. Some variations were noted for the IGM-40. Since the results obtained were generally consistent between both techniques, it is claimed that the newly implemented frequency domain system is a viable alternative for the rapid measurement of intrinsic properties in the Ku band.

FREQUENCY DOMAIN MEASUREMENTS OF MICROWAVE ABSORBER DESIGN MATERIALS

I. Introduction

The application of radar absorber design material to the concealment of aircraft and missiles hinges on a knowledge of the intrinsic properties of complex permittivity (ϵ) and permeability (μ) of the microwave absorber design materials over a wide frequency range (Ruck and Barrick, 1970; Crispin, 1970). These two properties are a measure of the ability of materials to conduct electric and magnetic fields which are present in the radar environments (Hayt, 1974; Allen, 1976).

Background

The ability to design and test radar absorber design materials depends on the capability to accurately measure the intrinsic properties of complex μ and ϵ of the material over a wide frequency range. The Air Force Avionics Laboratory contracted the Sperry Rand Research Corporation to build a time domain measurement system that could measure complex μ and ϵ parameters of design materials over a frequency range from 0.1 to 16 GHz (Nicolson, 1971; Nicolson, 1974). Traditionally, such measurements have been made at fixed frequencies below 10 GHz using slotted-line and impedance-bridge configurations (Hippel, 1958).

Essentially, the time domain measurement system consists of a sub-nanosecond pulse generator and coaxial line system to hold samples of materials, a wideband sampling oscilloscope, and an electronic

system which scans and digitizes the transient response of microwave materials (Nicolson, 1970; Nicolson, 1971; Nicolson, 1974). The transient response is then Fourier transformed on a Hewlett-Packard 21MX computer to provide frequency domain scattering coefficients. Further computation provides printouts and graphs of complex μ and complex ϵ as a function of frequency. Although the time domain system works well, the Air Force Avionics Laboratory has a need for a measurement capability of complex permittivity and permeability of candidate design materials at frequencies higher than 16 GHz.

The National Bureau of Standards published a report dealing with radar absorber design material measurement techniques at frequencies above 20 GHz (Nahman, 1979). One area of the report reviews the existing time domain measurement system in use at AFAL and recommended a frequency domain approach as one possible way to extend the μ and ϵ measurement capability into the millimeter frequency range. This would involve the development and verification of a frequency domain technique that can be integrated into the present time domain measurement system with the minimum equipment modification possible. The time domain system uses two specialized generators. One of these generators produces a very narrow and sharp impulse-like signal, whose spectral content is primarily in the frequency range from 0.1 to 10 GHz (Nicolson, 1971). The second generator emits a radio frequency burst, whose spectral content is between 9 and 16 GHz (Nicolson, 1974). Utilizing these two generators, two measurements then characterize the permeability and permittivity of a sample from 0.1 to 16 GHz. A sampling oscilloscope is used to sample the transient response for digitizing, so that scattering parameters can be computed at discrete frequencies.

The technological limitations of the sampling oscilloscope provides the impetus to develop a frequency domain measurement system (Nahman, 1979). The frequency domain approach would delete the requirement for the two special radio frequency generators and instead utilize a continuous wave generator, frequency synthesizer, tuned from discrete frequency to discrete frequency. The continuous wave radio frequency signals would also negate the requirement for sampling the transient signal response. Instead, the reflected and transmitted signals would be at a set frequency and could be digitized and processed using analog-to-digital (A/D) techniques.

Problem and Scope

The problem addressed in this thesis is that of experimentally developing a millimeter frequency domain measurement system, and demonstrating the system capabilities by measuring the intrinsic properties of several common materials at the Ku band (12.4 to 18 GHz). Existing material properties obtained from the time domain system can be used for comparison. The computer code should be modified to automate the measurement process by putting the frequency synthesizer under computer control and reading the network analyzer phase and amplitude outputs with the computer's A/D converter.

After demonstration of the concept feasibility, the Air Force Avionics Laboratory personnel would later modify the measurement setup to apply the technique at frequencies between 20 and 100 GHz.

This thesis contains a description of the fully automated frequency domain measurement system and data comparisons for fiberglass, two thicknesses of plexiglas, teflon, and FGL-40 absorber materials measured

in both the time domain and the frequency domain systems. The frequency domain measurement system is depicted in Figure 1. The frequency domain setup consists of two H-plane sectoral horns (Barrow and Chu, 1939) which are placed mouth to mouth. The system is used to measure the reflection and transmission coefficients from a single rectangular sample of the design material.

Five specific samples were evaluated, fiberglass, two thicknesses of plexiglas, teflon, and an FGM-40 absorber. To show concept feasibility, data were compared for the five samples tested on both the time domain system and the frequency domain system. The samples prepared for use in the time domain system were of such small dimension that a good uniformity of thickness could be expected; however, samples used in the frequency domain system were larger (7.60 sq cm) and were subject to slight nonuniformity of thickness. Therefore, the thickness value used for the computation of relative μ and ϵ in the frequency domain system is the average thickness across the sample.

The H-plane sectoral horn assembly is assumed to produce a transverse electromagnetic plane wavefront at the sample interface (Jasik, 1961). The plane wavefront approximation was sought because it provides a means to calculate μ and ϵ values using relatively uncomplicated mathematics.

Assumptions

In the frequency domain measurement setup, it will be assumed that the electromagnetic fields normally incident on the sample material interface approximate a plane wave. This assumption is discussed in the theory section. The theoretical phase variation in the mouth of the

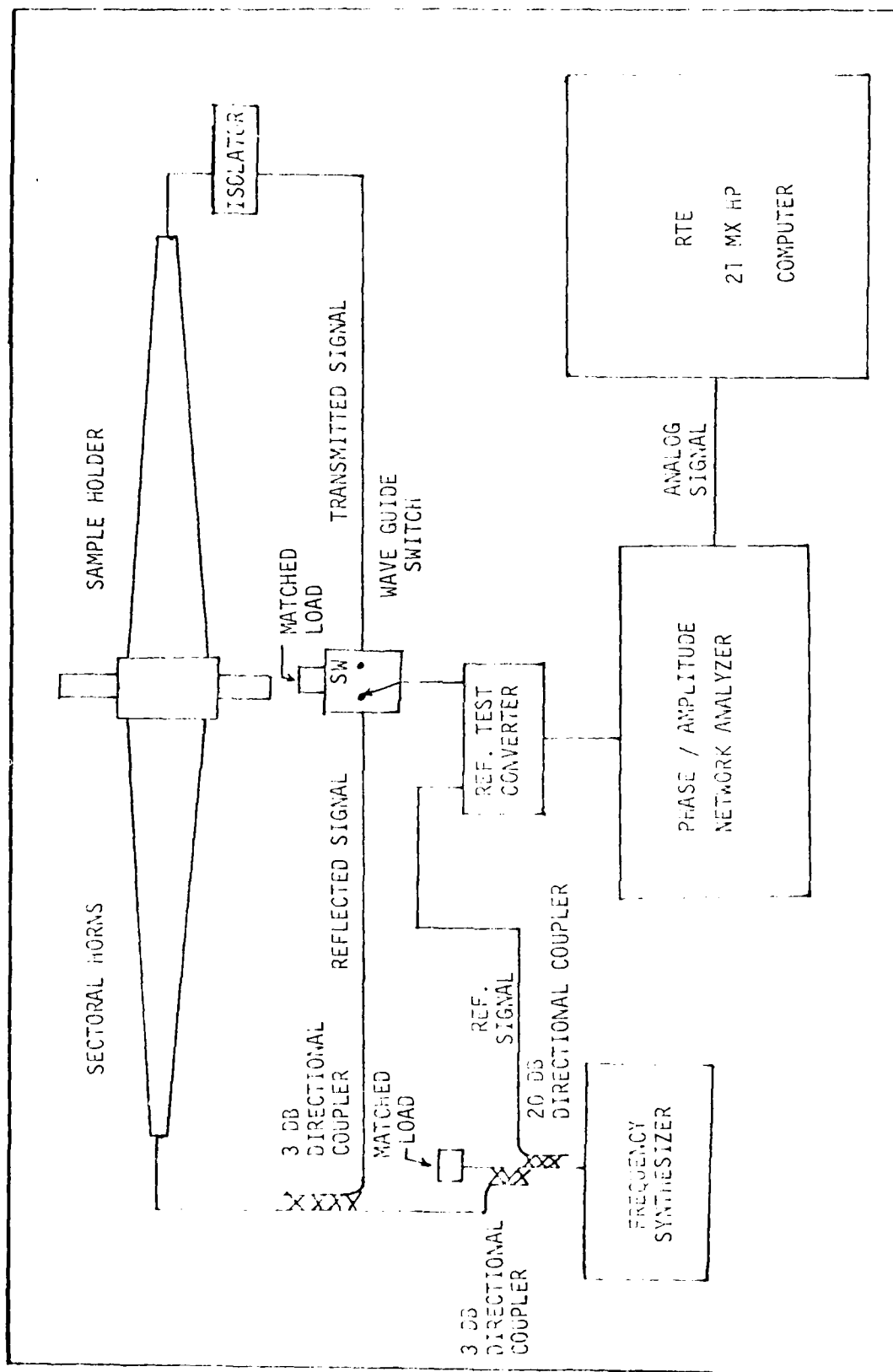


Figure 1. Frequency Domain Measurement System

H-plane sectoral horn ranges from 11.8° at 12.4 GHz to 16.24° at 18 GHz, using the dimensions of $L_h = 150$ cm and $a = 9.5$ cm in the equation $\Delta\phi = \left[\frac{a^2}{8\lambda L_h} \right] 360^\circ$ (Jasik, 1961).

General Approach

The research reported in this thesis involved eight major areas:

1. We studied the existing time domain measurement system.
2. We analyzed literature material associated with the sample holder, network analyzer, frequency synthesizer, and waveguide components used in the measurement system.
3. We performed an initial determination of the test setup and the actual assembly of the test system.
4. We modified the existing time domain computer program to delete portions of code associated with the Fourier Transform and added computer code to accept the frequency domain measured values as input.
5. We automated the test setup, putting the frequency synthesizer under computer control and reading the network analyzer's phase and amplitude outputs through the computers A/D converter.
6. We measured the sample materials and compared μ and ϵ from both the time domain and frequency domain systems.
7. We extended the ideas developed in building the test system and designed and built a final frequency domain system that could measure reflection and transmission coefficients from a single, small sample.

8. We took the measured values of μ and ϵ from the final frequency domain system and compared it to data obtained from the time domain system.

Sequence of Presentation

The material in the thesis is presented in the following manner:

1. The theory underlying the measurement technique is presented in Section II.
2. A description of the equipment used in the frequency domain setup is given in Section III.
3. The sample measurement procedures are presented in Section IV.
4. The results are given in Section V.
5. Finally, the conclusions and recommendations are presented in Section VI.

II. Theory

As an introduction to the theory used in developing the frequency domain measurement system for the intrinsic property measurements of radar absorber design materials, let's look first at a brief description of the properties themselves.

Dielectric Materials and Permittivity

A dielectric is a substance in which the electrons are so well bound or held near their equilibrium positions that they cannot be detached by the application of ordinary electric fields. The important characteristic in a dielectric is its permittivity ϵ . The permittivity (Dielectric Constant) relates the electric field intensity \vec{E} to the electric flux density \vec{D} by the equation $\vec{D} = \epsilon \vec{E}$. As ϵ increases for a material, the material will have an increased electric flux density present within (Ramo, 1965).

Because the permittivity of a dielectric is always greater than the permittivity of vacuum ϵ_0 , it is convenient to use the relative permittivity ϵ_r of the dielectric, that is to say $\epsilon_r = \frac{\epsilon}{\epsilon_0}$, where ϵ_0 is the permittivity of space $\approx (1/36\pi) \times 10^{-9}$ farads per meter and ϵ_r characterizes the effect of the atomic and molecular dipoles in the material. This relative permittivity is a dimensionless quantity (Ramo, 1965; Kraus, 1953). At higher frequencies, typically above 0.1 GHz, the dielectric material

experiences energy losses. The relative permittivity can be expressed as a complex number to account for such losses,

$$\epsilon_r^* = \epsilon_r' - j\epsilon_r'' \text{ (Hippel, 1958).}$$

Magnetic Materials and Permeability

All materials show some magnetic effects. Depending on their magnetic behavior, substances can be classified as diamagnetic, paramagnetic, and ferromagnetic. In diamagnetic materials, the magnetization is opposed to the applied field, while in paramagnetic materials the magnetization is in the same direction as the field. The materials in these two groups, however, show only weak magnetic effects. Materials in the ferromagnetic group, on the other hand, show very strong magnetic effects. Magnetization occurs in the same direction as the field, as it does in paramagnetic materials.

The level of magnetization of materials can be quantized by referring to the relative permeability μ_r defined as $\mu_r = \frac{\mu}{\mu_0}$. By definition, the relative permeability of free space is unity. The relative permeability of ferromagnetic materials is generally much greater than one. The magnetic flux density \vec{B} is related to the magnetic intensity \vec{H} by $\vec{B} = \mu\vec{H} = \mu_r\mu_0\vec{H}$ where μ_0 is the permeability of space = $4\pi \times 10^{-7}$ henrys per meter and μ_r measures the effect of the magnetic dipole moments of the atoms comprising the medium (Ramo, 1965).

In extending the concept of permeability to frequency dependent magnetization in ferromagnetic materials, it is convenient to

introduce the idea of a complex permeability. As frequency increases, the following effects can be accounted for by a complex relative permeability $\mu_r^* = \mu_r' - j\mu_r''$. This physical fact is that in a sinusoidally varying magnetic field a phase angle θ arises between \vec{B} and \vec{H} due to energy losses associated with magnetic resonance and relaxation phenomena. Such losses arise physically from reorientation of the magnetic moments.

Theoretical Development

The theoretical development presented here is an extension of theory from the standpoint of classical boundary value solution techniques for plane waves (Kraus, 1953; Hayt, 1974) and subsequent relationship to the scattering coefficients S_{11} and S_{21} (Ramo, 1965) for reflection and transmission parameters respectively. The theory of the H-plane sectoral horn will be given by presenting a few key points from the work of Barrow and Chu (1939).

The scattering coefficients S_{21} and S_{11} are a measure of the forward- and back-scattered energy respectively (Nicolson, 1970). These scattering coefficients are used to calculate the complex permeability $\mu_r^* = \mu_r' - j\mu_r''$ and permittivity $\epsilon_r^* = \epsilon_r' - j\epsilon_r''$ of the test sample. The sample will be examined under the assumption of plane waves normally incident at the interface.

Consider a slab of homogenous, isotropic, nonconducting material with permittivity $\epsilon = \epsilon_0 \epsilon_r^*$ and permeability $\mu = \mu_0 \mu_r^*$ and thickness d positioned in a free space medium with characteristic impedance Z_0 with region three infinite in extent, as shown in Figure 2. Within the region $0 \leq x \leq d$ the impedance of the slab

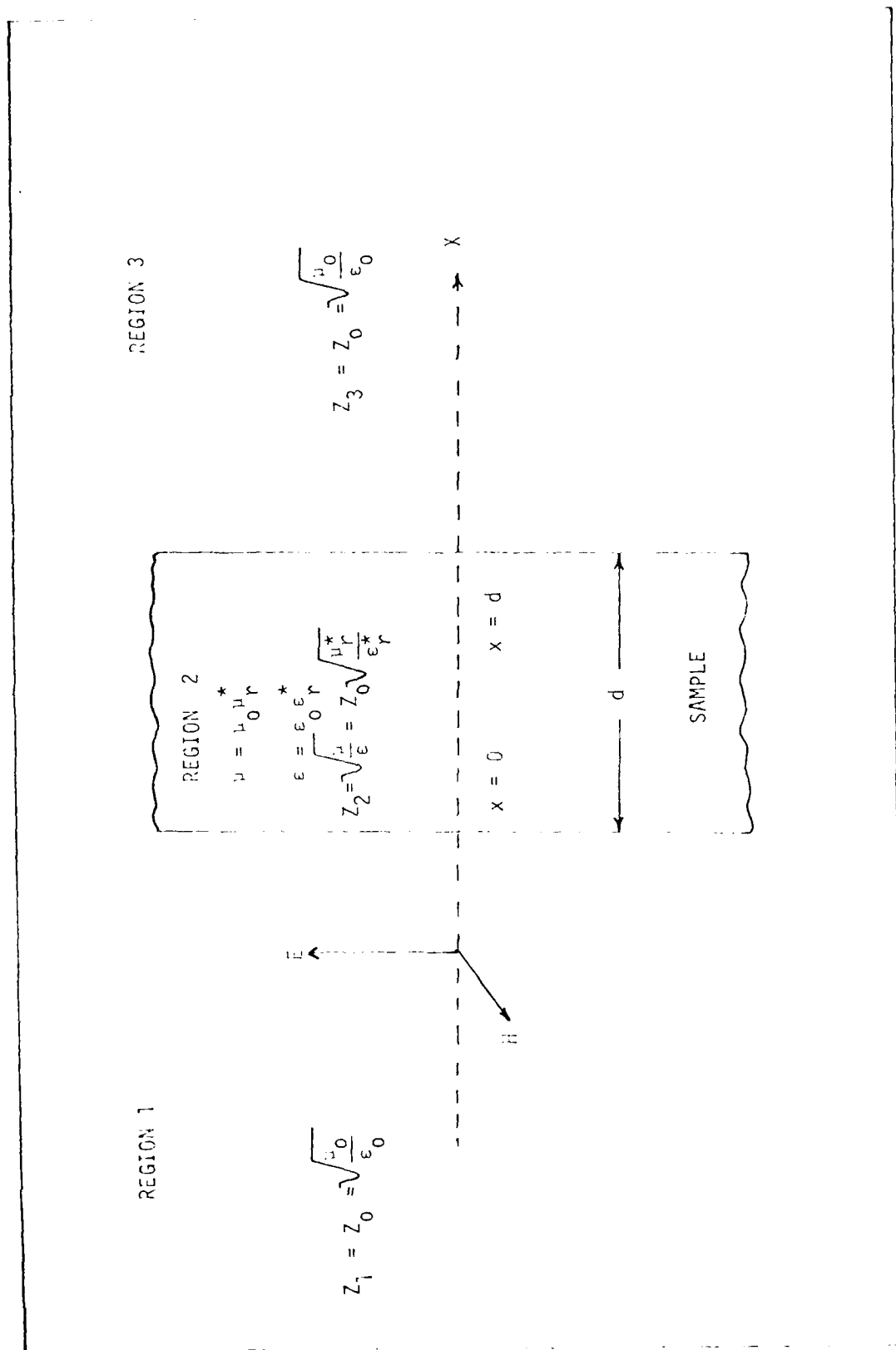


Figure 2. Plane Wave at Sample

will be $Z = \sqrt{\frac{\mu_r^*}{\epsilon_r^*}} \sqrt{\frac{\mu_0}{\epsilon_0}} = \sqrt{\frac{\mu_r^*}{\epsilon_r^*}} Z_0$. If d were infinite, then the reflection coefficient of a plane wave normally incident on the interface would simply be (Nicolson, 1970)

$$\Gamma = \frac{Z - Z_0}{Z + Z_0} = \frac{\sqrt{\frac{\mu_r^*}{\epsilon_r^*}} - 1}{\sqrt{\frac{\mu_r^*}{\epsilon_r^*}} + 1} \quad (1)$$

According to Maxwell's curl equations,

$$\nabla \times \vec{H} = \vec{J} + \frac{\partial \vec{D}}{\partial t} \quad (2)$$

$$\nabla \times \vec{E} = - \frac{\partial \vec{B}}{\partial t} \quad (3)$$

and since a nonconducting media is assumed, $\vec{J} = 0$ in Eq (2). Taking the curl operation of Eq (3) and substituting Eq (2), the wave equation is obtained,

$$\nabla^2 \vec{E} = -\mu\epsilon \frac{\partial^2 \vec{E}}{\partial t^2} \quad (4)$$

For a linearly polarized plane wave traveling in the x direction, the solution of the wave equation reduces to a term that is a function of position multiplied by the time variation term $\exp(j\omega t)$ (Hayt, 1974). Defining the complex propagation constant as $\gamma = \alpha + j\beta$,

the position term of the electric field in region one is

$$E_1 = E_i [e^{-\gamma_1 x} + e^{+\gamma_1 x}] \quad (5)$$

where E_i is the incident field and E_1 is the total field made up of the incident and reflected components of the fields. In region two (within the sample), the corresponding electric field term is

$$E_2 = A e^{-\gamma_2 x} + B e^{+\gamma_2 x} \quad (6)$$

And, in region three we obtain

$$E_3 = i E_i e^{-\gamma_3 x} \quad (7)$$

The magnetic field in region one expressed in terms of the incident electric field is

$$H_1 = j \frac{E_i}{\omega \mu_1} [-\gamma_1 e^{-\gamma_1 x} + \gamma_1 e^{+\gamma_1 x}] \quad (8)$$

In region two (within the sample) the magnetic field is

$$H_2 = j \frac{1}{\omega \mu_2} [-A \gamma_2 e^{-\gamma_2 x} + B \gamma_2 e^{+\gamma_2 x}] \quad (9)$$

And, in region three the magnetic field is

$$H_3 = -j \frac{E_i \gamma_3}{\omega \mu_3} e^{-\gamma_3 x} \quad (10)$$

The components E_1 , E_2 , E_3 , H_1 , H_2 , and H_3 of the electric fields E and magnetic fields H , respectively, in these expressions are complex quantities independent of time and depend on the space variables only. The actual field is the real part of $Ee^{j\omega t}$ and of $He^{j\omega t}$.

The reflection coefficient ρ and transmission coefficient τ will now be found using boundary value solution techniques (Kraus, 1953; Hayt, 1974; Hippel, 1958). Since the tangential components of the electric field in Eqs (5) and (6) are continuous at the boundaries, then at $x = 0$

$$E_i [1 + \rho] = A + B \quad (11)$$

and from Eqs (6) and (7), at $x = d$

$$A e^{-\gamma_2 d} + B e^{\gamma_2 d} = \tau E_i e^{-\gamma_3 d} \quad (12)$$

The tangential components of the magnetic fields are continuous at the boundaries, thus at $x = 0$

$$j \frac{\gamma_1 E_i}{\omega \mu_1} [\rho - 1] = j \frac{\gamma_2}{\omega \mu_2} [B - A] \quad (13a)$$

Using the substitution $Z = j \frac{\omega \mu_1}{\gamma}$ where $j \frac{\omega \mu_1}{\gamma} = j \frac{\omega \mu_1}{\sqrt{j\omega\epsilon_1(1+j\sigma_1/\omega)}}$ and since the slab is a nonconductor $\sigma = 0$, then

$Z = j \frac{\omega \mu_1}{\sqrt{j\omega\epsilon_1}} = \sqrt{\frac{\mu_1}{\epsilon_1}}$ which represents the impedance of the medium.

For the system being described in Figure 2, $Z_1 = Z_3 = Z_0$, where Z_0 is the characteristic impedance of free space; however, this derivation is for the general case, hence

$$\frac{E_i}{Z_1} [\rho - 1] = \frac{1}{Z_2} [B - A] \quad (13b)$$

And at $x = d$

$$\frac{1}{Z_2} [A e^{-\gamma_2 d} - B e^{+\gamma_2 d}] = \frac{\tau E_i}{Z_3} e^{-\gamma_3 d} \quad (14)$$

The variables A and B are eliminated from these equations by multiplying Eq (13b) by Z_2 and then adding Eq (11) to get

$$2B = E_i [(1 + \rho) - \frac{Z_2}{Z_1} (1 - \rho)] \quad (15)$$

Equation (14) is multiplied by Z_2 and added to Eq (12) to get

$$2A = \tau E_i e^{(\gamma_2 - \gamma_3)d} [1 + \frac{Z_2}{Z_3}] \quad (16)$$

Equation (13b) is multiplied by Z_2 and Eq (11) is subtracted off to get

$$2A = E_i [(1 + \rho) + \frac{Z_2}{Z_1} (1 - \rho)] \quad (17)$$

Equation (14) is multiplied by Z_2 and subtracted off Eq (12) to get

$$2B = \tau E_i e^{-(\gamma_2 + \gamma_3)d} \left[1 - \frac{Z_2}{Z_3}\right] \quad (18)$$

Equating Eqs (16) and (17) gives

$$\tau e^{(\gamma_2 - \gamma_3)d} \left[1 + \frac{Z_2}{Z_3}\right] = \left[(1 + \rho) + \frac{Z_2}{Z_1} (1 - \rho)\right] \quad (19)$$

And, equating Eqs (15) and (18) gives

$$\tau e^{-(\gamma_2 + \gamma_3)d} \left[1 - \frac{Z_2}{Z_3}\right] = \left[(1 + \rho) - \frac{Z_2}{Z_1} (1 - \rho)\right] \quad (20)$$

Equation (20) is solved for the transmission coefficient τ and it is substituted into Eq (19) to yield the reflection coefficient ρ .

$$\tau e^{-(\gamma_2 + \gamma_3)d} \frac{Z_3 - Z_2}{Z_3} = \left[\frac{Z_1(1 + \rho) - Z_2(1 - \rho)}{Z_1} \right] \quad (21a)$$

$$\tau = e^{(\gamma_2 + \gamma_3)d} \frac{Z_3}{Z_1} \left[\frac{Z_1(1 + \rho) - Z_2(1 - \rho)}{Z_3 - Z_2} \right] \quad (21b)$$

$$\tau e^{(\gamma_2 - \gamma_3)d} \frac{Z_3 + Z_2}{Z_3} = \left[\frac{Z_1(1 + \rho) + Z_2(1 - \rho)}{Z_1} \right] \quad (22a)$$

$$e^{(\gamma_2 + \gamma_3)d} \frac{z_3}{z_1} \left[\frac{z_1(1+\rho) - z_2(1-\rho)}{z_3 - z_2} \right] e^{(\gamma_2 - \gamma_3)d} \left[\frac{z_3 + z_2}{z_3} \right] = \left[\frac{z_1(1+\rho) + z_2(1-\rho)}{z_1} \right] \quad (22b)$$

$$e^{2\gamma_2 d} \left[z_1(1+\rho) - z_2(1-\rho) \right] \left[\frac{z_3 + z_2}{z_3 - z_2} \right] = \left[z_1(1+\rho) + z_2(1-\rho) \right] \quad (22c)$$

$$e^{2\gamma_2 d} \left[(z_1 - z_2) + \rho(z_1 + z_2) \right] \left[\frac{z_3 + z_2}{z_3 - z_2} \right] = \left[(z_1 + z_2) + \rho(z_1 - z_2) \right] \quad (22d)$$

$$\rho \left[e^{2\gamma_2 d} \left(\frac{z_3 + z_2}{z_3 - z_2} \right) (z_1 + z_2) \right] - (z_1 - z_2) = \left[(z_1 + z_2) - e^{2\gamma_2 d} \left(\frac{z_3 + z_2}{z_3 - z_2} \right) (z_1 - z_2) \right] \quad (22e)$$

$$\rho = \frac{\left[(z_1 + z_2) - e^{2\gamma_2 d} \frac{z_3 + z_2}{z_3 - z_2} (z_1 - z_2) \right]}{\left[e^{2\gamma_2 d} \left(\frac{z_3 + z_2}{z_3 - z_2} \right) (z_1 + z_2) - (z_1 - z_2) \right]} \left[\frac{e^{-2\gamma_2 d} \left(\frac{z_3 - z_2}{z_3 + z_2} \right) \left(\frac{1}{z_1 + z_2} \right)}{e^{-2\gamma_2 d} \left(\frac{z_3 - z_2}{z_3 + z_2} \right) \left(\frac{1}{z_1 - z_2} \right)} \right] \quad (22f)$$

Defining

$$\Gamma_{1,2} = \frac{z_2 - z_1}{z_2 + z_1} \quad (22g)$$

$$\Gamma_{2,3} = \frac{z_3 - z_2}{z_3 + z_2} \quad (22h)$$

$$\rho = \frac{\left[e^{-2\gamma_2 d} \left(\frac{Z_3 - Z_2}{Z_2 + Z_3} \right) - \left(\frac{Z_1 - Z_2}{Z_1 + Z_2} \right) \right]}{\left[1 - e^{-2\gamma_2 d} \left(\frac{Z_3 - Z_2}{Z_2 + Z_3} \right) \left(\frac{Z_1 - Z_2}{Z_1 + Z_2} \right) \right]} = \frac{\left[e^{-2\gamma_2 d} (\Gamma_{2,3}) - (-\Gamma_{1,2}) \right]}{\left[1 - e^{-2\gamma_2 d} (\Gamma_{2,3}) (-\Gamma_{1,2}) \right]} \quad (22i)$$

Since regions one and three are free space, the following is true

$$\Gamma_{2,3} = -\Gamma_{1,2} \quad (22j)$$

and Eq (22i) reduces to

$$\rho = \Gamma_{1,2} \left[\frac{1 - e^{-2\gamma_2 d}}{1 - \Gamma_{1,2}^2 e^{-2\gamma_2 d}} \right] = \Gamma \left[\frac{1 - Z^2}{1 - \Gamma^2 Z^2} \right] \quad (22k)$$

The solution for the transmission coefficient τ follows from Eq (19)

$$\tau e^{(\gamma_2 - \gamma_3)d} \left[\frac{Z_2 + Z_3}{Z_3} \right] = \left[\frac{Z_1(1 + \rho) + Z_2(1 - \rho)}{Z_1} \right] \quad (23a)$$

$$\tau = e^{\gamma_3 d} e^{-\gamma_2 d} \left[\frac{Z_3}{Z_2 + Z_3} \right] \left[\frac{1}{Z_1} \right] [(Z_1 + Z_2) + \rho(Z_1 - Z_2)] \quad (23b)$$

$$\tau = e^{\gamma_3 d} e^{-\gamma_2 d} \left[\frac{Z_1 + Z_2}{Z_2 - Z_3} \right] \left[\frac{Z_3}{Z_1} \right] \left[1 + \rho \left(\frac{Z_1 - Z_2}{Z_1 + Z_2} \right) \right] \quad (23c)$$

For the system being studied, $Z_1 = Z_3$ and $\Gamma = \Gamma_{1,2}$

$$\tau = e^{\gamma_3^d} e^{-\gamma_2^d} [1 - \rho \Gamma] \quad (23d)$$

The expression for the reflection coefficient ρ in Eq (22k) is substituted into Eq (23d) to give

$$\tau = e^{\gamma_3^d} e^{-\gamma_2^d} \left[1 - \Gamma \left(\frac{1 - e^{-2\gamma_2^d}}{1 - \Gamma^2 e^{-2\gamma_2^d}} \right) \Gamma \right] \quad (23e)$$

$$\tau = e^{\gamma_3^d} e^{-\gamma_2^d} \left[\frac{1 - \Gamma^2}{1 - \Gamma^2 e^{-2\gamma_2^d}} \right] = e^{\gamma_3^d} Z \left[\frac{1 - \Gamma^2}{1 - \Gamma^2 Z^2} \right] \quad (23f)$$

In order to use scattering coefficients S_{11} and S_{21} to calculate the complex permittivity and permeability of radar absorber design material, they must be extracted from the measured reflection coefficient ρ and transmission coefficient τ . The relationship between ρ , τ , S_{11} and S_{21} becomes apparent when the signal flow graph in Figure 3 is used to evaluate closed form expressions for the scattering coefficients S_{11} and S_{21} .

The development of closed form expressions for S_{11} and S_{21} will follow that which was presented in a technical memorandum published for the Air Force Avionics Laboratory (Kent, 1979). This material is also an extension of the signal flow graph ideas presented by Nicolson (1970).

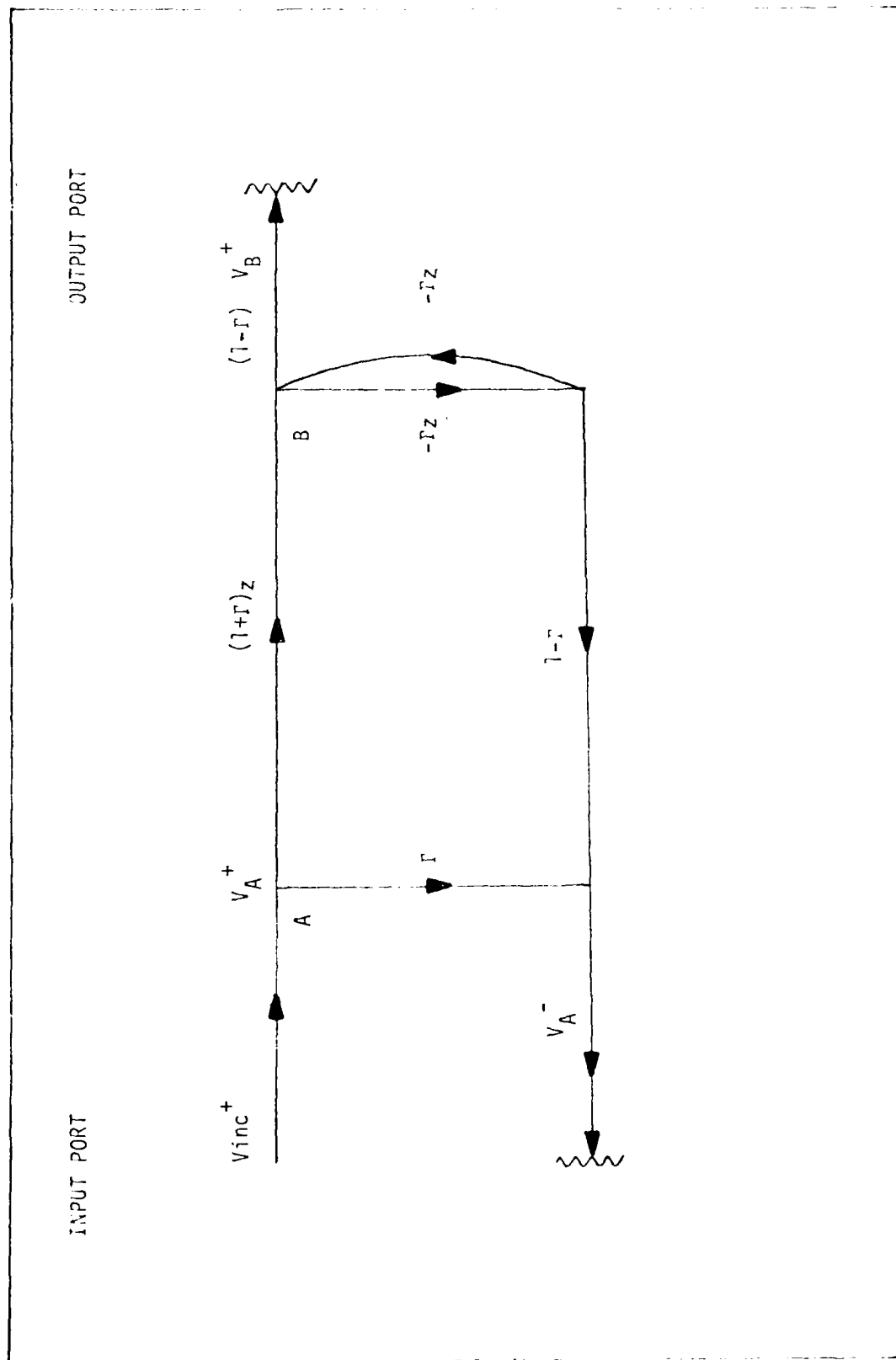


Figure 3. Signal Flow Graph for Sample

When the incident wave strikes the front face of the sample, part of the wave is transmitted and part is reflected. The amplitude of the reflected wave, in terms of the amplitude of the incident wave, denoted V_A^- , is easily calculated from the signal flow graph to be

$$|V_A^-| = \Gamma V_{inc}^+ \quad (24)$$

where

$$\Gamma = \frac{Z_2 - Z_0}{Z_2 + Z_0} \quad (25)$$

The amplitude of the transmitted wave, at $x = 0$, is found to be

$$|V_A^+| = (1 + \Gamma) V_{inc}^+ \quad (26)$$

where

$$(1 + \Gamma) = \frac{2Z_2}{Z_2 + Z_0} \quad (27)$$

Once the transmitted wave strikes the far face of the sample ($x = d$, or point B), part of this wave is reflected back and part is transmitted out the end. Since our substance of interest is electrically and magnetically lossy, complex μ and ϵ , the wave amplitude will suffer some attenuation as it travels through the sample with a propagation constant $\gamma = \alpha + j\beta$. Therefore, the propagation constant

is $\gamma = \alpha + j\beta = j\sqrt{\mu\epsilon} = j\frac{\omega}{c}\sqrt{\mu_r^*\epsilon_r^*}$. The magnitude of the incident wave at B will be reduced by the attenuation portion of

$\exp(-j\frac{\omega}{c}\sqrt{\mu_r^*\epsilon_r^*}d)$ from that of its amplitude at $x = 0$ or point A. By defining $z = \exp(j\frac{\omega}{c}\sqrt{\mu_r^*\epsilon_r^*}d)$ where $\mu_r^* = \mu_r' - j\mu_r''$ and $\epsilon_r^* = \epsilon_r' - j\epsilon_r''$, the incident wave at $x = d$ is found to be

$$|V_{Binc}^+| = z|V_A^+| = z(1 + \Gamma) V_{inc}^+ \quad (28)$$

The fraction of the incident wave transmitted out to the far end is

$$V_B^+ = (\frac{2Z_0}{Z_2 + Z_0}) zV_A^+ = (1 - \Gamma) zV_A^+ = (1 - \Gamma)(1 + \Gamma) zV_{inc}^+ \quad (29)$$

So, as a first approximation, the magnitude of the reflected and transmitted wave amplitudes through this sample can be found as follows:

- (a) Incident wave amplitude: V_{inc}^+
- (b) Reflected wave amplitude: $V_A^- = \Gamma V_{inc}^+$
- (c) Transmitted wave amplitude: $V_B^+ = z(1 - \Gamma^2)V_{inc}^+$

This approximation fails to consider second, third, and higher order internal reflections within the sample, which could make a significant contribution to the total reflected and transmitted wave amplitudes. If the measurement system is to work for any homogeneous unknown, how

many internal reflections must be taken into account? To precisely answer this question, consider the signal flow graph that simplifies the description of this system without loss of accuracy.

If one takes "n" interactions of the loop representing the internal reflections of the samples and allows the number n to approach infinity, then the amplitude of the transmitted wave can be expressed as an infinite series of the following form

$$V_B^+ = V_{inc}^+ \{ (1+\Gamma)(1-\Gamma)z + (1+\Gamma)(1-\Gamma)z(-\Gamma z)(-\Gamma z) + (1+\Gamma)(1-\Gamma)z(-\Gamma z)^2(-\Gamma z)^2 + \dots \} \quad (30a)$$

$$V_B^+ = V_{inc}^+ \{ z(1-\Gamma^2) + z^3\Gamma^2(1-\Gamma^2) + z^5\Gamma^4(1-\Gamma^2) + \dots + z^{2n+1}\Gamma^{2n}(1-\Gamma^2) \} \quad (30b)$$

$$V_B^+ = V_{inc}^+ (1-\Gamma^2)(z) \{ 1 + z^2\Gamma^2 + z^4\Gamma^4 + z^6\Gamma^6 + \dots + z^{2n}\Gamma^{2n} \} \quad (30c)$$

$$V_B^+ = V_{inc}^+ \frac{(1-\Gamma^2)(z)}{(1-\Gamma^2 z^2)} \{ 1 + z^2\Gamma^2 + z^4\Gamma^4 + z^6\Gamma^6 + \dots + z^{2n}\Gamma^{2n} \} (1-\Gamma^2 z^2) \quad (30d)$$

$$V_B^+ = V_{inc}^+ \frac{(1-\Gamma^2)z}{(1-\Gamma^2 z^2)} \quad (30e)$$

As one can see, the above is a very convenient closed form expression for the transmission scattering coefficient. Since this transmission scattering coefficient is, in general, a function of frequency, it follows that

$$S_{21}(\omega) = \frac{V_B^+}{V_{inc}^+} \quad (31)$$

which can be conveniently expressed as follows

$$S_{21}(\omega) = \frac{z(1 - \Gamma^2)}{(1 - \Gamma^2 z^2)} \quad (32)$$

Similarly, the amplitude of the reflected wave can be expressed as an infinite series. A closed form is also desired.

$$V_A^- = V_{inc}^+ \{ \Gamma + (1+\Gamma)(1-\Gamma)z(-\Gamma z) + (1+\Gamma)(1-\Gamma)z(-\Gamma z)(-\Gamma z)^2 + \dots \} \quad (33a)$$

$$V_A^- = V_{inc}^+ \Gamma \{ 1 - (1-\Gamma^2)z^2 - (1-\Gamma^2)z^4\Gamma^2 - (1-\Gamma^2)z^6\Gamma^4 - \dots - (1-\Gamma^2)z^{2n+2}\Gamma^{2n} \} \quad (33b)$$

$$V_A^- = V_{inc}^+ \frac{(1-\Gamma^2 z^2)}{(1-\Gamma^2 z^2)} \{ 1 - (1-\Gamma^2)z^2 - (1-\Gamma^2)z^4\Gamma^2 - (1-\Gamma^2)z^6\Gamma^4 - \dots - (1-\Gamma^2)z^{2n+2}\Gamma^{2n} \} \quad (33c)$$

$$V_A^- = V_{inc}^+ \frac{\Gamma}{(1-\Gamma^2 z^2)} \{ 1 - z^2 + \Gamma^2 z^2 - z^4\Gamma^2 + z^4\Gamma^4 - z^6\Gamma^4 + z^6\Gamma^6 - \dots - z^{2n+2}\Gamma^{2n} + z^{2n+2}\Gamma^{2n+2} - \Gamma^2 z^2 + z^4\Gamma^2 - z^4\Gamma^4 + z^6\Gamma^4 - z^6\Gamma^6 + \dots + z^{2n+2}\Gamma^{2n} - z^{2n+2}\Gamma^{2n+2} \} \quad (33d)$$

$$V_A^- = V_{inc}^+ \frac{(1 - z^2)\Gamma}{(1 - \Gamma^2 z^2)} \quad (33e)$$

A closed form relation between the incident wave amplitude and the reflected wave amplitude has been obtained. As with the transmission scattering coefficient, the reflection scattering coefficient can also be defined as a function of frequency.

$$S_{11}(\omega) = \frac{V_A^-}{V_{inc}^+} = \frac{(1 - z^2)\Gamma}{(1 - \Gamma^2 z^2)} \quad (34)$$

Therefore, it becomes apparent that the measured value of reflection coefficient ρ is equal to the reflection scattering coefficient and the transmission coefficient τ differs from the transmission scattering coefficient by the phase term $\exp(\gamma_0 d)$.

$$S_{11} = \rho = \frac{(1 - z^2)\Gamma}{(1 - \Gamma^2 z^2)} \quad (35)$$

$$S_{21} = \frac{\tau}{e^{\gamma_0 d}} = e^{\gamma_0 d} \frac{z(1 - \Gamma^2)}{(1 - \Gamma^2 z^2)} \left(\frac{1}{e^{\gamma_0 d}} \right) = \frac{z(1 - \Gamma^2)}{(1 - \Gamma^2 z^2)} \quad (36)$$

where

$$\gamma_0 = j\omega \sqrt{\mu_0 \epsilon_0} \quad (37)$$

The reflection and transmission scattering coefficients can thus be determined. The following details show how they are used to calculate the complex μ and ϵ values of a radar absorber design material

ample (Nicolson, 1970). Several intermediate variables are introduced to aid in the calculation.

The sum and difference of the scattering coefficients are found as

$$V_1 = S_{21} + S_{11} \quad (38)$$

$$V_2 = S_{21} - S_{11} \quad (39)$$

A variable x will be defined as the ratio of $1 - V_1 V_2$ and $V_1 - V_2$.

$$x = \frac{1 - V_1 V_2}{V_1 - V_2} \quad (40)$$

By direct substitution of the defining expressions for the scattering coefficients into Eq (40) yields the following equation

$$x = \frac{(1 + \Gamma^2)(1 - z^2)}{2\Gamma(1 - z^2)} = \frac{\Gamma^2 + 1}{2\Gamma} \quad (41)$$

This equation can be solved for Γ .

$$\Gamma = x \pm \sqrt{x^2 - 1} \quad (42)$$

where the plus or minus sign is chosen to restrict Gamma's magnitude to less than one in absolute value.

Again, direct substitution of the defining expressions for the scattering coefficients, in Eq (38), yields an equation for z in terms of V_1 and Γ .

$$z = \frac{V_1 - \Gamma}{1 - V_1 \Gamma} \quad (43)$$

From Eq (1), define

$$C_1 = \frac{\mu_r^*}{\epsilon_r^*} = \left(\frac{1 + \Gamma}{1 - \Gamma} \right)^2 \quad (44)$$

and from the definition of $z = \exp(-j \frac{\omega}{c} \sqrt{\mu_r^* \epsilon_r^*} d)$, define

$$C_2 = \mu_r^* \epsilon_r^* = - \left(\frac{c}{d \omega} \ln \left(\frac{1}{z} \right) \right)^2 \quad (45)$$

Then,

$$\mu_r^* = \sqrt{C_1 C_2} \quad (46)$$

$$\epsilon_r^* = \sqrt{\frac{C_2}{C_1}} \quad (47)$$

Thus, the complex permittivity and permeability are easily calculated from a knowledge of the reflection and transmission scattering coefficients. Because the reflection coefficient is measured using an H-plane sectoral horn, the theory that underlies this horn will be presented next.

The following theory on the H-plane sectoral horn was taken from a published article by W. L. Barrow and L. J. Chu (1939). It is presented here for the special case which was implemented as part of this thesis.

Using the geometry of the sectoral horn depicted in Figure 4, Maxwell's equations in a form suitable for our problem yield the following components of electric field (E_y) and magnetic field (H_ρ , H_ϕ).

$$E_y = B \cos(mv\phi) K_{mv} \left(2\pi \frac{\rho}{\lambda} \right) \quad (48)$$

$$H_\rho = B \frac{mv}{j\omega\mu\rho} \sin(mv\phi) K_{mv} \left(2\pi \frac{\rho}{\lambda} \right) \quad (49)$$

$$H_\phi = -Bj\sqrt{\frac{\epsilon}{\mu}} \cos(mv\phi) K'_{mv} \left(2\pi \frac{\rho}{\lambda} \right) \quad (50)$$

In these expressions, the complex quantities are independent of the time and depend on the space variable only. The actual field is the real part of $Ee^{j\omega t}$ and $He^{j\omega t}$. Here K'_{mv} is the derivative of K_{mv} , the Hankel function, with respect to its argument $\left(2\pi \frac{\rho}{\lambda} \right)$ and λ is the wavelength of a plane wave in an unbounded medium of constant μ and ϵ . The remaining components of field are zero, i.e., $H_y = E_\rho = E_\phi = 0$.

The metal is assumed to have an infinitely high conductivity. The boundary conditions require that the tangential component of the electric field vanish at the boundary. There is no electric field in our wave tangential to the top and bottom surfaces of the horn, hence

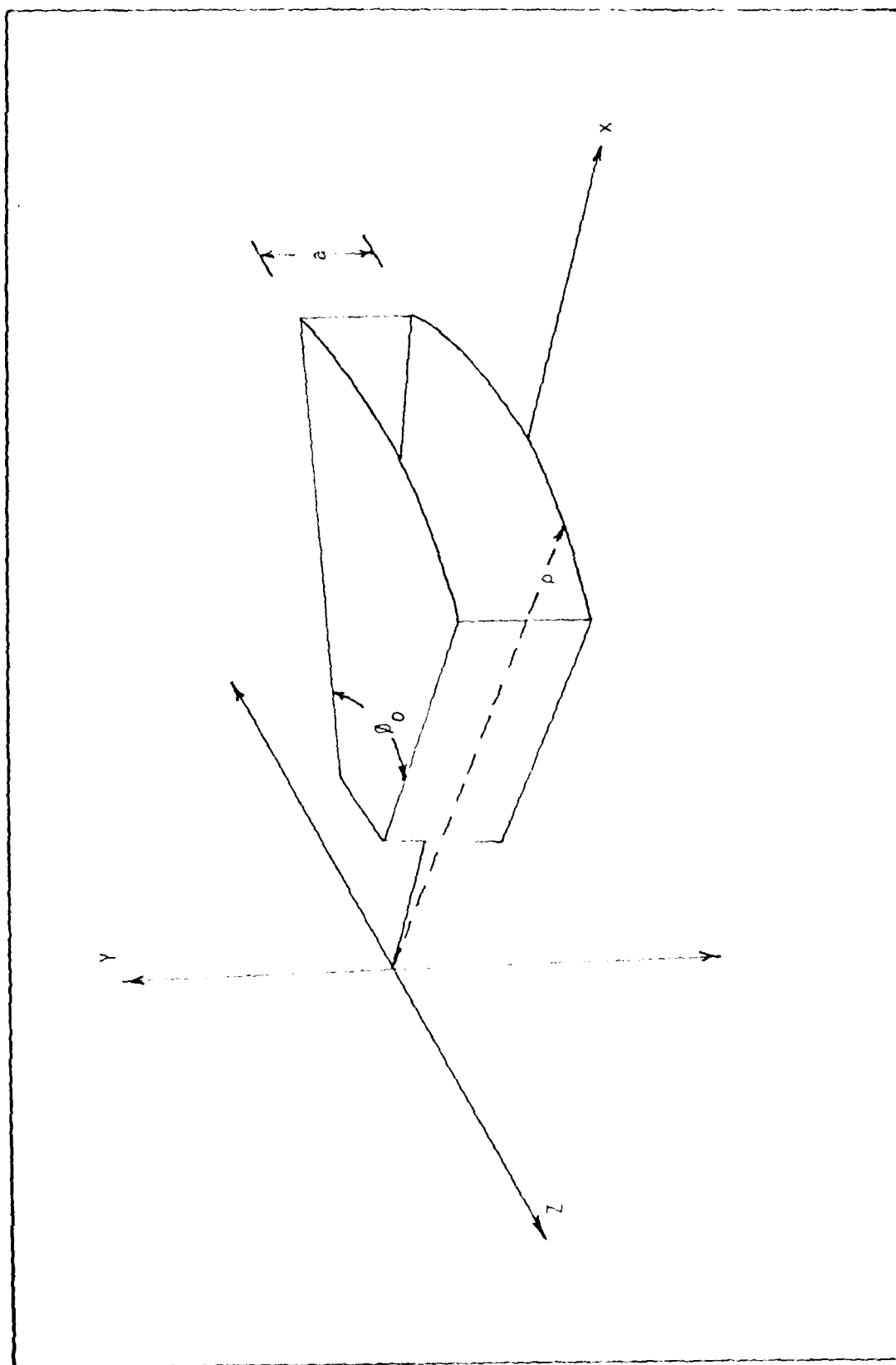


Figure 4. Sectoral Horn and Cylindrical Coordinate System

the boundary conditions are automatically satisfied for $y = 0, a$.
 At the two sides, where $\phi = \pm\phi_0/2$, E_y must vanish, so we must have

$$\cos (mv\phi_0/2) = 0$$

This equation can be satisfied by letting the integer m be odd
 (1, 3, 5, ...) and

$$v = \frac{\pi}{\phi_0} \quad (52)$$

The integer m specifies the order of the wave. Physically, it indicates the number of half-period sinusoidal variations between the two sides of any component of the field along an arc $\rho = \text{constant}$. The constant v depends only on the flare angle ϕ_0 , as specified by Eq (52). Since m is always associated with v as a product, the product

$$mv = \frac{m\pi}{\phi_0} \quad (53)$$

determines the behavior of the wave inside the horn. Only those $H_{m,0}$ waves which have an electric field of even symmetry about the center of the horn radiate beams with a central lobe.

Several advantages are gained by using the sectoral horn for the measurement of reflection and transmission coefficients. Near the

throat, the radial component of the magnetic field is still of considerable magnitude, but in the more distant parts of the horn, where ρ is large, the component H_ρ becomes negligible compared to the other two field components. Both the magnetic and electric field lines are normal to each other and to the direction of propagation, and the waves at the mouth of the horn behave very much as do transverse electromagnetic waves in free space. Thus, a sample placed at the mouth of a sectoral horn with a large radius (ρ) would experience a closely approximated normally incident plane wave condition.

Lower signal power requirements can be realized by using the sectoral horn to approximate a normally incident plane wave on the sample. The usual technique to obtain a plane wavefront is to remove the sample far from the transmitting source. In this case, power loss increases with separation. The sectoral horn allows the sample to be placed within the mouth area, as if inside a wave guide, where the power is reduced only by wall losses.

The total area of the sample used for measurements is typically greater than that of samples used in the time domain. This aspect would reduce some of the delicate machining needed to make small samples.

III. Equipment

During the course of this work, there were two operating systems developed. The first system was a test setup and used an anechoic chamber and a modified H-plane sectoral horn to measure the transmission and reflection coefficients, respectively. A full description of this setup is provided in Appendix B. The second system utilizes the two H-plane sectoral horns. It is this second system which is reported on in the main body of the thesis.

The major pieces of equipment used in the frequency domain measurement system will be described first. Then a full description of how these major pieces of equipment are assembled for intrinsic property measurements will be given.

The equipment used to support this thesis project consisted of a frequency synthesizer which served as the signal source, a network analyzer used for making relative decibel amplitude and phase measurements, a two sectoral horn assembly and sample holder used to measure reflection and transmission coefficient parameters, and a Hewlett-Packard 21MX RTE computer used to control the measurement setup. The complete measurement setup is diagrammed in Figure 1.

Frequency Synthesizer

The signal source is a Watkins and Johnson model 1204-1; rapidly tunable over a frequency range of 0.1 to 26 GHz. The following information was taken from the Watkins and Johnson 1204-1 specification sheet. The frequency resolution is 10 kHz from 100 MHz to 249.99 MHz,

100 kHz from 250 MHz to 1.9999 GHz, and 1 MHz from 2 - 26 GHz. The frequency is displayed with a five-digit LED, in GHz, with floating decimal. The frequency accuracy is $\pm 0.00035\%$ for 180 days over a 0 - 50° C range. A single frequency can be selected on the keyboard with the enter, ENT, button and displayed on the LED. The frequency can be slewed up or down in 1, 10, and 100 MHz steps as selected on the INCREMENT controls. The synthesizer sweeps repetitively upward within the following bands: 0.1 - 1 GHz, 1 - 2 GHz, 2 - 8 GHz, 8 - 13 GHz, 13 - 18 GHz, and 18 - 26 GHz. The ΔF symmetrical sweep about phase-locked center frequency F which is displayed on the LED readout is 0 to $\pm 0.1\%$ of F . The synthesizer provides 0 dBm (1 mW) minimum leveled output power. The variations in leveled power for the 0 dB attenuator setting is ± 1 dB over the range of 0.1 - 26 GHz. The output power can be attenuated over a range of 0 to 90 dB in 10 dB steps. The output power accuracy (meter reading plus attenuator setting) is: 0 dB attenuator setting, 0.1 - 18 GHz, ± 1 dB and 18 - 26 GHz, ± 1 dB; 10 dB - 90 dB attenuator setting, ± 2 dB and 18 - 26 GHz, ± 2.5 dB.

Network Analyzer

The network analyzer is a Hewlett-Packard Model 8410A with a phase-gain indicator. The 8413A phase-gain indicator uses a meter display. The 8411A harmonic frequency converter provides RF-to-IF conversion. The 8411A converter has been modified under Option 018 to work across the Ku band. The VSWR at the reference and test port under Option 018 increases to 10 at 18 GHz. Measurements are based

on the use of two wideband samplers to convert the input frequencies to a constant IF frequency. RF-to-IF conversion takes place entirely in the harmonic frequency converter, which converts frequencies over a range of 12.4 - 18 GHz to 20 MHz IF signals. The phase and amplitude of the two RF input signals are maintained in the IF signal. The network analyzer mainframe provides the phase-lock circuitry to maintain the 20 MHz IF frequency while frequency is being swept, takes the ratio of the reference and test channels by use of identical AGC amplifiers, and then converts down to a second IF at 278 kHz. It also has a precision 0 to 69 dB IF attenuator with 10 and 1 dB steps for accurate IF substitution measurements of gain or attenuation. The frequency domain measurement setup utilized the following piece of equipment during data measurements: a plug-in for the 8410A mainframe, the 8413A phase-gain indicator. It compares the amplitudes of the two IF signals and provides a meter readout of their ratio directly in dB with 0.1 dB resolution. It also compares phase in degrees over a 360° unambiguous range with 0.2° resolution on the meter. Phase difference is presented on the same meter when the appropriate function button is depressed. This plug-in has two analog output ports accessible from the front, one for dB amplitude, 20 mv/dB, and one for phase, 50 mv/degree.

Horn Assembly

The H-plane sectoral horn assembly and sample holder is constructed from aluminum. There are three major parts comprising this assembly. The two horns, the sample holder/reference slide section, and the

sample holder itself. The individual pieces are depicted in Figure 5.

The two sectoral horns are placed mouth to mouth and form the central part of the measurement system. The full length of the horn section is 310.5 cm. The inner dimensions at the end flange region are 1.6 cm x 0.8 cm, and at the mouth 9.5 cm x 0.8 cm. The two horns are connected at the sample holder area.

The sample holder section is made up of a 6 cm x 5 cm x 15 cm solid block slider which fits inside the 10.5 cm x 11 cm x 15 cm rectangular housing. There are three windows cut along the length of the slider section. In the center window, the slider section has a shorting plate made of stainless steel used to obtain the reference for making reflection coefficient measurements. At one end of the slider, there is an open rectangular window measuring 9.5 cm x 0.8 cm which is used to obtain the reference for making transmission coefficient measurements. The third window is used to hold the sample during measurement.

The sample holder is removed from the slider section during sample installation. The overall dimensions of the sample holder are 11.3 cm x 5 cm x 3 cm. A 9.5 cm x 0.8 cm window in the sample holder serves to accommodate the sample. A set screw at one side is used to apply a small amount of pressure on the sample to hold it in place so it does not become misaligned during installation of the sample holder in the slider.

A gauge block is used when mounting the sample material into the sample holder. The gauge block provides a means to position the sample's front face at the same plane as the shorting plate for

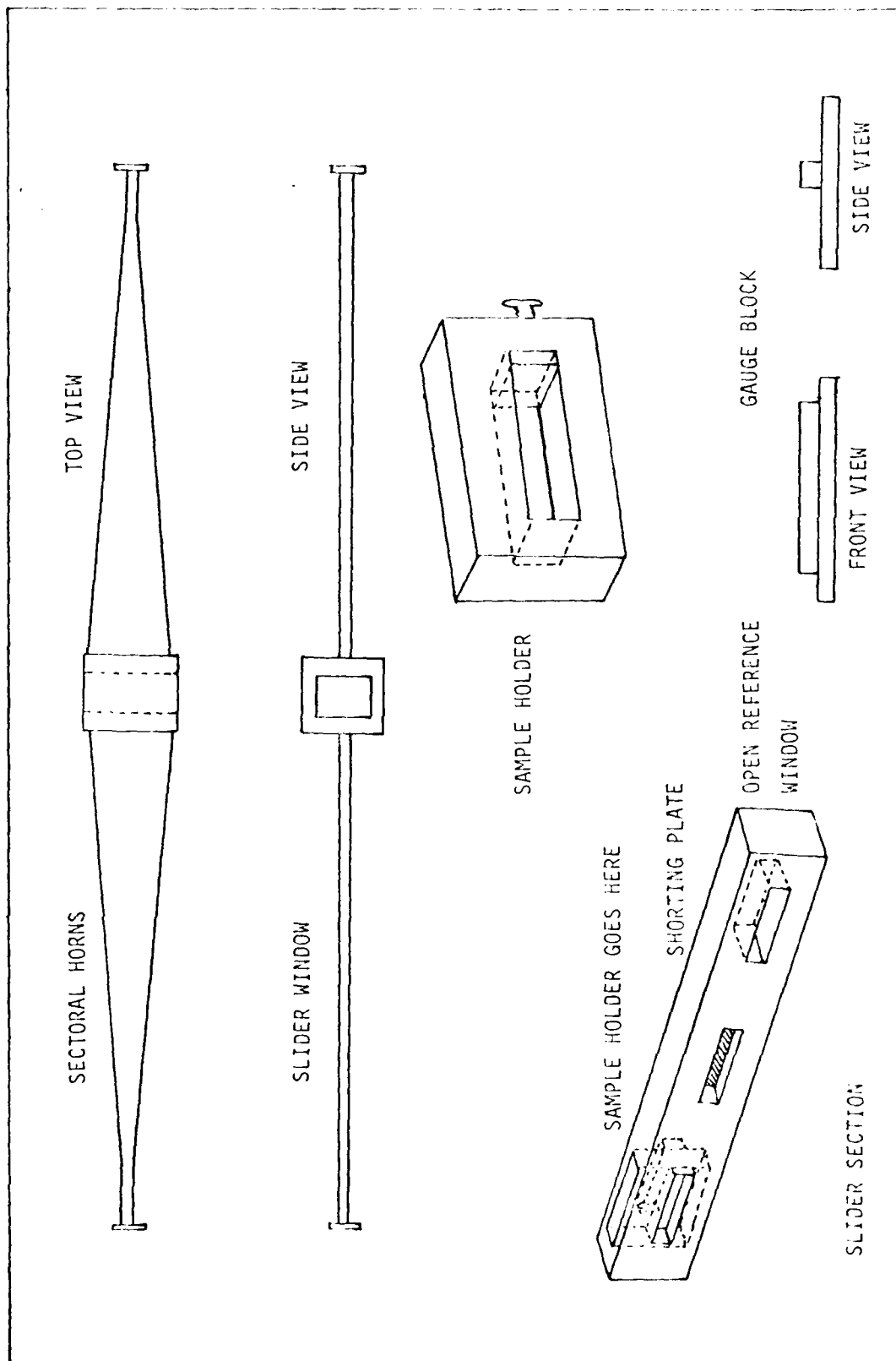


Figure 5. Sectoral Horns and Sample Holder

reflection coefficient measurements. The sample holder is placed on the gauge block with the 1.119 cm raised section inserted in the sample window. The sample is placed in the sample window and forced firmly against the raised section as the set screw is tightened.

21MX Computer

The Hewlett-Packard 21MX computer is used to control the data measurement. The frequency synthesizer is commanded to a discrete frequency by the computer and a data measurement taken through the computer A/D converter connected to the outputs of the network analyzer. The disk subsystem and I/O devices are used to store, process, and display the results of a data run. The computer software is provided in Appendix A.

With some insight into the main parts of the frequency domain measurement system, the rest of this chapter will deal with describing the system as a whole and how it is interconnected. This description is an amplification of Figure 1.

Measurement System

The Watkins and Johnson 1204-1 Synthesizer serves as the signal source. It is commanded by the 21MX computer to discrete frequencies as part of the intrinsic property measurement routine. The RF signal is routed from the signal synthesizer to the Ku band wave guide by means of a six foot coaxial cable (C1803-72 B&W Associates, Inc., Burlington, MA). The cable connects into a Narda 4609, 12.4 to 18 GHz, coaxial to wave guide adapter. The Narda adapter is attached to a

20 dB Hewlett-Packard (HP) directional coupler, model number P752D. The 20 dB coupler couples a portion of the signal into the reference port of the HP 8411 Harmonic Frequency Converter (modified with Option 018 to extend its capability from 12.4 to 18 GHz). The main RF signal is fed into a second directional coupler. This second HP directional coupler, Model P752A, couples 3 dB of the signal into a third directional coupler and sends the rest of the signal into a matched load. The third HP coupler, model number P752A, is used to couple 3 dB of reflected signal from the sample or short into an FXR model Y641A switch and then into the test port of the harmonic frequency converter during reflection coefficient measurements. During transmission coefficient measurements, any reflected signal coupled through this 3 dB coupler is switched into a Waveline Type 754 matched load.

For transmission coefficient measurements, the RF signal which transmits through the sample is routed into the test port of the harmonic frequency converter through a PRD Electronics, Inc. Type 1208 Isolator and the switch. The transmitted signal through the sample is terminated in a matched load at the switch during reflection coefficient measurements.

The harmonic frequency converter provides the IF signal to the HP 8410B Network Analyzer. The analog amplitude and phase ports on the front of the HP 8413A Phase-Gain Indicator are read by the computer. An HP Plug-In 20 KHz Analog-to-Digital Interface Sybsystem located in the 21MX computer, machine model HP2108A, converts the analog inputs to digital values used for computation. A Tektronix 4006-1 CRT

Terminal is the operator control center for sample measurements. Finally, the processed μ and epsilon data are routed from the computer to the HP 2635A Line Printer or, for plots of μ and epsilon, to the Tektronix 4631 Hard Copy Unit.

IV. Procedure

1. The sample is prepared by cutting a 9.5 x 0.8 cm rectangular piece from the material to be measured.
 - 1a. The sample is cut to fill the sample window completely.
 - 1b. The thickness of the sample in mils is determined for use in the computer program.
2. The frequency synthesizer and network analyzer are turned on for a half hour before any measurements are to be taken.
3. The frequency synthesizer and network analyzer are adjusted for making measurements. The slider section in the sample holder assembly is positioned with the shorting plate in the sectoral horn and the reflected signal line is switched to the test port of the harmonic frequency converter as shown in Figure 1.
 - 3a. The local/remote switch at the back of the frequency synthesizer is placed in local.
 - 3b. The Ku band midrange frequency of 15 GHz is entered at the frequency synthesizer keyboard and the output signal power level is set to +3 dbm.
 - 3c. The network analyzer is adjusted to read 0 dB on the 3 dB amplitude scale by means of the amplitude vernier and the amplitude gain amplifier.
 - 3d. The amplitude meter is switched to the 30 dB scale and an additional 30 dB is added to the test signal amplitude.

gain amplifier to insure an adequate operating range when making measurements.

- 3e. The phase offset dial on the network analyzer is placed at +20°. This value is arbitrary since the coefficient phase measurements are only difference values between a reference phase and the phase associated with reflections off and transmissions through the sample.
 - 3f. The local/remote switch on the frequency synthesizer is set to remote. This mode enables communications between the computer and frequency synthesizer.
4. The computer program is initiated and a statement about the sample is typed in for use as a heading on the relative mu/epsilon output data at the line printer.
- 4a. The sample thickness in mils is entered for use in calculating the relative mu/epsilon data of the sample.
 - 4b. The beginning and ending frequencies in GHz are entered next.
 - 4c. The number of frequencies to be measured is entered. The frequency increment is determined in the computer routine by the equation

$$\Delta F = \frac{\text{End Frequency} - \text{Start Frequency}}{\text{No. of Frequencies to be Measured} - 1}$$

This routine allows the first frequency measured to be the start frequency.

4d. The main command listing is displayed on the CRT and the characteristic of the system can now be measured.

5. Under ideal conditions, the relative mu and epsilon values are determined using the free space values μ_0 and ϵ_0 . However, it is possible to measure a μ_0 and ϵ_0 value for the frequency domain system which has slight deviations from the free space values. These new measured values of μ_0 and ϵ_0 can be complex and characterize how well the frequency domain measurement system approximates free space. A typical plot of μ_0 and ϵ_0 characterizing the measurement system is given in Figure 6A and 6B. The system measured values of μ_0 and ϵ_0 are used to renormalize the relative mu and epsilon data calculated for the sample prior to output.

5a. The sample holder with no sample installed is used in the system characteristic measurement.

5b. The reporting plate is placed at the center of the horn assembly and the reflection signal line is switched into the test port of the harmonic frequency converter.

5c. The reflection coefficient measurement routine is entered and the reference values are measured and stored.

5d. At the end of the reference measurement routine, the sample holder window is placed at the center of the horn assembly and the sample measurement routine entered.

5e. At the end of the sample measurement routine, the computer has calculated and stored the reflection coefficient values.

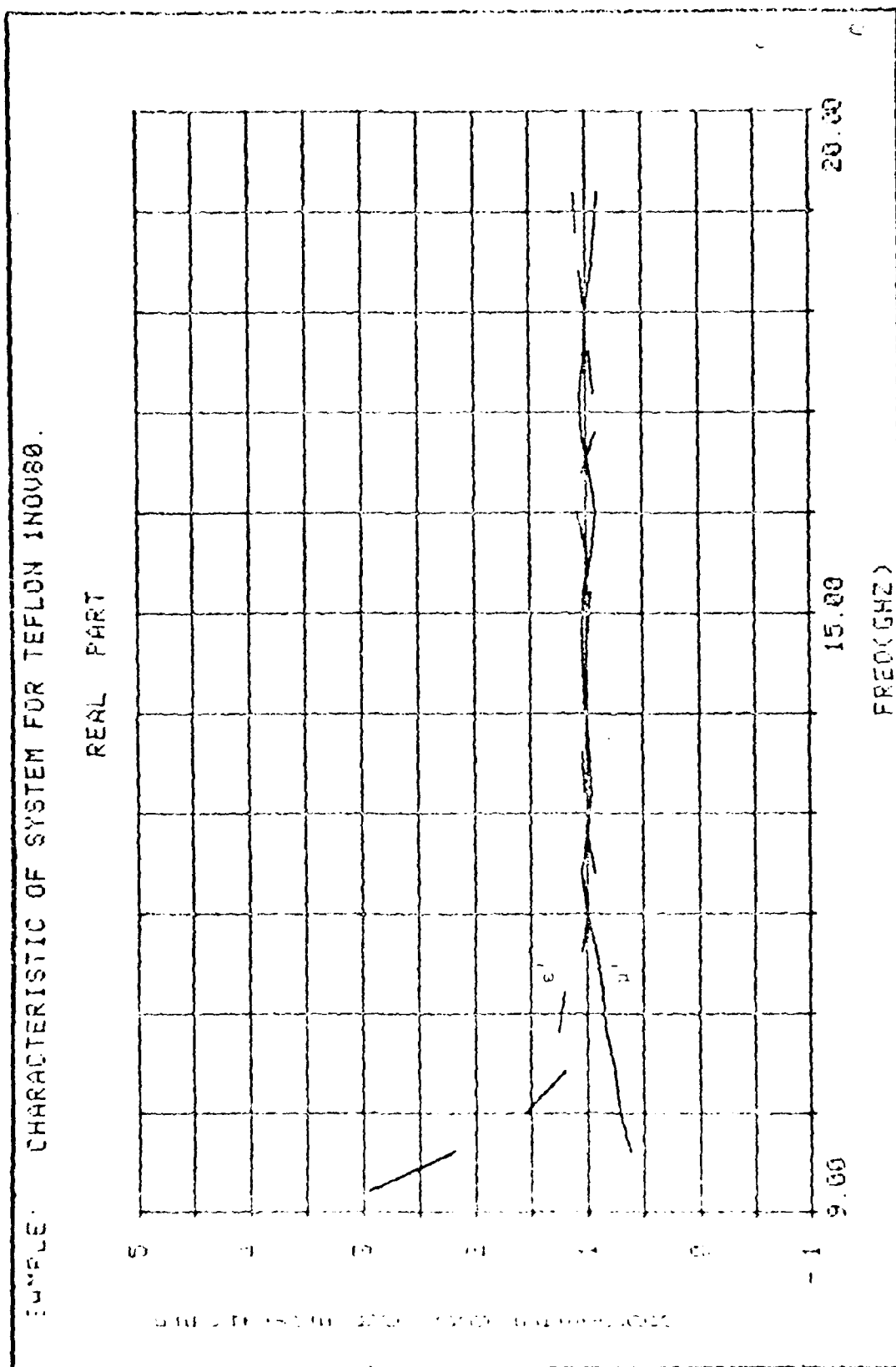


Figure 6A. Frequency Domain (Real) Characteristic of Mu and Epsilon

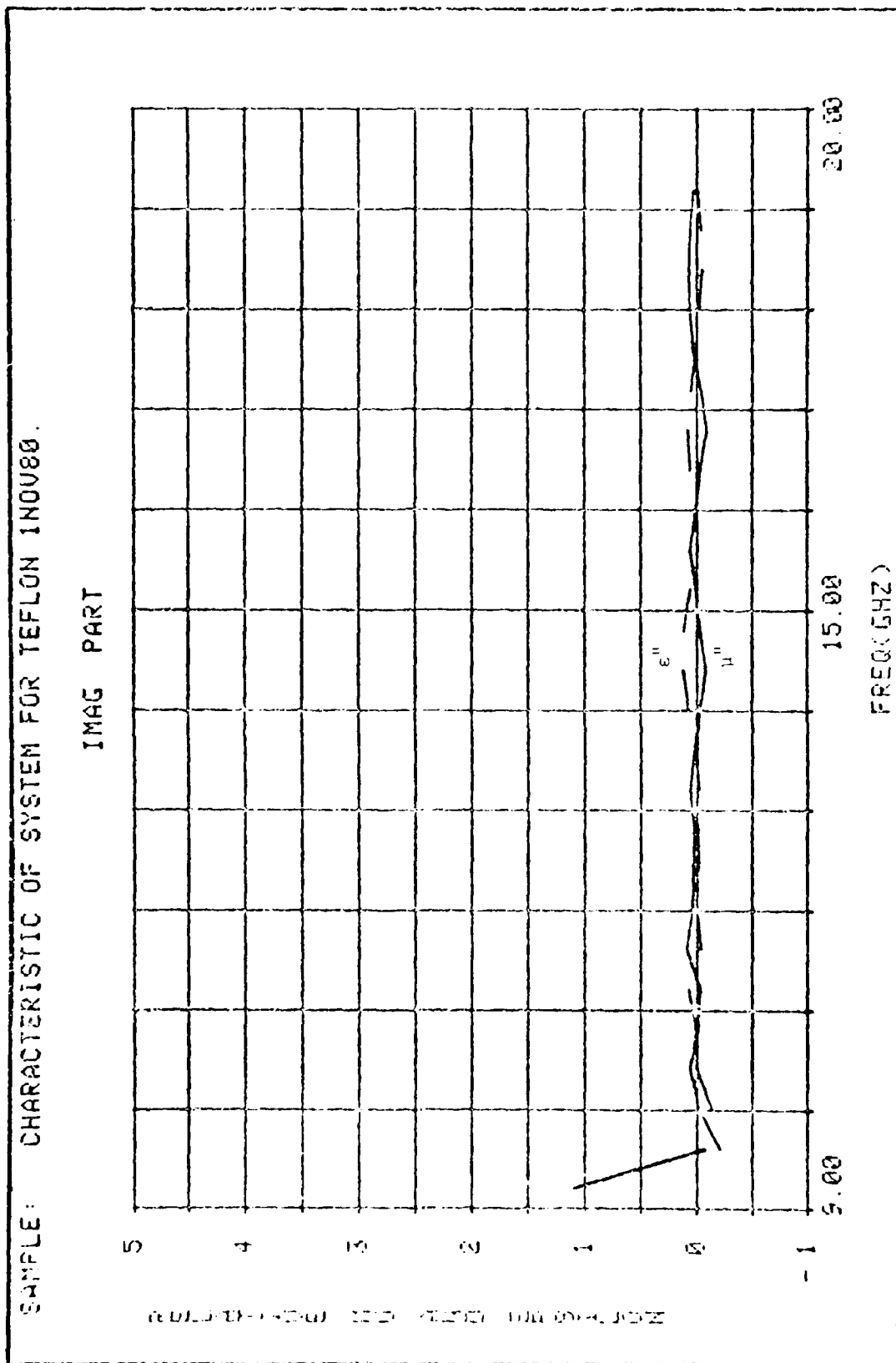


Figure 63. Frequency Domain (Imaginary) Characteristic of Mu and Epsilon

- 5f. At this time, the slider is repositioned with the open reference window at the center of the horn assembly and the transmission signal line is switched into the test port of the harmonic frequency converter.
 - 5g. The transmission coefficient measurement routine is entered and the reference values through the open window are measured and stored.
 - 5h. When the reference measurements are complete, the sample window is again slid to the center of the horn assembly and the sample measurement routine entered. The transmission coefficient is calculated and stored.
 - 5i. At this point, the μ/ϵ calculation routine is entered. During this calculation, the thickness value used for computation of μ and ϵ is 200 mils if this is the first measurement run after entering the program. If this is not the first measurement run after entering the program, the thickness value used for calculation is that thickness entered at the beginning of the program for the sample.
 - 5j. The system characteristic values are stored for renormalization of sample relative μ and ϵ values.
6. The reflection coefficient measurement routine is re-entered and the sample to be measured is installed in the sample holder.
- 6a. The sample holder is removed from the slider section and placed on the gauge block with the raised section inserted

in the sample window such that the set screw is to the right. The sample is inserted and pressed firmly against the raised section of the gauge block. The set screw is adjusted to hold the sample tightly.

- 6b. The sample holder is re-installed in the slider section with the set screw away from the shorting plate.
- 6c. The μ and epsilon values are determined by following the steps from 5b to 5i.

7. The relative μ and epsilon values calculated for the sample are renormalized and then routed as numeric data output to the line printer or as plots to the hard copy unit. When the plot option is used to display the output data, a statement about the sample must be entered to serve as a title for the plots.

V. Results

To demonstrate the feasibility of the frequency domain measurement system, fiberglass, two thicknesses of plexiglas, teflon, and an FGM-40 absorber were measured and their relative permittivity and permeability values calculated. These values were compared to the relative permittivity and permeability for the same fiberglass, plexiglas, teflon, and FGM-40 absorber materials measured on the time domain system. Because the frequency domain system was designed to operate in the Ku band, 12.4 to 18 GHz, and the time domain data were valid below 16 GHz (Nicolson, 1974), the data were compared between the two systems only from 12.4 to 16 GHz.

Expected Results

The relative permittivity values measured for fiberglass, plexiglas, and teflon materials are provided in the table of dielectric materials given below (Hippel, 1958).

Dielectric Material	T °C		.1 GHz	.3 GHz	3 GHz	10 GHz
Laminated Fiberglass	24	ϵ'	4.8	4.54	4.40	4.37
		$\tan \delta$	260	240	290	360
Plexiglas	27	ϵ'	---	2.66	2.60	2.59
		$\tan \delta$	---	62	57	67
Teflon	22	ϵ'	2.1	2.1	2.1	2.08
		$\tan \delta$	< 2	1.5	1.5	3.7

Values for $\tan \delta$ are multiplied by 10^4 .

The permeability value for these dielectrics is, of course,
 $\mu = \mu_r \mu_0$ where $\mu_r = 1$.

It is not known whether the laminated fiberglass listed in the table above was the same type of fiberglass material used in the thesis work. However, the permittivity value given above compares extremely well with that value obtained on the time domain system at 10 GHz.

Fiberglass Sample

The time domain data for the fiberglass sample are given in Figure 7A and 7B. The plot of the time domain data is for a single measurement run. The frequency domain data for the fiberglass sample are presented graphically in Figure 8A and 8B. The frequency domain data are the statistically averaged relative epsilon and mu values from ten separate measurement runs. It is assumed that the data values at any given frequency are normally distributed. The standard deviation is depicted on the plot as a vertical line above and below the mean. A complete listing of the average values of relative permittivity and permeability, along with the standard deviation, is presented in Table I. The complex permittivity and permeability values calculated for the fiberglass sample are compared for the frequency range of 12.4 to 16 GHz in Table II.

First Plexiglas Sample

The complex permittivity and permeability values measured on the time domain for the 64.5 mil plexiglas sample are plotted in Figure 9A and 9B. Again, these data are for a single measurement run. The

SAMPLE: FIBER GLASS 134.5 MILS 10-9-80

REAL PART

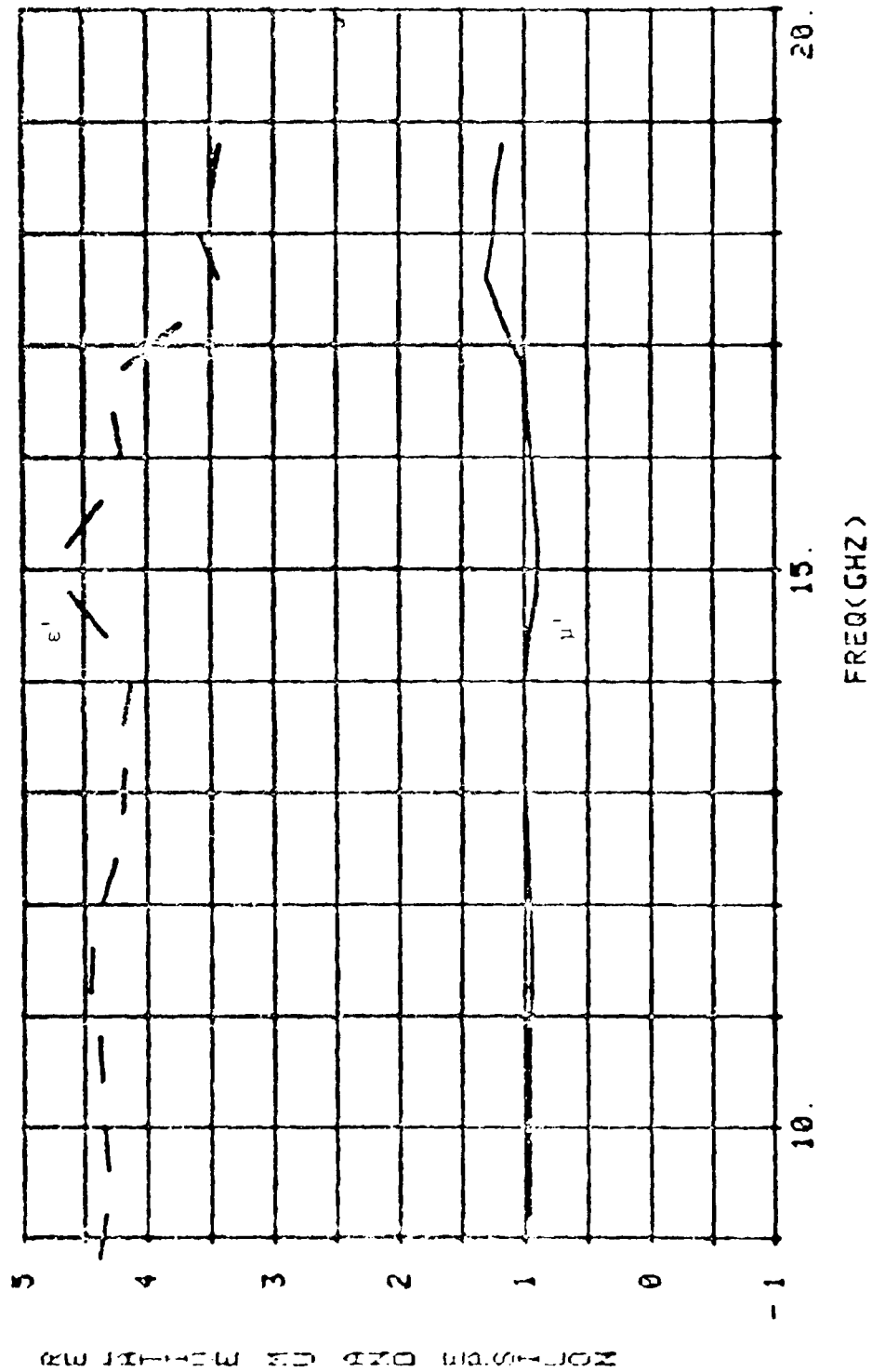


Figure 70. Time Domain (Peal) Data for 134.5 mil Fiberglass Sample

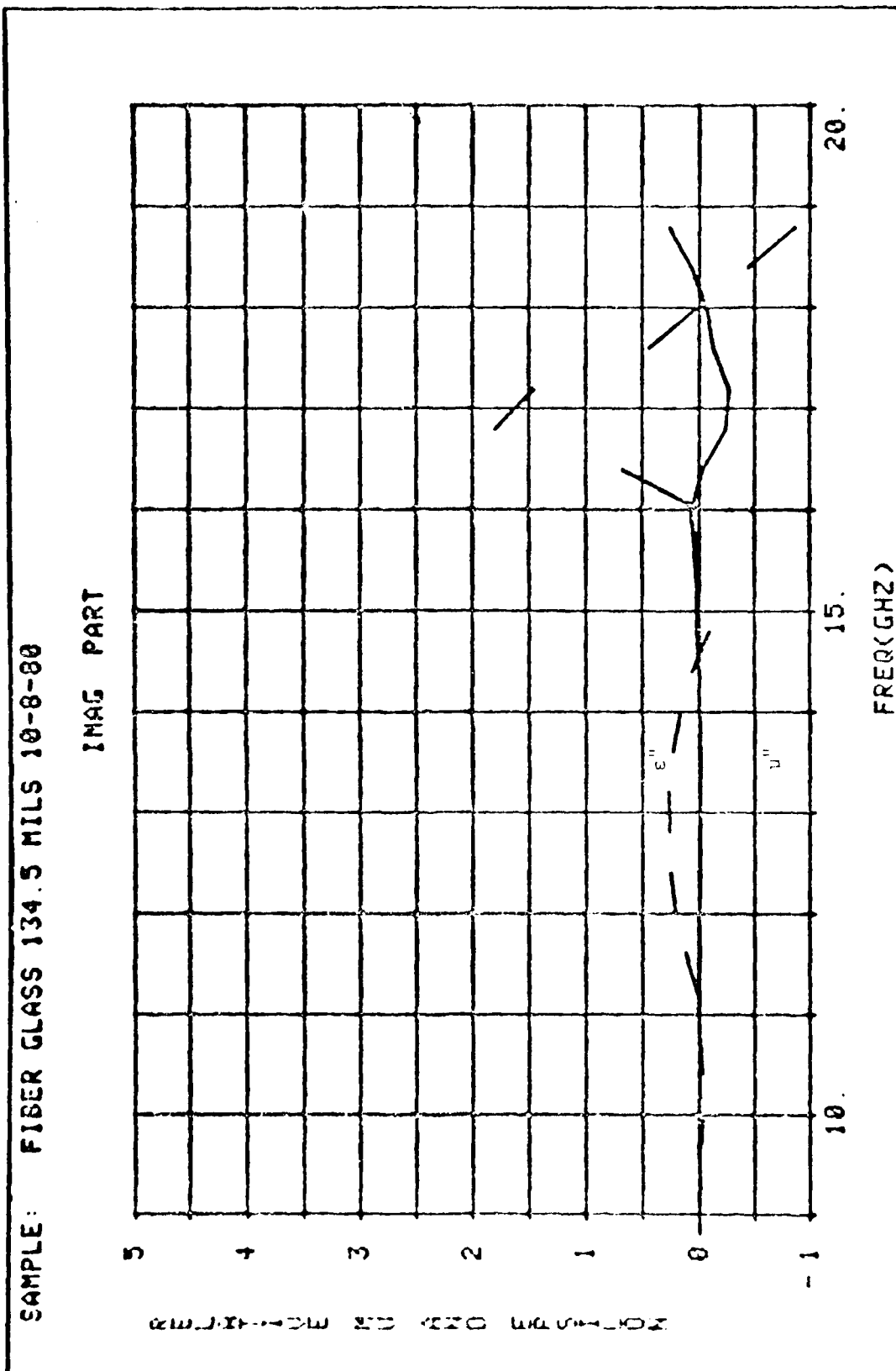


Figure 73. Time Domain (Imaginary) Data for 134.5 mil Fiberglass Sample

SAMPLE: 01: FIBERGLAS THICKNESS = 135 MILS.

REAL PART

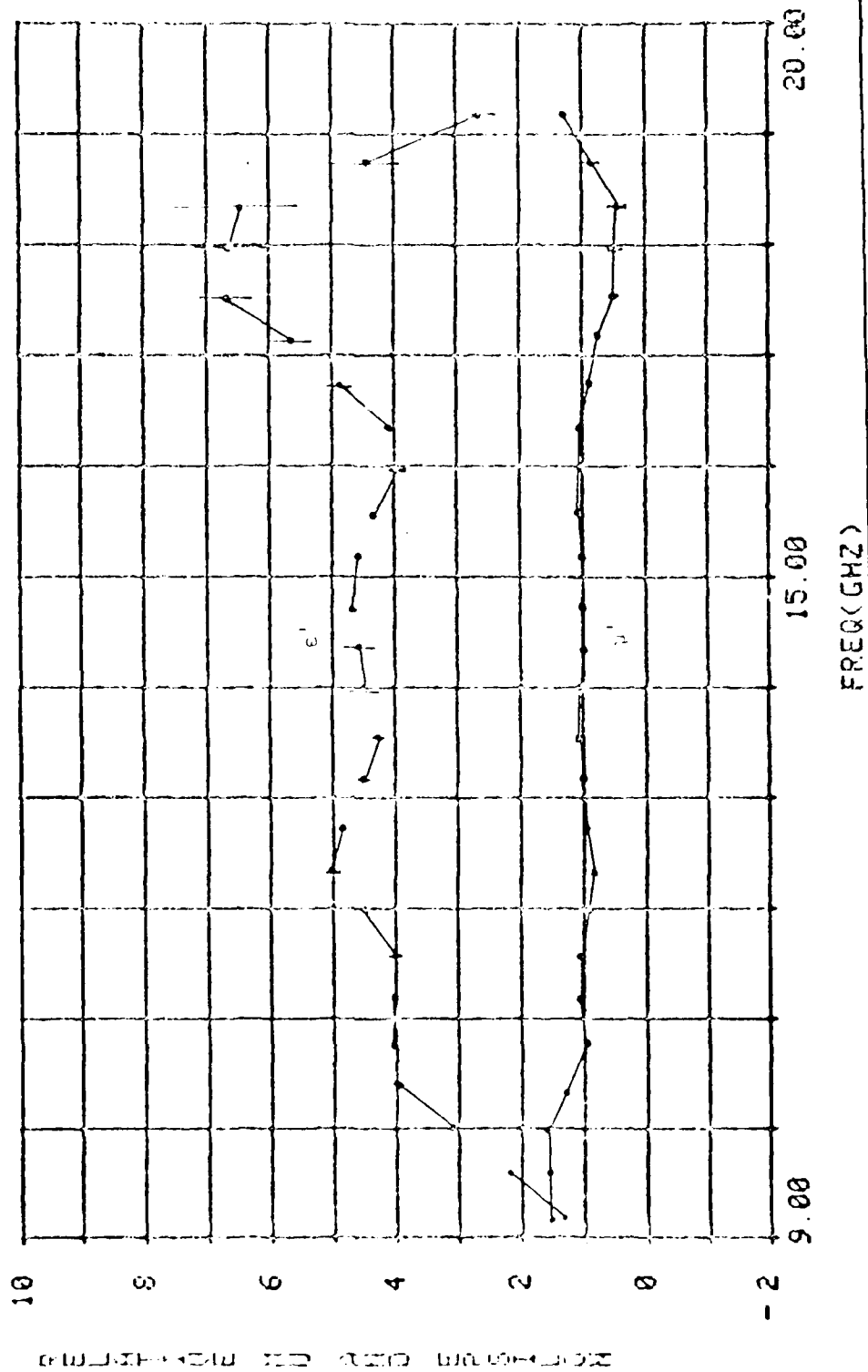


Figure 8A. Frequency Domain (Real) Data for 135 mil Fiberglass Sample

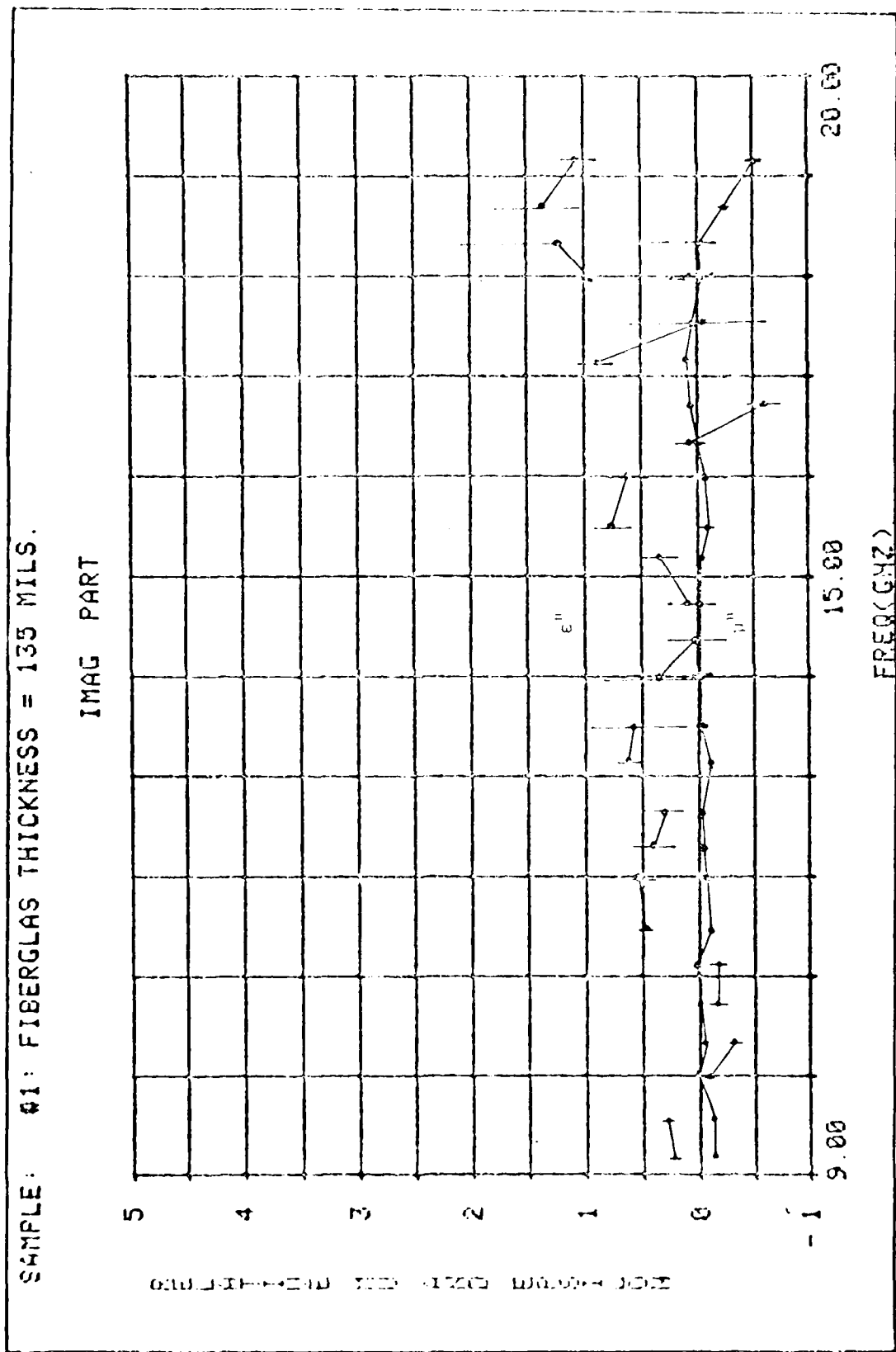


Figure 63. Frequency Domain (Imaginary) Data for 135 mil Fiberglass Sample

TABLE I

SAMPLE: FIBERGLASS

FREQUENCY DOMAIN DATA

THICKNESS = 134.5 MILS

FREQUENCY (GHz)	ϵ'	s	ϵ''	s	μ'	s	μ''	s
9.2	1.25	.05	.26	.04	1.39	.04	-.11	.03
9.6	2.17	.05	.30	.07	1.44	.04	-.11	.03
10.0	3.07	.07	-.11	.06	1.48	.04	.01	.02
10.4	3.96	.09	-.38	.06	1.21	.02	-.06	.02
10.8	4.13	.05	-.19	.10	1.00	.02	-.00	.01
11.2	4.07	.11	-.18	.08	1.02	.02	.04	.01
11.6	4.08	.12	.48	.13	1.01	.03	-.12	.03
12.0	4.60	.14	.54	.26	.94	.02	-.08	.04
12.4	5.01	.21	.47	.27	.88	.02	-.07	.03
12.8	4.83	.17	.36	.16	.92	.02	-.06	.02
13.2	4.46	.18	.68	.17	1.00	.02	-.14	.03
13.6	4.26	.15	.57	.37	1.05	.02	-.07	.08
14.0	4.48	.25	.42	.41	1.05	.01	-.04	.11
14.4	4.69	.23	.03	.34	.98	.01	.03	.08
14.8	4.74	.11	.16	.19	.96	.01	-.03	.03
15.2	4.63	.05	.37	.14	.99	.01	-.05	.03
15.6	4.27	.08	.76	.14	1.03	.01	-.11	.08
16.0	3.97	.10	.61	.15	1.09	.01	-.11	.03
16.4	4.14	.10	.13	.14	1.05	.01	-.00	.02
16.8	4.88	.14	-.60	.15	.91	.01	.09	.02
17.2	5.72	.27	-.94	.29	.78	.03	.10	.03
17.6	6.78	.59	-.04	.62	.67	.06	.02	.08
18.0	6.70	.68	.99	.85	.65	.08	-.06	.13
18.4	6.56	1.16	1.25	.91	.67	.11	-.07	.11
18.8	4.45	.54	1.44	.46	.92	.09	-.27	.07
19.2	2.67	.22	1.09	.20	1.37	.06	-.53	.10

TABLE II

SAMPLE: FIBERGLASS

FREQUENCY DOMAIN SYSTEM

THICKNESS = 135 MILS

TIME DOMAIN SYSTEM

THICKNESS = 134.5 MILS

<u>FREQUENCY (GHz)</u>	<u>EPSILON</u>	<u>MU</u>	<u>FREQUENCY (GHz)</u>	<u>EPSILON</u>	<u>MU</u>
12.4	4.25+J.25	.97-J.01	12.4	5.01+J.47	.88-J.07
12.8	4.19+J.25	.99-J.01	12.8	4.83+J.36	.92-J.06
13.2	4.18+J.27	1.00-J.01	13.2	4.46+J.68	.99-J.14
13.6	4.19+J.23	1.00-J.01	13.6	4.20+J.51	1.05-J.07
14.0	4.12+J.17	1.00+J.00	14.0	4.47+J.42	1.18-J.04
14.4	4.32+J.51	.96+J.00	14.9	4.69+J.03	.93+J.03
14.8	4.62-J.09	.90+J.02	14.8	4.74+J.16	.90-J.03
15.2	4.64+J.02	.89+J.02	15.2	4.63+J.37	.99-J.05
15.6	4.36+J.01	.92+J.04	15.6	4.27+J.76	1.03-J.11
16.0	4.20-J.01	.94+J.07	16.0	3.97+J.61	1.09-J.11

SAMPLE: PLEXIGLAS 64.5 MILS 10-1-00

REAL PART

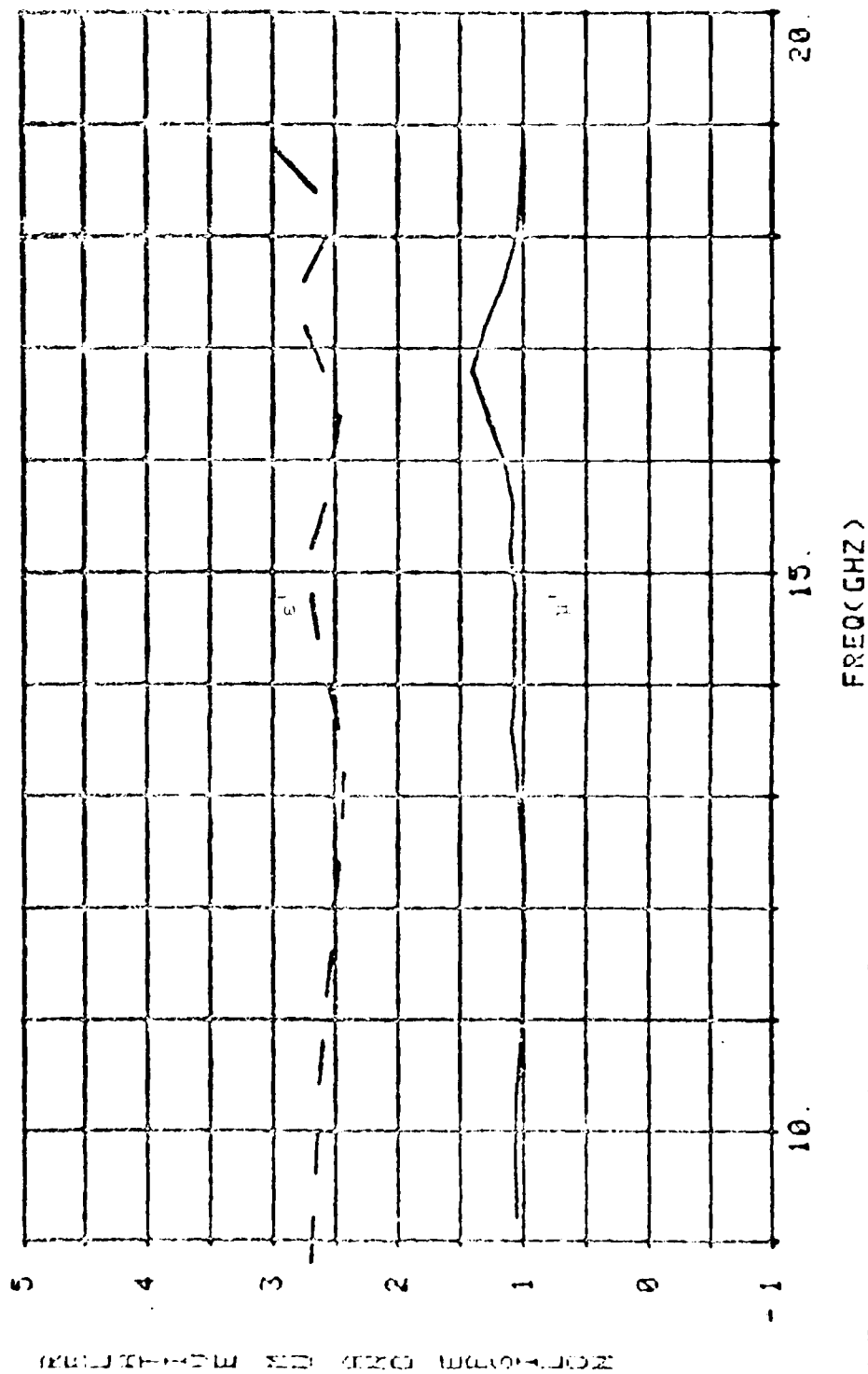


Figure 9A. Time Domain (Real) Data for 64.5 mil Plexiglas Sample

SAMPLE: PLEXIGLAS 64.5 MILS 10-1-80

IMAG PART

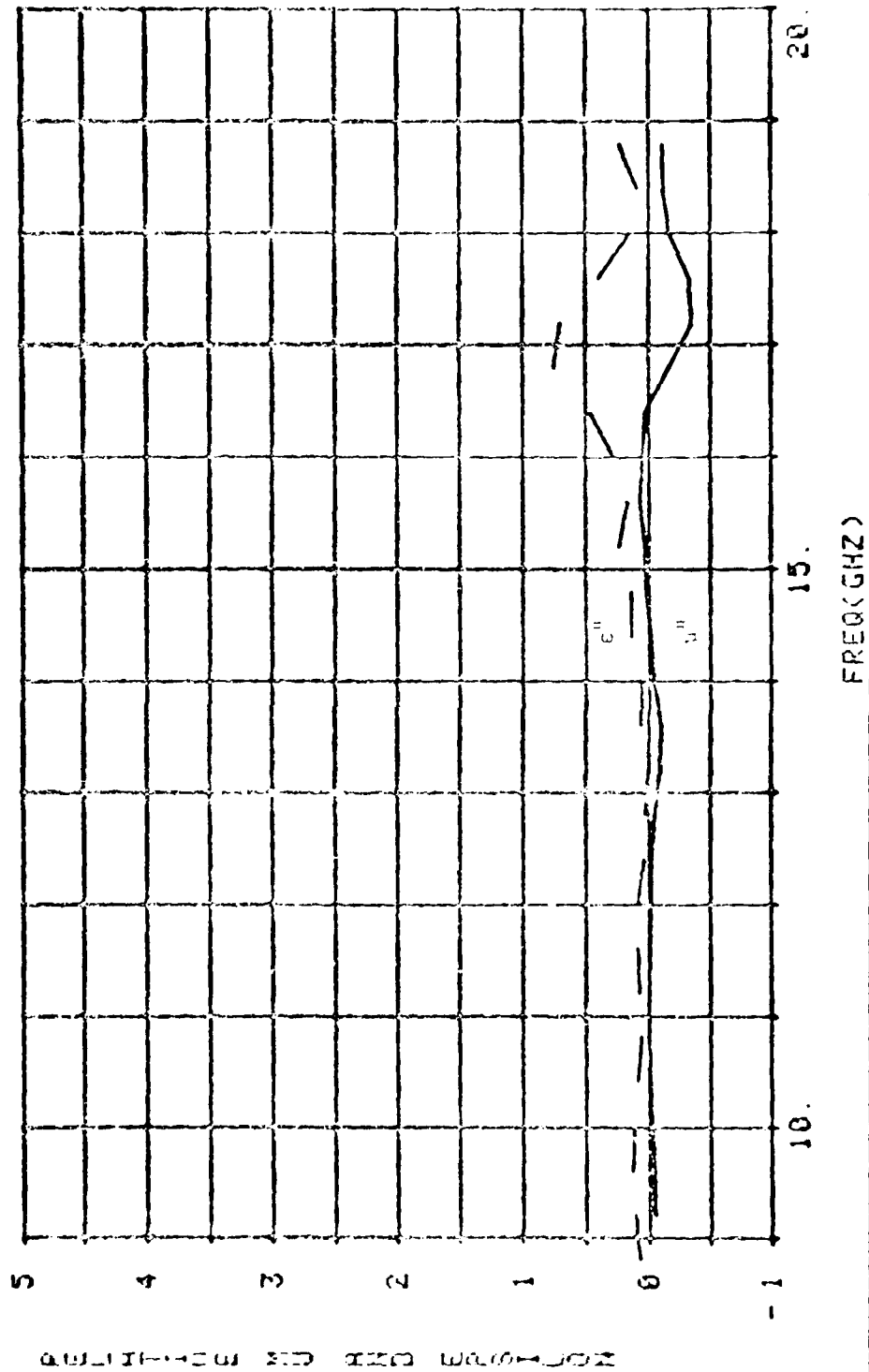


Figure 90. Time Domain (Imaginary) Data for 64.5 mil Plexiglas Sample

frequency domain data for a 65.5 mil plexiglas sample is shown in Figure 10A and 10B. As before, this frequency domain data is the mean and standard deviation for ten data runs. The mean and standard deviation calculated for the μ and ϵ values are presented in Table III. The comparison for the time domain and frequency domain data is presented in Table IV for the frequency range from 12.4 to 16 GHz.

Second Plexiglas Sample

The time domain data obtained for the 174 mil plexiglas sample are presented graphically in Figure 11A and 11B for a single measurement run. The frequency domain data for the 174 mil plexiglas sample are presented in Figure 12A and 12B. As before, the frequency domain data are the mean values of ten runs and the standard deviations are presented in Table V. The comparison of the 174 mil plexiglas data for the time and frequency domain systems from 12.4 to 16 GHz are given in Table VI.

Repeatability

The statistics developed for the frequency domain data measurements show the repeatability of the measurement technique. During each of the data runs the network analyzer was turned off and on, or the sample was removed from the sample holder and re-installed. The system configuration did not allow for power removal from the computer or the frequency synthesizer.

SAMPLE: 02: PLEXIGLAS THICKNESS = 65.5 MILS.

REAL PART

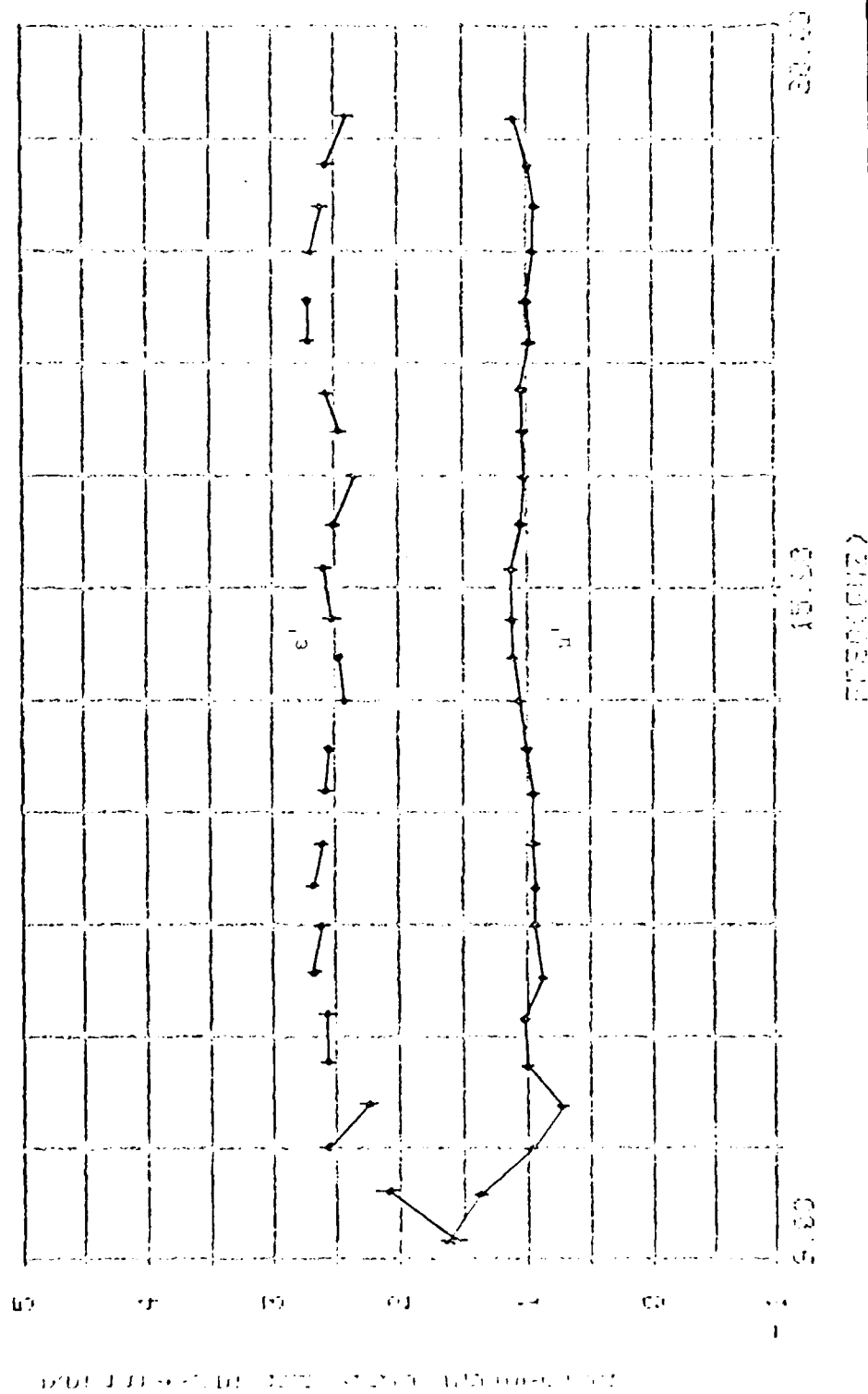


Figure 10A. Frequency Domain (Real) Data for 65.5 mil Plexiglas Sample

SAMPLE: #2: PLEXIGLAS THICKNESS = 65.5 MILS.

IMAG PART

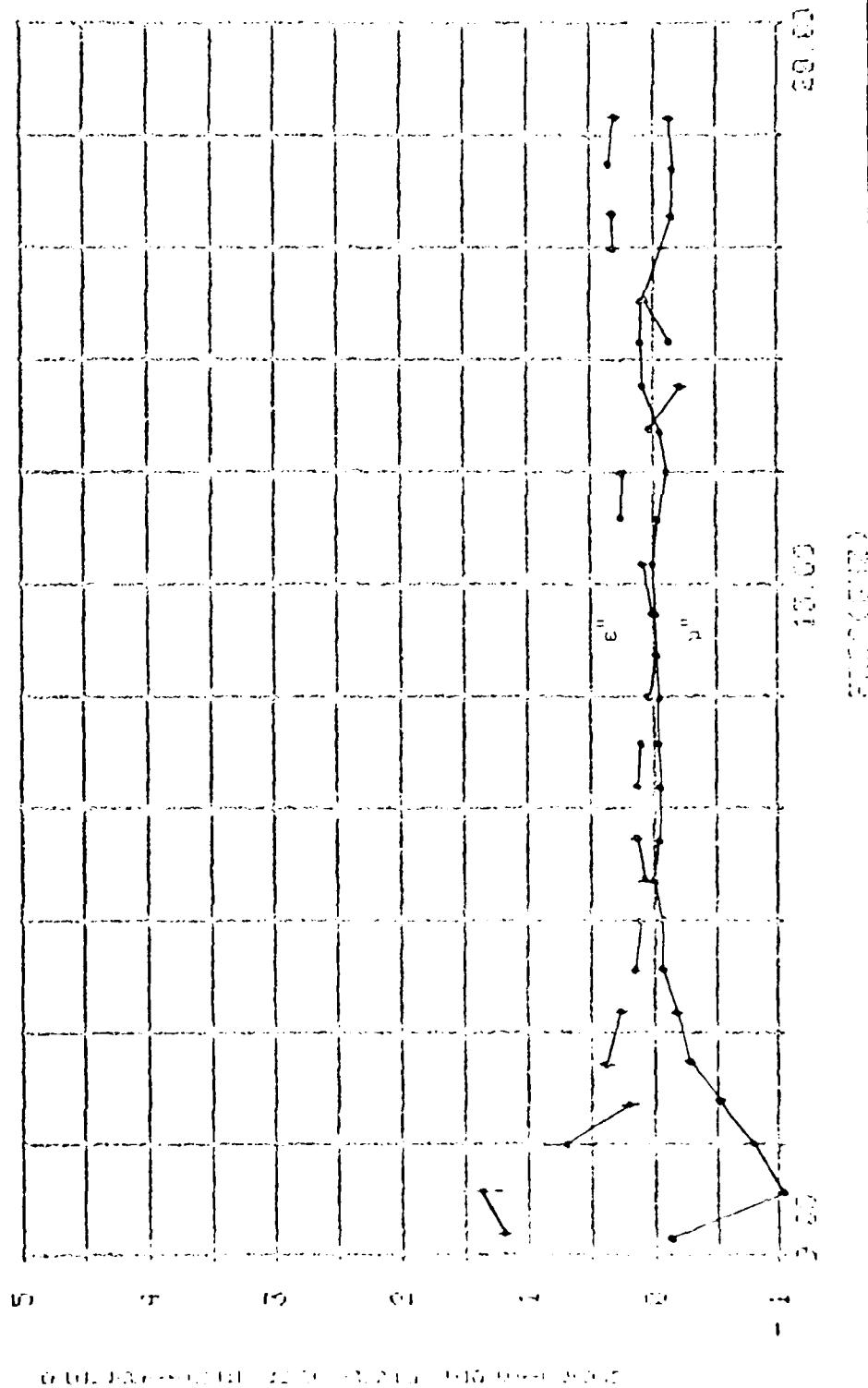


Figure 113. Frequency Domain (Imaginary) Data for 65.5 mil Plexiglas Sample

TABLE III

SAMPLE: PLEXIGLAS

FREQUENCY DOMAIN DATA

THICKNESS = 65.5 MILS

FREQUENCY (GHz)	ϵ'	s	ϵ''	s	μ'	s	μ''	s
9.2	1.57	.12	1.22	.05	1.65	.02	-.15	.03
9.6	2.10	.11	1.40	.18	1.39	.06	-1.12	.03
10.0	2.54	.11	.69	.21	.93	.05	.83	.09
10.4	2.23	.06	.25	.07	.73	.05	-.52	.03
10.8	2.66	.05	.43	.05	1.00	.04	-.31	.03
11.2	2.57	.07	.35	.04	1.04	.03	-.21	.04
11.6	2.68	.04	.23	.04	.83	.01	-.10	.05
12.0	2.62	.04	.16	.06	.89	.02	-.05	.05
12.4	2.71	.04	.11	.07	.94	.03	-.03	.04
12.8	2.63	.06	.21	.05	.96	.03	.07	.04
13.2	2.60	.05	.26	.05	.94	.04	-.09	.03
13.6	2.53	.04	.19	.02	1.01	.03	-.06	.03
14.0	2.45	.04	.05	.03	1.10	.03	-.04	.04
14.4	2.47	.02	-.06	.02	1.12	.03	-.01	.02
14.8	2.53	.05	.07	.04	1.15	.03	.00	.01
15.2	2.60	.05	.17	.06	1.13	.03	.03	.02
15.6	2.51	.03	.32	.03	1.05	.04	-.04	.02
16.0	2.38	.03	.29	.03	1.03	.03	-.13	.02
16.4	2.48	.03	.05	.04	1.05	.02	-.06	.02
16.8	2.61	.04	-.25	.04	1.06	.03	-.09	.01
17.2	2.75	.05	-.18	.03	1.00	.02	.10	.03
17.6	2.73	.03	.10	.03	1.00	.03	.01	.02
18.0	2.72	.04	.30	.03	.95	.03	-.08	.03
18.4	2.65	.05	.38	.04	.95	.03	-.18	.03
18.8	2.56	.05	.37	.03	1.01	.02	-.21	.04
19.2	2.42	.06	.30	.06	1.15	.04	-.18	.04

TABLE IV
SAMPLE: PLEXIGLAS

TIME DOMAIN SYSTEM
THICKNESS = 64.5 MILS

FREQUENCY DOMAIN SYSTEM
THICKNESS = 65.5 MILS

<u>FREQUENCY (GHz)</u>	<u>EPSILON</u>	<u>MU</u>	<u>FREQUENCY (GHz)</u>	<u>EPSILON</u>	<u>MU</u>
12.4	2.47+J.04	.93-J.02	12.4	2.71+J.11	.94+J.03
12.8	2.44+J.03	1.02-J.05	12.8	2.63+J.21	.96-J.07
13.2	2.43+J.00	1.05-J.09	13.2	2.60+J.26	.94-J.09
13.6	2.47+J.06	1.09-J.10	13.6	2.53+J.19	1.01-J.06
14.0	2.64+J.06	1.07-J.04	14.0	2.45+J.05	1.10-J.04
14.4	2.69+J.14	1.07-J.02	14.4	2.47-J.06	1.12+J.01
14.8	2.69+J.14	1.06+J.02	14.8	2.53+J.07	1.15+J.00
15.2	2.69+J.24	1.10+J.03	15.2	2.60+J.17	1.13+J.03
15.6	2.58+J.17	1.08+J.07	15.6	2.51+J.32	1.05-J.04
16.0	2.52+J.28	1.15+J.05	16.0	2.38+J.29	1.03-J.13

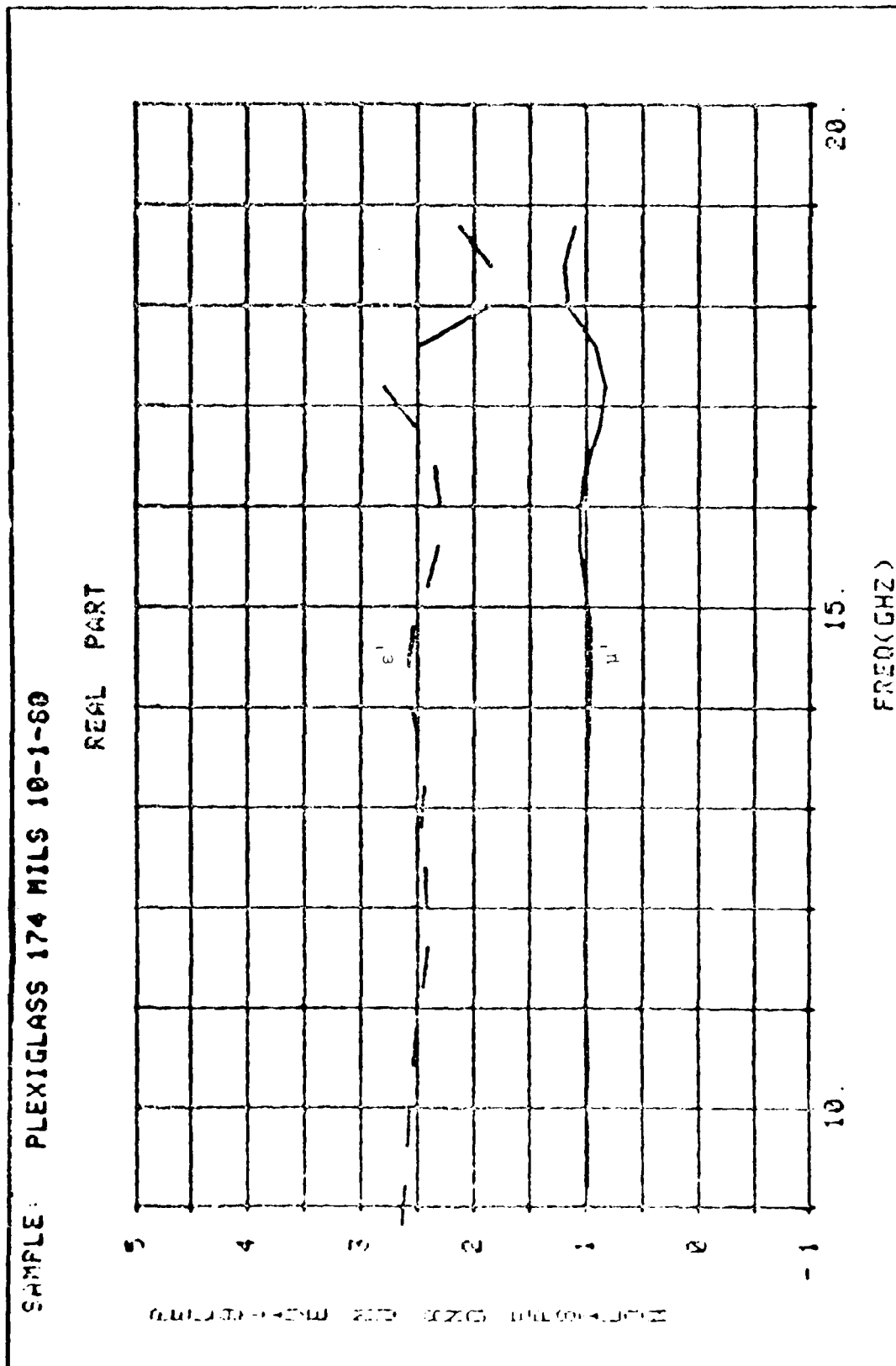


Figure 17A. Time Domain (Real) Data for 174 mil Plexiglas Sample

SAMPLE: PLEXIGLAS 174 MILS 10-1-80

IMAG PART

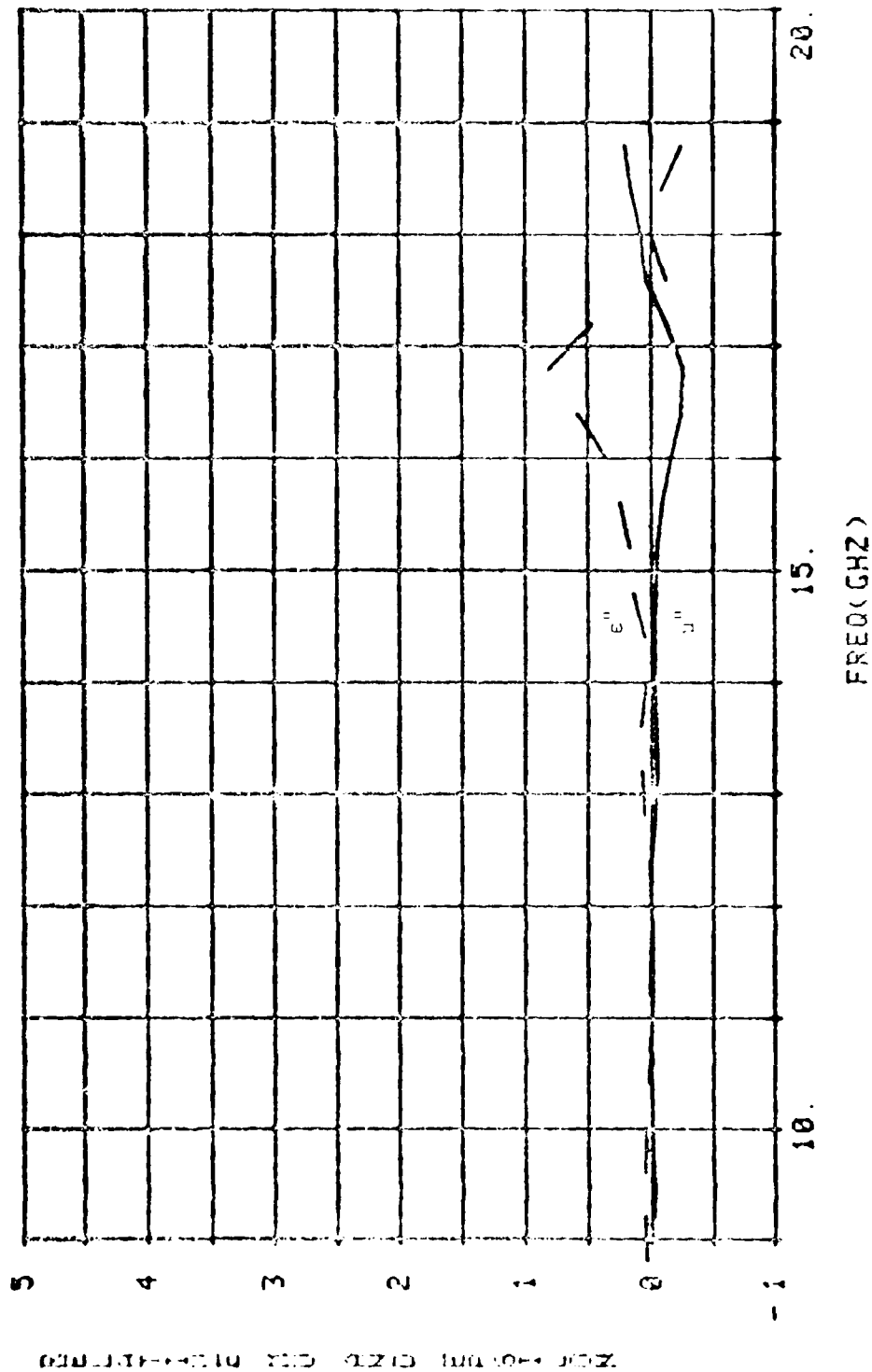


Figure 113. Time Domain (Imaginary) Data for 174 mil Plexiglas Sample

SAMPLE: #3: PLEXIGLAS THICKNESS = 174 MILS.

REAL PART

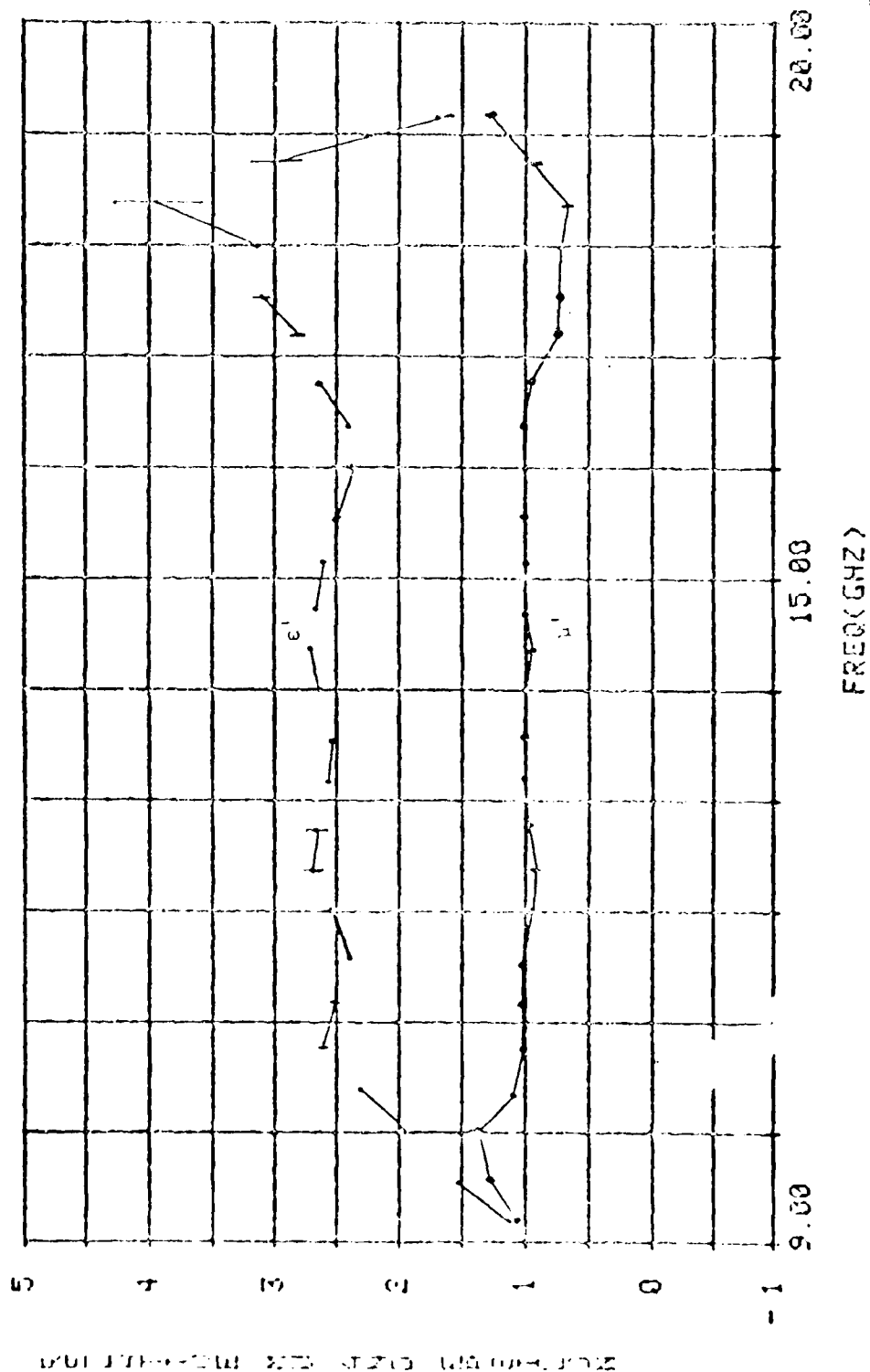


Figure 12A. Frequency Domain (Real) Data for 174 mil Plexiglas Sample

SAMPLE: 03: PLEXIGLAS THICKNESS = 174 MILS.

IMAG PART

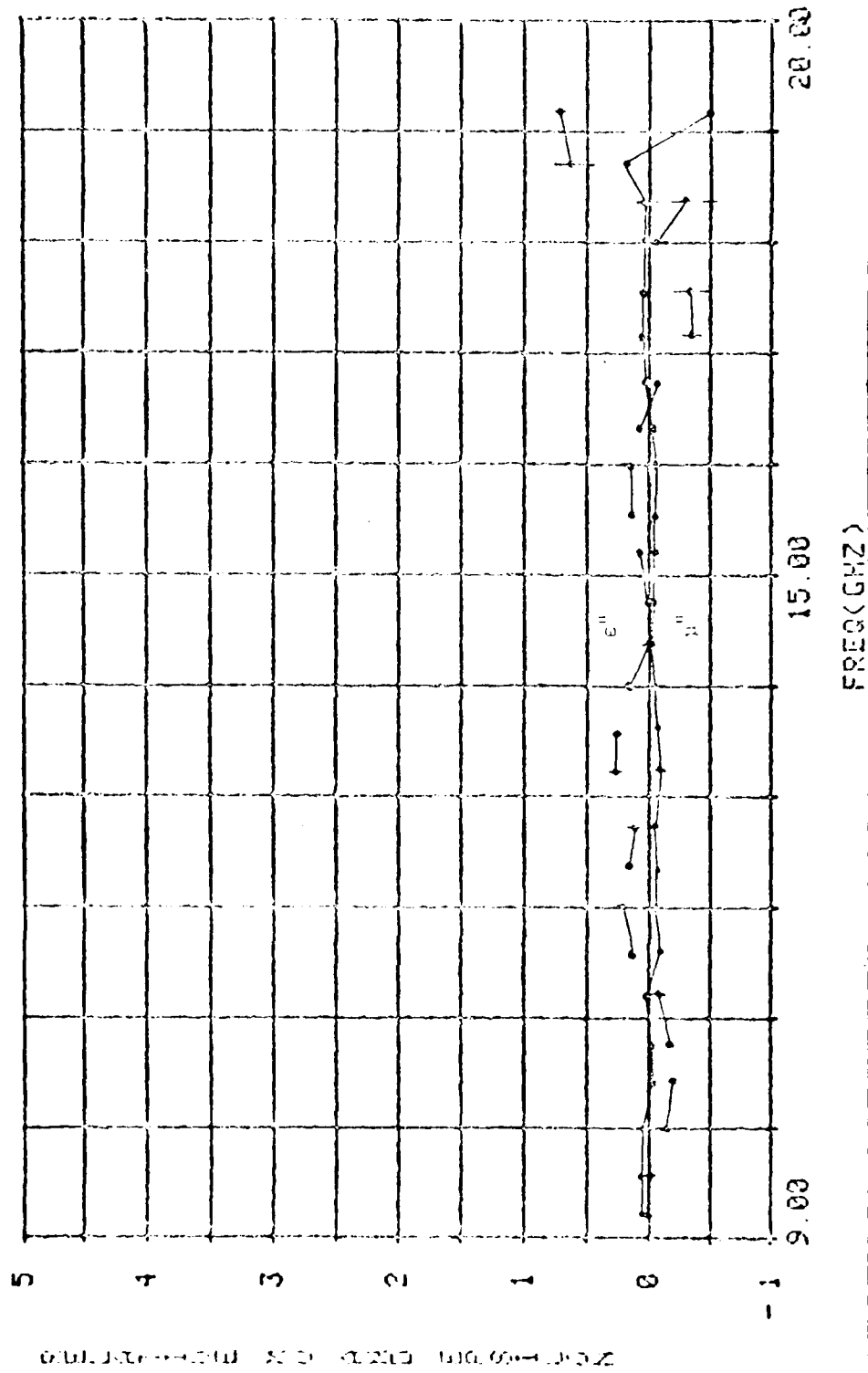


Figure 128. Frequency Domain (Imaginary) Data for 174 mil Plexiglas Sample

TABLE V

SAMPLE: PLEXIGLAS

FREQUENCY DOMAIN DATA

THICKNESS = .174 MILS

FREQUENCY (GHz)	ϵ'	S	ϵ''	S	μ'	S	μ''
9.2	1.12	.03	.01	.04	1.09	.03	.06
9.6	1.52	.05	-.00	.07	1.29	.05	.05
10.0	1.95	.07	-.13	.09	1.38	.07	.03
10.4	2.39	.03	-.21	.04	1.13	.02	-.08
10.8	2.60	.04	-.11	.04	1.00	.01	-.01
11.2	2.51	.07	-.08	.05	1.02	.02	.01
11.6	2.45	.04	.21	.04	1.04	.03	-.10
12.0	2.54	.07	.25	.05	.94	.03	-.07
12.4	2.71	.10	.21	.07	.91	.01	-.07
12.8	2.69	.10	.15	.07	.95	.01	-.07
13.2	2.57	.05	.30	.06	1.01	.01	-.10
13.6	2.56	.04	.32	.05	1.01	.02	-.07
14.0	2.64	.03	.25	.04	1.01	.01	-.04
14.4	2.76	.03	.01	.05	.95	.01	-.00
14.8	2.72	.04	.06	.03	.98	.01	-.03
15.2	2.60	.03	.10	.02	1.00	.01	-.04
15.6	2.51	.03	.20	.04	1.03	.01	-.06
16.0	2.39	.04	.17	.05	1.07	.01	-.06
16.4	2.44	.04	.16	.04	1.05	.02	-.02
16.8	2.68	.04	-.08	.04	.96	.01	.05
17.2	2.83	.08	-.38	.08	.88	.01	.10
17.6	3.14	.08	-.37	.09	.83	.02	.06
18.0	3.19	.10	-.07	.07	.84	.03	-.00
18.4	3.94	.39	-.31	.26	.72	.04	.02
18.8	2.96	.24	.66	.11	.90	.04	-.19
19.2	1.63	.07	.77	.06	1.31	.04	-.53

TABLE VI

SAMPLE: PLEXIGLAS

TIME DOMAIN SYSTEM

FREQUENCY DOMAIN SYSTEM

THICKNESS = 174 MILS

THICKNESS = 174 MILS

<u>FREQUENCY (GHz)</u>	<u>EPSILON</u>	<u>MU</u>	<u>FREQUENCY (GHz)</u>	<u>EPSILON</u>	<u>MU</u>
12.4	2.43+J.01	1.00+J.00	12.4	2.71+J.21	.91-J.07
12.8	2.46+J.03	.99-J.03	12.8	2.69+J.15	.95-J.07
13.2	2.44+J.04	.99-J.05	13.2	2.57+J.30	1.01-J.10
13.6	2.49+J.08	.98-J.04	13.6	2.56+J.32	1.01-J.07
14.0	2.55+J.04	.97-J.03	14.0	2.64+J.25	1.01-J.04
14.4	2.53+J.05	.96-J.03	14.4	2.76+J.01	.95-J.00
14.8	2.54+J.14	.96-J.04	14.8	2.72+J.06	.99-J.03
15.2	2.41+J.17	1.01-J.05	15.2	2.63+J.10	1.00-J.04
15.6	2.32+J.25	1.06-J.09	15.6	2.81+J.20	1.03-J.06
16.0	2.30+J.35	1.05-J.16	16.0	2.39+J.17	1.07-J.06

Teflon Sample

The time domain data for the teflon sample are given in Figure 13A and 13B. The plot of the time domain data is for a single measurement run. The frequency domain data for the teflon sample is presented graphically in Figure 14A and 14B. The frequency domain data plots are for a single measurement run. A complete listing of the frequency domain data is given in Table VII. The comparison of time and frequency domain data is presented in Table VIII for the frequency range from 12.4 to 16 GHz.

FCM-40 Absorber Sample

The FCM-40 absorber is composed of ferrites in silicon rubber. It is an Eccosorb high-loss microwave absorber. The relative μ and epsilon values calculated for the FCM-40 absorber on the time domain system are presented graphically in Figure 15A and 15B. The frequency domain data of relative μ and epsilon are graphically presented in Figure 16A and 16B. Both the time domain and frequency domain plots are for a single measurement run. The complete listing of relative μ and epsilon values measured with the frequency domain system is given in Table IX. The comparison for the time domain and frequency domain data from 12.4 to 16 GHz is given in Table X.

Comparison of time and frequency domain data points up a problem in the frequency domain data. Although the permeability follows a similar trend as that from the time domain, it is seen that the real part of the permittivity was approximately 25% below the values

SAMPLE: TEFLON NDS GEN 181 SCOPE 100-00

REAL PART

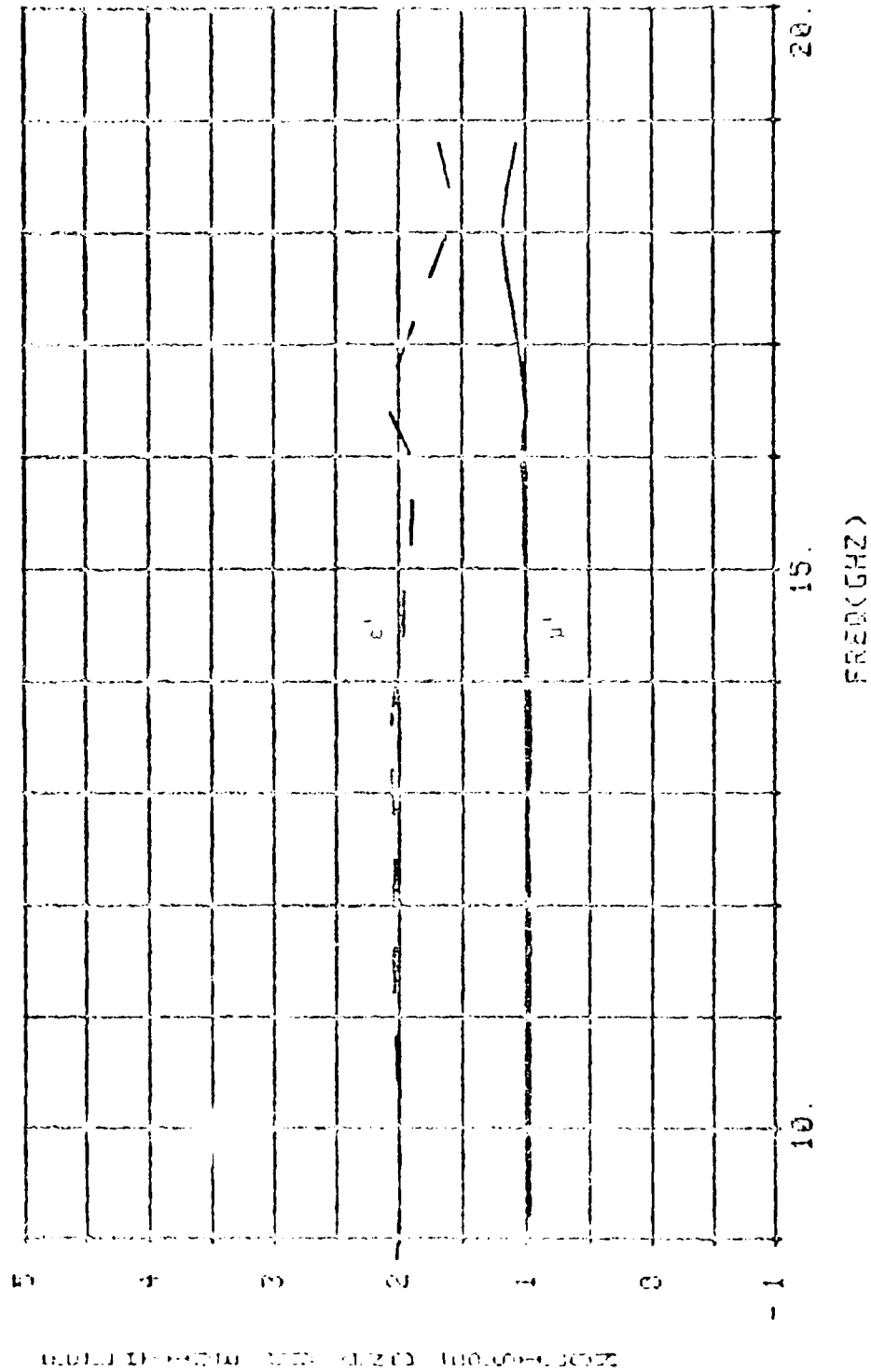


Figure 13A. Time Domain (Real) Data for 181 mil Teflon Sample

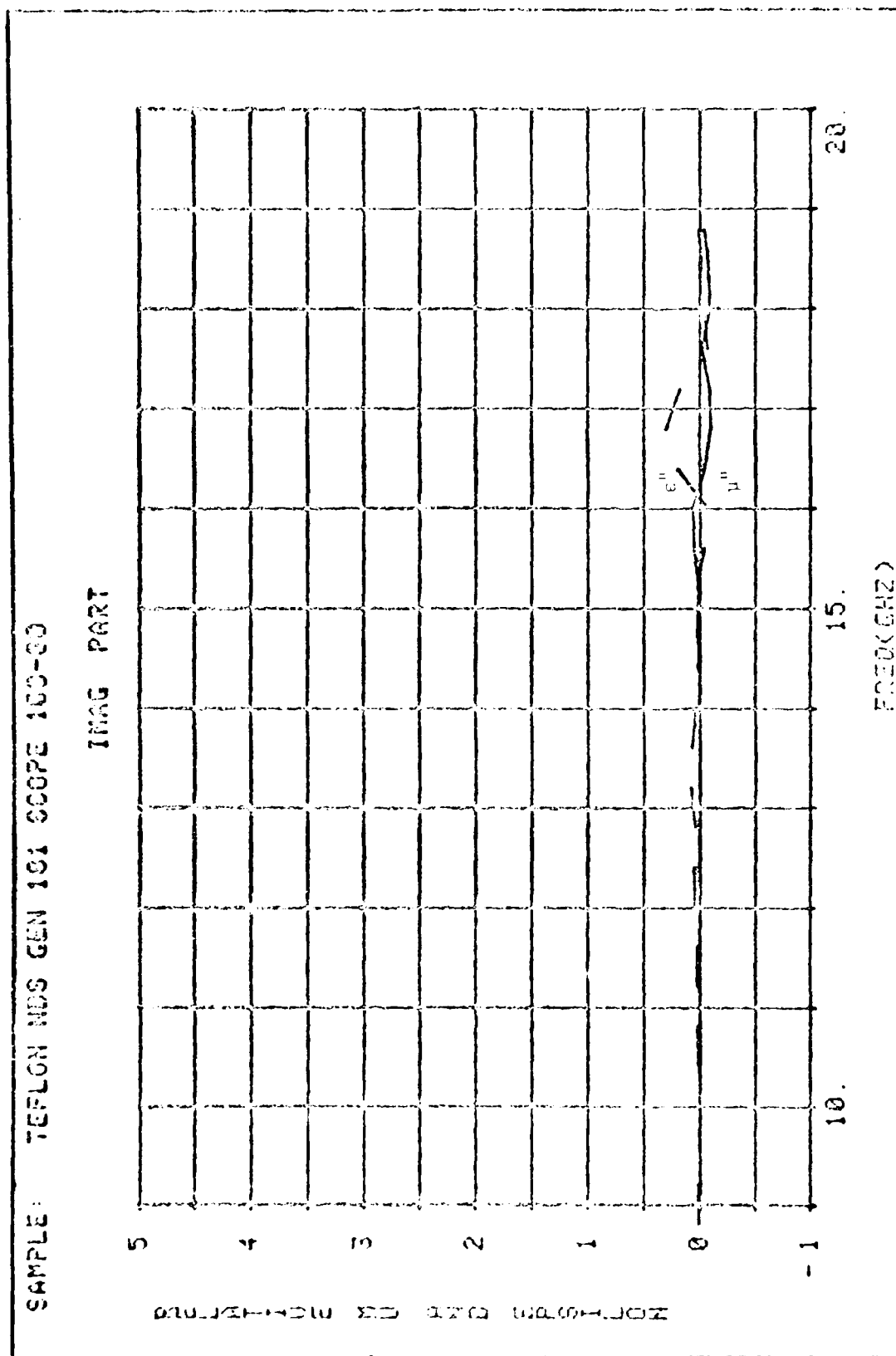


Figure 136. Time Domain (Imaginary) Data for 181 mil Teflon Sample

SAMPLE: TEFLON THICKNESS = 160 MILS INOV80 NORM.

REAL PART

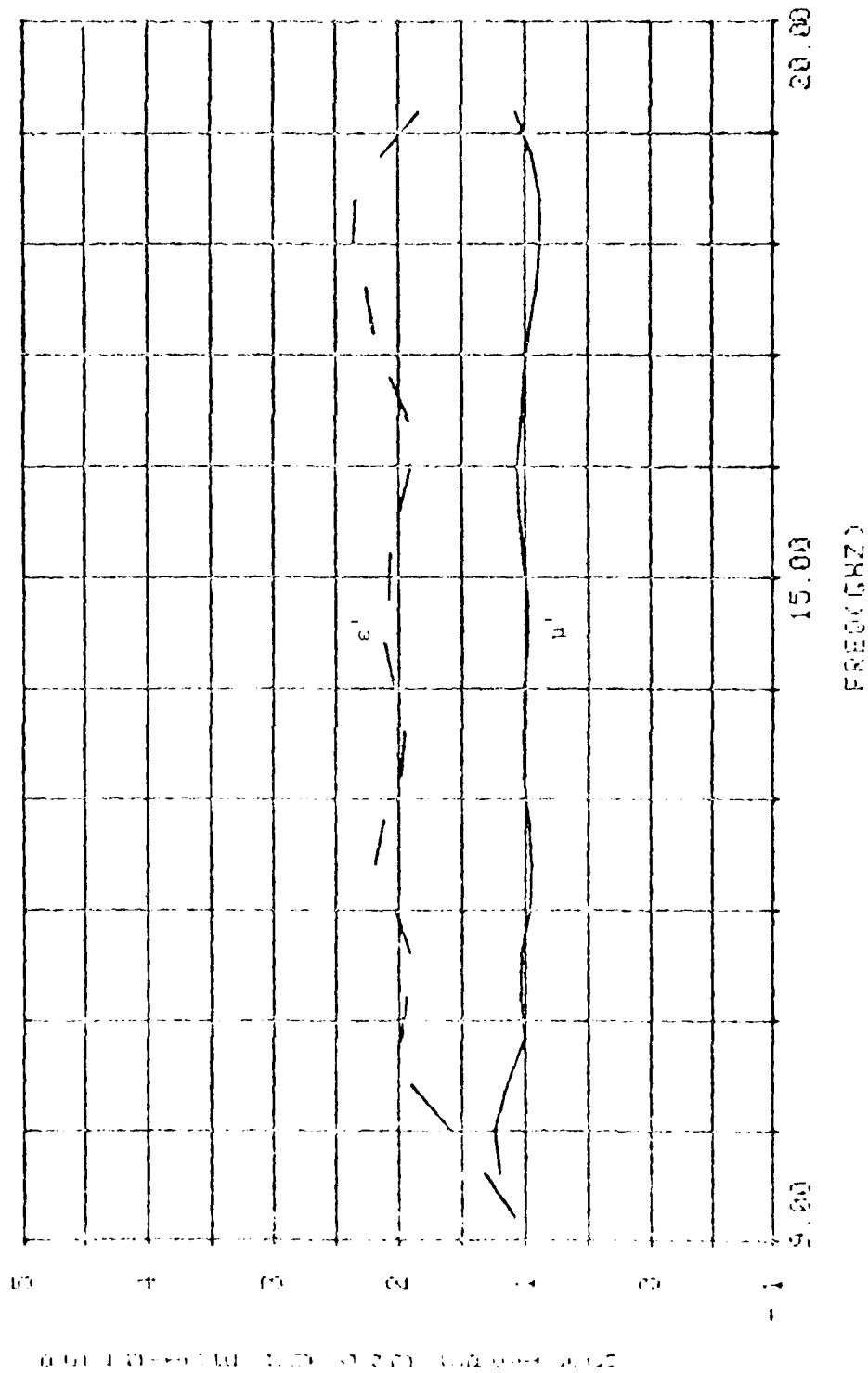


Figure 14A. Frequency Domain (Real) Data for 160 mil Teflon Sample

SAMPLE: TEFLON THICKNESS = 180 MILS 1N0U80 NORM.

INAG PART

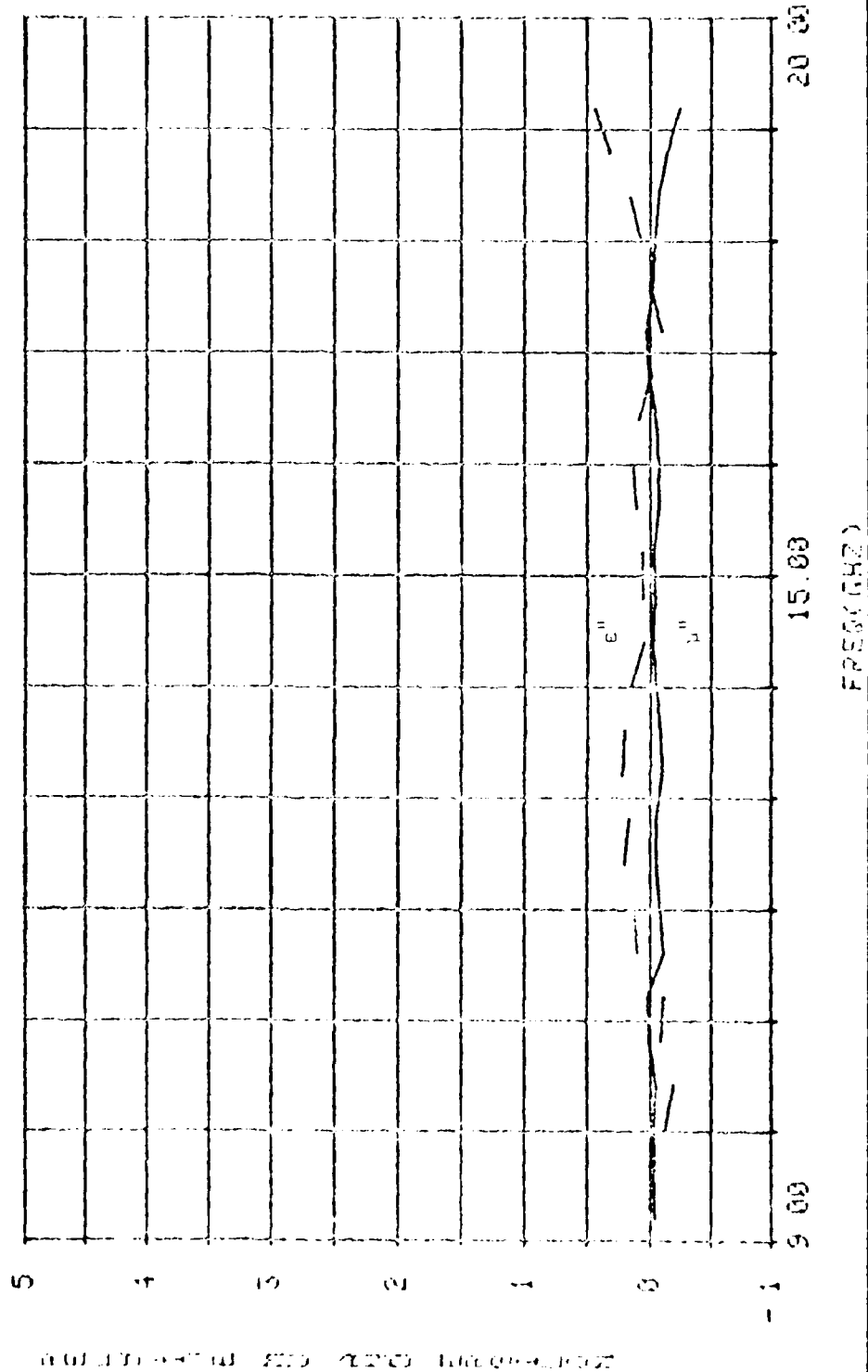


Figure 143. Frequency Domain (Imaginary) Data for 180 mil Teflon Sample

TABLE VII

SAMPLE: TEFLON

FREQUENCY DOMAIN DATA

THICKNESS = 160 MILS

<u>FREQUENCY (GHz)</u>	<u>EPSILON</u>	<u>MU</u>
9.2	1.08-J.04	1.05+J.01
9.6	1.32-J.03	1.20-J.04
10.0	1.59-J.12	1.24-J.03
10.4	1.90-J.19	1.14-J.05
10.8	1.98-J.09	1.01+J.01
11.2	1.94-J.11	1.04+J.02
11.6	1.91+J.10	1.03-J.11
12.0	2.03+J.13	.96-J.08
12.4	2.19+J.21	.95-J.05
12.8	2.12+J.17	.97-J.05
13.2	1.98+J.22	1.01-J.10
13.6	1.95+J.21	1.01-J.08
14.0	2.04+J.16	1.01-J.05
14.4	2.11+J.05	.98-J.02
14.8	2.08+J.06	.98-J.04
15.2	2.07+J.06	1.02-5.03
15.6	1.99+J.11	1.05-J.07
16.0	1.90+J.14	1.06-J.07
16.4	1.92+J.09	1.03-J.05
16.8	2.07-J.01	1.01+J.01
17.2	2.20-J.10	.97+J.03
17.6	2.26+J.00	.01-J.02
18.0	2.36+J.07	.88-J.04
18.4	2.34+J.16	.98-J.07
18.8	2.14+5.32	.94-J.14
19.2	1.84+J.44	1.07-J.24

TABLE VIII

SAMPLE: TEFLON

FREQUENCY DOMAIN SYSTEM

THICKNESS = 180 MILS

TIME DOMAIN SYSTEM

THICKNESS = 181 MILS

<u>FREQUENCY (GHz)</u>	<u>EPSILON</u>	<u>MU</u>	<u>FREQUENCY (GHz)</u>	<u>EPSILON</u>	<u>MU</u>
12.4	2.03+J.05	.98+J.00	12.4	2.19+J.21	.95-J.05
12.8	2.04+J.04	.99+J.00	12.8	2.12+J.17	.97-J.05
13.2	2.05+J.08	.97+J.00	13.2	1.98+J.22	1.01-J.10
13.6	2.06+J.07	.97+J.00	13.6	1.95+J.21	1.01-J.06
14.0	2.02+J.03	.98+J.00	14.0	2.04+J.16	1.01-J.05
14.4	1.96+J.01	1.00+J.00	14.4	2.11+J.05	.98-J.02
14.8	1.96+J.00	.99+J.02	14.8	2.08+J.06	.98-J.04
15.2	1.93+J.02	1.01+J.01	15.2	2.07+J.06	1.02-J.03
15.6	1.89-J.04	1.00+J.05	15.6	1.99+J.11	1.05-J.07
16.0	1.90-J.07	1.03+J.06	16.0	1.90+J.14	1.06-J.07

FGM-40 (37 mils) 30 Jan 76 209/JK

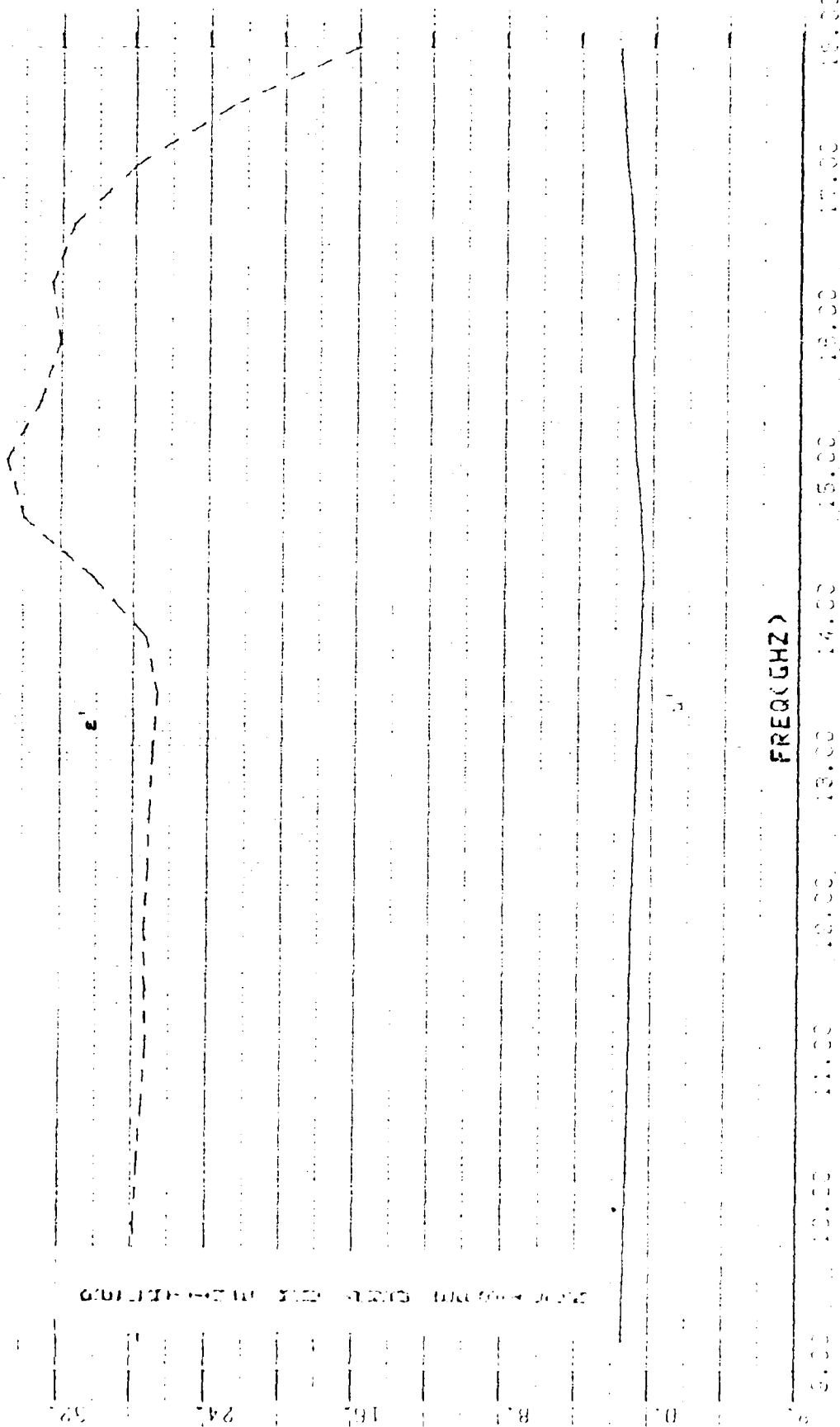
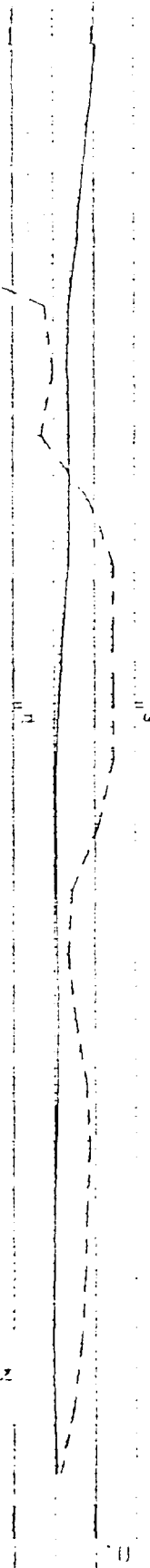


Figure 15A. Time Domain (Real) Data for 37 mil FGM-40 Sample

FGM-40 (37 mils) 30 Jan 76 209/JK

TIME (SECONDS) 0.00 1.00 2.00 3.00 4.00 5.00 6.00 7.00 8.00 9.00 10.00 11.00 12.00 13.00 14.00 15.00 16.00 17.00 18.00 19.00 20.00 21.00 22.00 23.00 24.00 25.00 26.00 27.00 28.00 29.00 30.00 31.00 32.00 33.00 34.00 35.00 36.00 37.00 38.00 39.00 40.00 41.00 42.00 43.00 44.00 45.00 46.00 47.00 48.00 49.00 50.00 51.00 52.00 53.00 54.00 55.00 56.00 57.00 58.00 59.00 60.00 61.00 62.00 63.00 64.00 65.00 66.00 67.00 68.00 69.00 70.00 71.00 72.00 73.00 74.00 75.00 76.00 77.00 78.00 79.00 80.00 81.00 82.00 83.00 84.00 85.00 86.00 87.00 88.00 89.00 90.00 91.00 92.00 93.00 94.00 95.00 96.00 97.00 98.00 99.00 100.00



FREQ(GHZ)

9.00 10.00 11.00 12.00 13.00 14.00 15.00 16.00 17.00 18.00 19.00

Figure 155. Time Domain (Imaginary) Data for 37 mil FGM-40 Sample

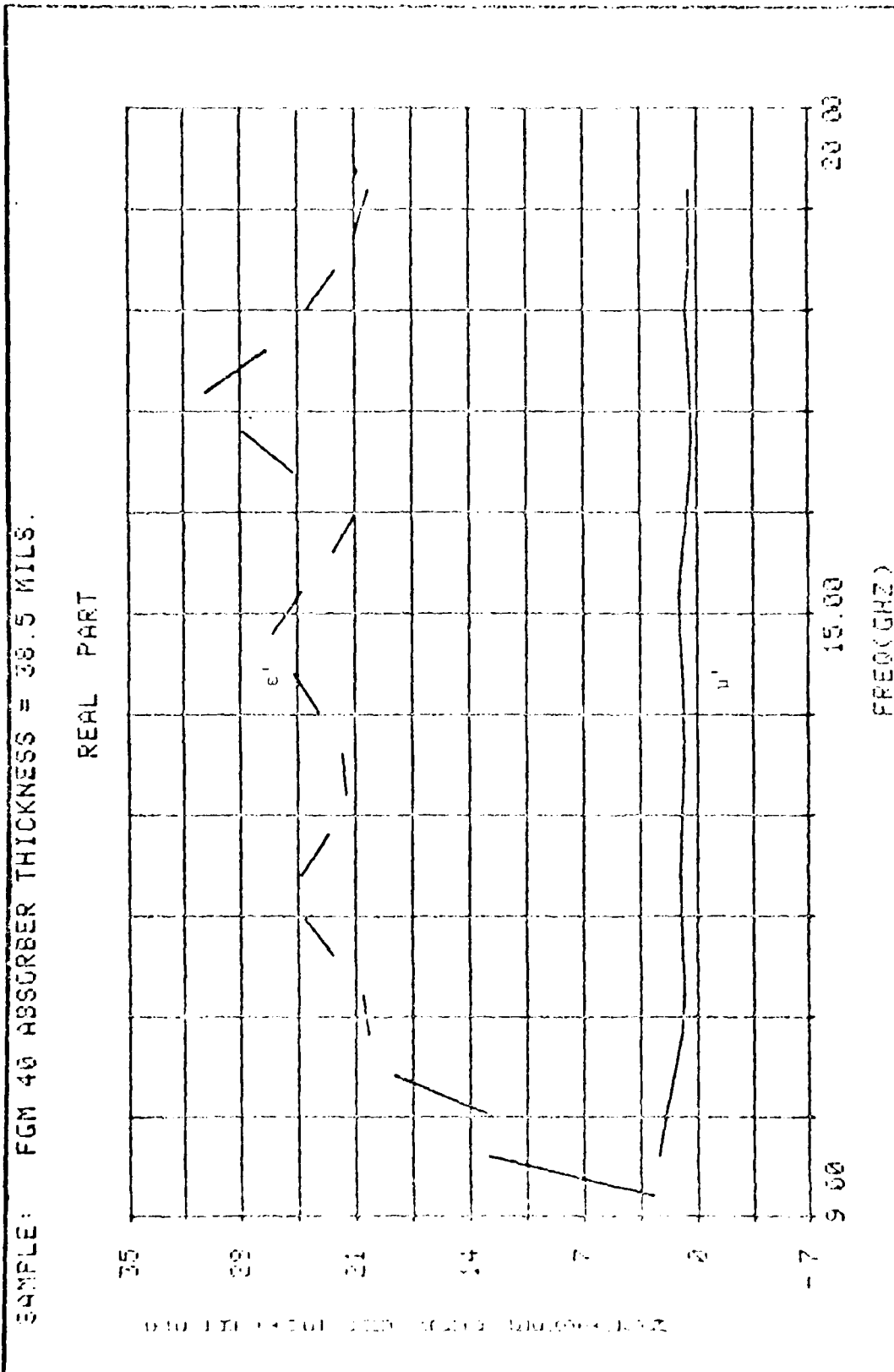


Figure 10A. Frequency Domain (Real) data for 38.5 mil FGM-40 Sample

SAMPLE: FGM 40 ABSORBER THICKNESS = 38.5 MILS.

IMAG PART

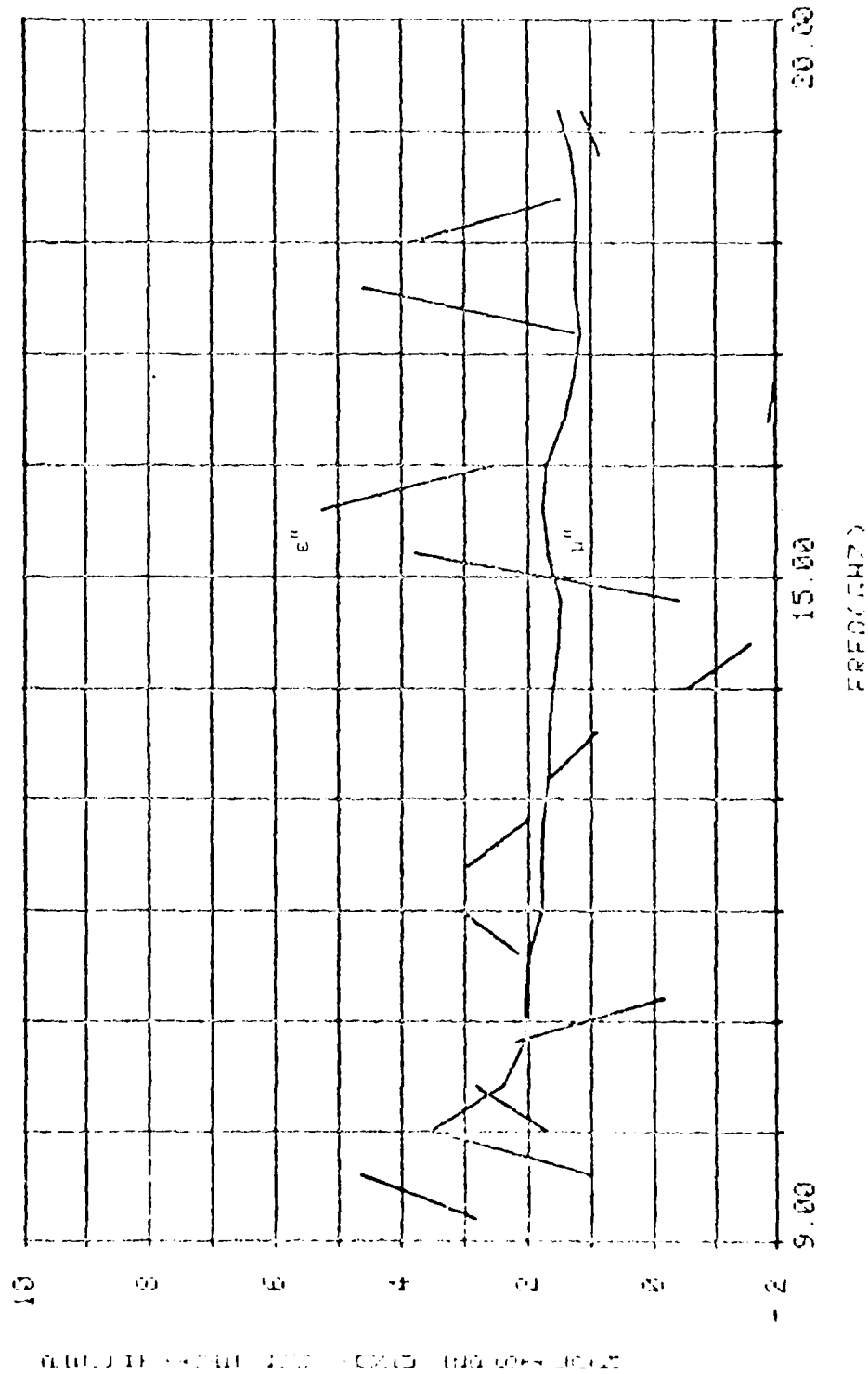


Figure 160. Frequency Domain (Imaginary) Data for 38.5 mil FGM-40 Sample

TABLE IX

SAMPLE: FGM-40 ABSORBER

FREQUENCY DOMAIN DATA

THICKNESS = 38.5 MILS

<u>FREQUENCY (GHz)</u>	<u>EPSILON</u>	<u>MU</u>
9.2	2.78+J2.83	1.42-J.57
9.6	12.87+J4.64	2.43+J.98
10.0	12.73+J1.71	2.02+J3.53
10.4	18.63+J2.21	1.47+J2.40
10.8	20.27+J2.21	1.02+J2.06
11.2	20.57-J.15	.85+J2.05
11.6	22.38+J2.17	.91+J1.98
12.0	24.26+J3.07	1.00+J1.78
12.4	24.29+J2.95	1.07+J1.79
12.8	22.64+J2.02	1.03+J1.77
13.2	21.60+J1.63	.96+J1.69
13.6	21.77+J.93	.84+J1.67
14.0	23.15-J.54	.90+J1.52
14.4	24.76-J1.57	.91+J1.52
14.8	26.07-J.39	1.10+J1.48
15.2	24.34+J3.78	1.17+J1.68
15.6	22.34+J5.27	.94+J1.77
16.0	20.99+J2.55	.65+J1.71
16.4	24.83-J1.88	.48+J1.43
16.8	27.81-J2.77	.35+J1.27
17.2	30.15+J1.26	.44+J1.17
17.6	26.52+J4.60	.62+J1.24
18.0	24.03+J3.91	.71+J1.24
18.4	22.23+J1.48	.52+J1.22
18.8	20.94+J.87	.49+J1.31
19.2	20.17+J1.14	.54+J1.51

TABLE X

SAMPLE: FGM-40 ABSORBER

FREQUENCY DOMAIN SYSTEM

THICKNESS = 38.5 MILS

TIME DOMAIN SYSTEM

THICKNESS = 37.0 MILS

<u>FREQUENCY (GHz)</u>	<u>EPSILON</u>	<u>MU</u>	<u>FREQUENCY (GHz)</u>	<u>EPSILON</u>	<u>MU</u>
12.4	27.20+J1.20	1.00+J1.24	12.4	24.29+J2.95	1.07+J1.79
12.8	27.20+J1.20	.80+J1.92	12.8	22.64+J2.02	1.03+J1.77
13.2	27.20+J0.20	.80+J2.00	13.2	21.60+J1.63	.98+J1.69
13.6	26.72+J0.88	.80+J1.92	13.6	21.77+J0.93	.99+J1.67
14.0	27.20+J0.88	.60+J1.68	14.0	23.15+J0.54	.97+J1.61
14.4	36.20+J0.38	.40+J1.60	14.4	24.76+J1.54	.97+J1.52
14.8	34.00+J0.88	.72+J1.20	14.8	26.07+J0.39	1.10+J1.48
15.2	34.00+J0.40	.96+J1.20	15.2	24.34+J3.78	1.17+J1.68
15.6	33.20+J2.60	1.20+J2.72	15.6	22.34+J5.27	.94+J1.77
16.0	32.00+J2.00	1.20+J2.00	16.0	20.99+J2.55	.65+J1.71

measured on the time domain and the imaginary part of the permittivity from the frequency domain measurement could not be compared. During tests of the placement of the sample relative to the shorting plate, it was seen that the imaginary permittivity parameter was very sensitive to position within the sample holder. Also, the 10M-40 sample was seen to deform slightly when it was inserted into the sample window. This effect could not occur on the other harder samples of plexiglas, fiberglass and teflon. These factors may give a clue to the poor comparison of data for this sample. Unfortunately, time did not permit extensive investigation in this area.

VI. Conclusions and Recommendations

Conclusions

A frequency domain measurement system was developed. The intrinsic properties of fiberglass, two thicknesses of plexiglas, teflon, and an IGM-40 absorber were measured on the frequency domain and time domain systems and compared. On the basis of the results obtained from the frequency domain system, the following conclusions are drawn:

1. The feasibility of measuring intrinsic properties of materials using a frequency domain technique has been shown.
2. Repeatability was investigated for the two thicknesses of plexiglas and fiberglass. Repeatability of measurement was extremely good in the case of the two thicknesses of plexiglass, but began to show a problem in the imaginary part of the permittivity of fiberglass.
3. The comparison of data between the time domain and frequency domain system was good for the plexiglas and teflon. The fiberglass data began to show some error, especially in the area of the imaginary permittivity.
4. The greatest error was seen when measuring the IGM-40 absorber. Although the permeability compared well for both the time domain and frequency domain data, the real part of the permittivity was approximately 25% below that of the time domain and the imaginary

AD-A100 764

AIR FORCE INST OF TECH WRIGHT-PATTERSON AFB OH SCHOO--ETC F/G 20/3
FREQUENCY DOMAIN MEASUREMENTS OF MICROWAVE ABSORBER DESIGN MATE--ETC(U)
DEC 80 D 6 AGUIRRE
AFIT/GE/EE/80D-8

UNCLASSIFIED

NL

2 OF 2
AD A
100784

END
DATE
FILMED
7-81
DTIC

part of the permittivity was not comparable.

5. The refinement of the sample holder and slider section may result in smaller errors than those seen in this study. This observation is drawn from experience gained during trouble-shooting problems in the sample holder area.

6. A possible cause of error in the frequency domain data of the FGM-40 absorber material may have been distortion of the sample during insertion into the sample window. Unlike the other materials tested, the FGM-40 absorber was rubbery and easily compressed.

Recommendations

Based on the assumptions stated initially and observations made during the investigation, the following recommendations are proposed for further study:

1. The high VSWR, which ranged up to 10 at 18 GHz, at the test and reference ports of the frequency converter, could be investigated as a source of error.

2. The sensitivity of reflection coefficients to the reference shorting plate and sample position within the sample holder could be investigated.

3. A computer model could be developed to investigate the H-plane sectoral horn plane wave approximations to TEM waves used in

this thesis and how this approximation relates to the samples' intrinsic property measurements.

4. A system characteristic was used to renormalize the relative μ and ϵ values. An investigation could be done to determine if a better technique were possible for removing inherent system error.

Bibliography

1. Allen, J., et al. A Technology Plan for Electromagnetic Characteristics of Advanced Composition. New York: Rome Air Development Center, Air Force Systems Command, Griffiss Air Force Base (July 1976). (RADC-TR-76-206)
2. Barrow, W. L., L. J. Chu. "Theory of Electromagnetic Horn," Proceedings IRE, Vol. 27, pp 51-64 (1939).
3. Crispin, J. W., Jr. et al. Methods of Radar Cross Section Analysis. New York: Academic Press (1968).
4. Hayt, William H., Jr. Engineering Electromagnetics (Third Edition). New York: McGraw Hill Book Company (1974).
5. Hippel, Arthur R. von, ed. Dielectric Materials and Applications. New York: John Wiley and Sons, Inc. (1958).
6. Jasik, Henry, ed. Antenna Engineering Handbook. New York: McGraw Hill Book Company, pp 10-8, 10-9 (1961).
7. Kent, Brian M. Time Domain Measurements of Microwave Absorbers with Real Time Processing. Technical Memorandum. Wright-Patterson Air Force Base, Ohio: Air Force Avionics Laboratory (March 1979) (AFAL-TM-79-3-WP).
8. Kraus, John D. Electromagnetics. New York: McGraw Hill Book Company (1953).
9. Nahman, N. S., et al. Radar Absorber Measurement Techniques at Frequencies Above 20 GHz. Boulder, Colorado: National Bureau of Standards (August 1979) (NBSIR 79-1613).
10. Nicolson, A. M., et al. "Measurement of the Intrinsic Properties of Materials by Time Domain Techniques." IEEE Transactions on Instrumentation and Measurement, IM-19: pp 377-382 (November 1970).
11. Nicolson, A. M. Time Domain Measurement of Microwave Absorbers. Technical Report AFAL-TR-71-33. Sperry Rand Research Center, Sudbury, Massachusetts. (February 1971) (AD 884306).
12. Nicolson, A. M., et al. Time Domain Measurement of Microwave Absorbers, 9-16 GHz Frequency Band. Technical Report AFAL-TR-73-435. Sperry Rand Research Center, Sudbury, Massachusetts (April 1974) (AD 779815).
13. Ramo, Simon, et al. Fields and Waves in Communication Electronics. New York: John Wiley and Sons, Inc., 1965.
14. Fuck, George T., et al. Radar Cross Section Handbook. New York: Plenum Press (1970).

Appendix A

Control Software

The operating system controls the Hewlett-Packard network analyzer and Watkins and Johnson frequency synthesizer during parameter measurements. The software and system relationship is diagrammed below.

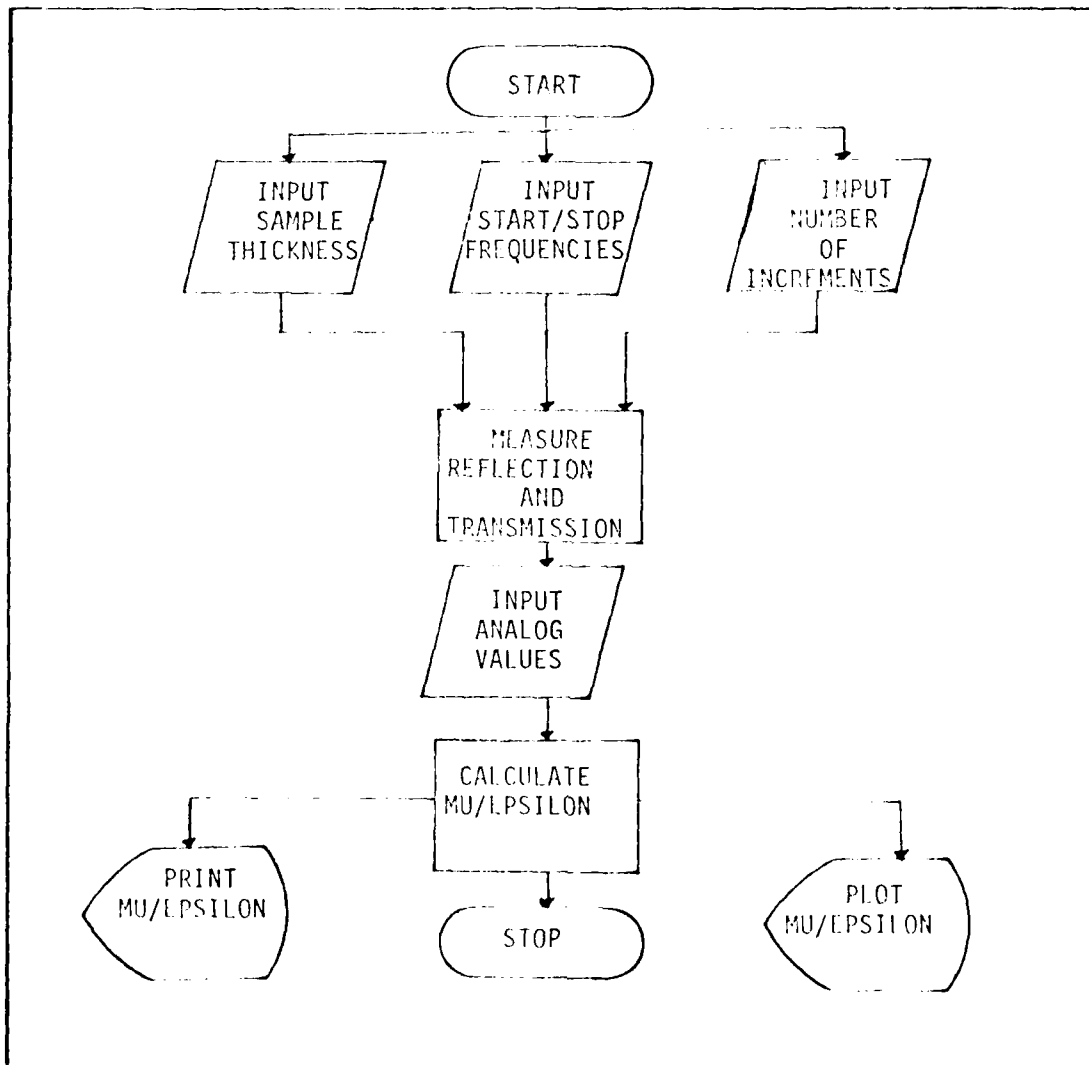


Figure 17. Software Control Diagram

ETN4
C39
ETN4

```

PROGRAM CPLN3
DIMENSION IPRER(120), IEPER(120), IEPI(120), MUR(120), MUI(
120), RMOD(120), RPHA(120), TMOO(120), TPHA(120), LU(5), IMD
2(32), INAME(3), IDATA(1024), J1(120), J2(120), J3(120), J4(120)

```

EXECUTABLE STATEMENTS FOLLOW

ZERO PRINCIPLE ARRAYS

```

CALL RMPAR(LU)
IMPER(1)=2HNUJ
IMHNER(2)=2HSE
IMHNER(3)=1HT
RES=PRER(9, INAME, 1)
DO 200 I=1, 120
  IPRER(I)=0.
  IEPER(I)=0.
  IEPI(I)=0.
  MUR(I)=0.
  MUI(I)=0.
  RMOD(I)=0.
  RPHA(I)=0.
  TMOO(I)=0.
  TPHA(I)=0.
200 CONTINUE

```

READ IN SAMPLE NAME AND THICKNESS

```

WRITE(LU, 10)
READ (LU, 11) (IMD(I), I=1, 32)

```

000

L73

```

      READ (LU,11) (IWD(I),I=1,32)
11  FORMAT (32A2)
18  FORMAT ("INPUT COMMENT ABOUT SAMPLE AND PRESS RETURN.")
28  WRITE (LU,28)
28  FORMAT ("PLEASE ENTER SAMPLE THICKNESS IN MILS AND PRESS RETURN.")

```

READ (LU,*) THT

00000

ESTABLISH START AND END FREQ AND NUMBER
OF STEP INCREMENTS.

```

4  WRITE (LU,4)
4  FORMAT ("INPUT BEGINNING FREQ IN GHZ AND PRESS RETURN.")
5  READ (LU,*) XMIN
5  WRITE (LU,5)
5  FORMAT ("INPUT END FREQUENCY IN GHZ AND PRESS RETURN.")
6  READ (LU,*) XMAX
6  WRITE (LU,6)
6  FORMAT ("INPUT NUMBER OF FREQUENCY STEPS DESIRED.")
7  READ (LU,*) N
7  WRITE (LU,*) N
7  DELF=(XMAX-XMIN)/(N-1)

```

0000

INITIAL COMMANDS FOR SYSTEM CONTROL

```

7  WRITE (LU,30)
30  FORMAT ("MEASUREMENT/OUTPUT COMMANDS",//,"Q=END",//
1  "I=REFLECTION MEASUREMENTS",//,"2=TRANSMISSION MEASUREMENTS",//,
2  "3=MU,EP CALCULATION",//
3  "4=LINE PRINT OF MU,EP DATA",//,"5=PLOT OF MU,EP DATA")
4  READ (LU,*) NCW
4  NENDW+1

```


130

```

N=NCH+1
GO TO (100,110,120,130,140,150),N
100 WRITE(LU,40)
140 FORMAT("PROGRAM COMPLEX END")
INAME(1)=CHND
INAME(2)=CHSE
INAME(3)=IHT
REGEXEC(9,INAME,0)
STOP
110 CALL REFL(LU,RMOD,RPHA,M,XMIN,DELF)
WRITE(LU,50)
50 FORMAT("REFLECTION MEASUREMENT COMPLETED.")
GO TO 7
120 CALL TRANS(LU,TMOD,TPHA,M,XMIN,DELF)
WRITE(LU,60)
60 FORMAT("TRANSMISSION MEASUREMENT COMPLETED.")
GO TO 7
130 CONTINUE
CHK=200
IF (KY.EQ.0) THK=THT
CALL CDATA(LU,RMOD,RPHA,TMOD,TPHA,IEPR,IEPI,MUR,MUI,
1 THK,XMIN,DELF,M,IFREQ)
IF (KY.EQ.0) GO TO 65
200=0
DO 61 I=1,M
J1(I)=IEPR(I)
J2(I)=IEPI(I)
J3(I)=MUR(I)
J4(I)=MUI(I)
61 CONTINUE
WRITE(LU,62)

```

L30

```

625 WRITE (LU,62)
635 FORMAT ("THE CHARACTERISTIC OF THE SYSTEM HAS BEEN RECORDED.")
640 CONTINUE
650 WRITE (LU,600)
655 FORMAT ("ENTER '99' TO NORMALIZE DATA.")
660 READ (LU,*) RN
665 IF (RN.EQ.99) GO TO 665
670 RN = 1.0
675 IF (RN.EQ.1.0) THEN
680   IEPR(I) = IEPR(I)/100.
685   IEPI(I) = IEPI(I)/100.
690   MUR(I) = MUR(I)/100.
695   MU(I) = MU(I)/100.
700   J1(I) = J1(I)/100.
705   J2(I) = J2(I)/100.
710   J3(I) = J3(I)/100.
715   J4(I) = J4(I)/100.
720   CPLEX = CPLEX/100.
725   CPLEX = CPLEX/100.
730   CPLEX = CPLEX/100.
735   CPLEX = CPLEX/100.
740   CPLEX = CPLEX/100.
745   CPLEX = CPLEX/100.
750   CPLEX = CPLEX/100.
755   CPLEX = CPLEX/100.
760   CPLEX = CPLEX/100.
765   CPLEX = CPLEX/100.
770   CPLEX = CPLEX/100.
775   CPLEX = CPLEX/100.
780   CPLEX = CPLEX/100.
785   CPLEX = CPLEX/100.
790   CPLEX = CPLEX/100.
795   CPLEX = CPLEX/100.
800   CPLEX = CPLEX/100.
805   CPLEX = CPLEX/100.
810   CPLEX = CPLEX/100.
815   CPLEX = CPLEX/100.
820   CPLEX = CPLEX/100.
825   CPLEX = CPLEX/100.
830   CPLEX = CPLEX/100.
835   CPLEX = CPLEX/100.
840   CPLEX = CPLEX/100.
845   CPLEX = CPLEX/100.
850   CPLEX = CPLEX/100.
855   CPLEX = CPLEX/100.
860   CPLEX = CPLEX/100.
865   CPLEX = CPLEX/100.
870   CPLEX = CPLEX/100.
875   CPLEX = CPLEX/100.
880   CPLEX = CPLEX/100.
885   CPLEX = CPLEX/100.
890   CPLEX = CPLEX/100.
895   CPLEX = CPLEX/100.
900   CPLEX = CPLEX/100.
905   CPLEX = CPLEX/100.
910   CPLEX = CPLEX/100.
915   CPLEX = CPLEX/100.
920   CPLEX = CPLEX/100.
925   CPLEX = CPLEX/100.
930   CPLEX = CPLEX/100.
935   CPLEX = CPLEX/100.
940   CPLEX = CPLEX/100.
945   CPLEX = CPLEX/100.
950   CPLEX = CPLEX/100.
955   CPLEX = CPLEX/100.
960   CPLEX = CPLEX/100.
965   CPLEX = CPLEX/100.
970   CPLEX = CPLEX/100.
975   CPLEX = CPLEX/100.
980   CPLEX = CPLEX/100.
985   CPLEX = CPLEX/100.
990   CPLEX = CPLEX/100.
995   CPLEX = CPLEX/100.

```

```

130
IF (RN.EQ.88) GO TO 65
CALL LIST (1,M,IFREQ,IEPR,IEPI,MUR,MUI,IMD)
WRITE (LU,88)
ECRMT ("HARD COPY OF MU.EP COMPLETED.")
GO TO 7
150 CONTINUE
      BUILD IDATA ARRAY THAT GOES ON DISC
      GO 1 I=1,128
      IDATA(I)=IEPR(I)
      IDATA(I+128)=IEPR(I)
      IDATA(I+248)=IEPI(I)
      IDATA(I+368)=MUR(I)
      IDATA(I+488)=MUI(I)
      CONTINUE
      IDATA(601)=M
      GO 2 I=1,423
      IDATA(601+I)=0
      CONTINUE
      DISC TRACK ALLOCATION (1 TRACK)
      IDISC=3
      ISECT=3
      ISTRK=3
      CALL EXEC(15,1,ISTRK,IDISC,ISECT)
      WRITE ARPHY DATA ON TRACKS
      CALL EXEC(2,2,IDATA,1024,ISTRK,0)
      INAME(1)=2HPL
      INAME(2)=2HT

```

L10

```
INAME(S)=ZHT  
INAME(S)=1H  
LL=LU(1)  
SCHEDULE PLOT PROGRAM (PLT)  
REG=EXEC9, INAME, ISTRK, 0, 0, 0, LL)  
RELEASE DISC TRACKS  
CALL EXEC(16, 1, ISTRK, IOISC)  
WRITE(10, 90)  
FORMAT ("PLOT COMPLETED.")  
GO TO 7  
END
```

90

```

L30
FTNA
      1
C      C      C
      PROGRAM WJSET
      DIMENSION IPRAM(5)
      WRITE(12,1)
      1  FORMAT ("WJSET PROGRAM ENTERED.")
C      THIS PROGRAM ALLOWS THE LOCAL AND REMOTE COMMANDS
C      TO BE SENT TO THE FREQUENCY SYNTHESIZER AT THE
C      START AND TERMINATION OF THE MAIN PROGRAM....
      CALL RXPAT(IPRAM)
      IF (IPRAM(1).EQ.1) CALL RMOTE(23)
      IF (IPRAM(1).EQ.0) CALL LOCL(13)
      END
      EOF

```

L30

```

END
SUBROUTINE REFL(LU,RMOD,RPHA,M,XMIN,DELF)
  DIMENSION RMOD(1),RPHA(1),A(200),B(200)
  1 WRITE (LU,2)
  2 FORMAT ("REFLECTION MEASUREMENT COMMANDS",/,
  1"1=RETURN TO MAIN PROGRAM",/,"2=MEASURE SHORT",
  2/,"3=MEASURE SAMPLE")
  READ (LU,X) NN
  GO TO (100,110,120),NN
100 RETURN
110 WRITE (LU,3)
  3 FORMAT ("WOULD YOU LIKE TO CONTROL SWEEP RANGE?",/,
  1"1=YES",/,"2=NO")
  READ (LU,X) KK
  GO TO (111,112),KK
111 NI=0.
  K=1
  AK1=0.
  AK2=0.
  4 WRITE (LU,5)
  5 FORMAT("ENTER START AND STOP FREQ.")
  READ (LU,X) AK1,AK2
  J=(AK2-AK1)/DELF
  DO 7 I=NI+1,J=NI+K
  FR=AK1+(FLOAT(I)*DELF)-(DELF*FLOAT(NI+K))
  WRITE (23,6) FR
  6 FORMAT (F5.3,"E")
  CALL WAIT(500)
  A(I)=0.
  B(I)=0.
  CALL READ(LU,A,B,I)

```

```

L30      CALL READ(LU,A,B,I)
        WRITE (12,33) A(I),B(I),FR
33      FORMAT(F7.3,10X,F7.3,10X,F7.3)
7      CONTINUE
        N1=I-1
        K=0
        IF (I-M) 4,1,1
112     DO 9 I=1,M
        F1=XMIN+(FLOAT(I-1)*DRLF)
        WRITE (23,8) F1
8      FORMAT (F5.3,"E")
        CALL WAIT(500)
        A(I)=0.
        B(I)=0.
        CALL READ (LU,A,B,I)
9      CONTINUE
        GO TO 1
120     WRITE (LU,10)
10     FORMAT("WOULD YOU LIKE TO CONTROL THE SWEEP RANGE?",
1/, "1=YES",/, "2=NO")
        READ (LU,x) KA
        GO TO (130,140),KA
130     N1=0.
        K=1
        AK1=0.0
        AK2=0.0
11     WRITE(LU,12)
12     FORMAT("ENTER START AND STOP FREQ.")
        READ (LU,x) AK1,AK2
        J=(AK2-AK1)/DRLF
        DO 14 I = N1+1,J+N1+K

```

L30

```

DO 14 I = N1+1, J+N1+K
FR=AK1+(FLOAT(I)*DELF)-(DELF*FLOAT(N1+K))
WRITE (23,13) FR
13 FORMAT (F3.3,"E")
CALL WAIT(500)
CALL READ (LU,A,B,I)
RMOD(I)=A(I)
RPHA(I)=B(I)
WRITE (12,99) A(I),B(I),FR
99 FORMAT(F7.3,10X,F7.3,10X,F7.3)
14 CONTINUE
N1=I-1
K=0
IF (I-M) 11,1,1
DO 16 I=1,M
F1=(XMIN+FLOAT(I-1)*DELF)
WRITE(23,15) F1
15 FORMAT(F3.3,"E")
CALL WAIT(500)
CALL READ (LU,A,B,I)
RMOD(I)=A(I)
RPHA(I)=B(I)
16 CONTINUE
GO TO 1
END
SUBROUTINE READ (LU,A,B,I)
DIMENSION A(1),B(1),IQRUF(14),ICHAN(2),IAD(2)

```

C
C
C
C

THIS SUBROUTINE READS DATA VALUES FROM THE
NETWORK ANALYZER THROUGH THE A/D DEVICE.

L30
C

```

      ICHAN(1)=2
      ICHAN(2)=3
      IRTN=0.
      CALL R2313(IQDUF,14)
      CALL S2313(9,IRTN)
      IF (IRTN-1) 3,4,3
100   CONTINUE
      4   CALL R2313(9,IRTN,0,2,ICAN,2,IAD,0)
      IF (IRTN) 110,100,120
110   WRITE (LU,5) IRTN
      5   FORMAT ("RETURN CODE ERROR",15)
      RETURN
120   V1=FLOAT(IAND(IAD(1),177760H))*.0003125
      V2=FLOAT(IAND(IAD(2),177760H))*.0003125
      A(I)=A(I)
      B(I)=B(I)
      A(I)=(V1*20.)-A(I)
      B(I)=(V2*100.)-B(I)
      RETURN
      END
      SUBROUTINE TRANS(LU,TMOD,TPHA,M,XMIN,DELF)
      DIMENSION TMOD(1),TPHA(1),A(120),B(120),C(120),D(120)
      1   WRITE(LU,2)
      2   FORMAT("TRANSMISSION COMMANDS",/,"1=RETURN TO MAIN PROGRAM",/,
      1"2=MEASURE OPEN REFERENCE WINDOW",/,
      2"3=MEASURE SAMPLE")
      READ (LU,x) N1
      GO TO (100,110,120),N1
100   RETURN
110   DO 4 I=1,M

```

```

L30
110 DO 4 I=1,M
    F1=XMIN+(FLOAT(I-1)*DELF)
    WRITE (23,3) F1
3   FORMAT (F5.3,"E")
    CALL WAIT(500)
    A(I)=0.
    B(I)=0.
    CALL READ (LU,A,B,I)
4   CONTINUE
    GO TO 1
120 WRITE (LU,5)
5   FORMAT ("SAMPLE MEASUREMENT COMMANDS",/,
1"1=END SAMPLE MEASUREMENT",/,"2=LEVEL SAMPLE RUN",/,
2"3=RAISED SAMPLE RUN")
    READ (LU,x) KK
    GO TO (121,122,123),KK
121 CONTINUE
    GO TO 1
122 DO 7 I=1,M
    C(I)=A(I)
    D(I)=B(I)
    F1=XMIN+(FLOAT(I-1)*DELF)
    WRITE(23,6) F1
6   FORMAT(F5.3,"E")
    CALL WAIT(500)
    CALL READ(LU,A,B,I)
    TMD(I)=A(I)
    TPHA(I)=B(I)
7   CONTINUE
    GO TO 120
123 CONTINUE
/

```

```

L30
123      CONTINUE
        N1=0.
        K=1
        AK1=0.
        AK2=0.
8      WRITE(LU,9)
9      FORMAT("ENTER START AND STOP FREQ.")
        READ(LU,*) AK1,AK2
        J=(AK2-AK1)/DELTA
        DO 11 I=N1+1,J+N1+K
            FR=(AK1+FLOAT(I)*DELTA)-(DELTA*FLOAT(N1+K))
            WRITE(23,10) FR
10         FORMAT(F5.3,"E")
            CALL WAIT(500)
            A(I)=C(I)
            B(I)=D(I)
            CALL READ(LU,A,B,I)
            TMOD(I)=(TMOD(I)+A(I))/2.
            TPHA(I)=(TPHA(I)+B(I))/2.
            WRITE (12,99) TMOD(I),TPHA(I),FR
99        FORMAT (F5.2,10X,F5.2,10X,F5.2)
11      CONTINUE
        N1=I-1
        K=0
        IF (I-M) 8,1,1
        END
        SUBROUTINE CDATA(LU,RNOD,RPHA,TMOD,TPHA,IEPR,IEPI,MUR,
1      MUI,THK,XMIN,DELTA,N2,IFREQ)
        DIMENSION RNOD(1),RPHA(1),TMOD(1),TPHA(1),IEPR(1),
1      IEPI(1),MUR(1),MUI(1),CCIR(120),CC2R(120),
2      CC2I(120),IFREQ(1)

```

```

L30      20021(120),IFREQ(1)
C
C      THE FOLLOWING SUBROUTINE CALCULATES MU AND EP.
C
      FACB=1.8798E6/THK
      FACA=1.0/FAICB
      M=1
      F=XMIN*1000.
      DEL=DELF*1000.
C      BIG LOOP FOR PROCESSING MU AND EP
      DO 400 I=1,N2
        REFR=0.
        REFI=0.
        DR=0.
        DI=0.
        AR=0.
        AT=0.
        TRAR=0.
        TRAI=0.
        DRR=0.
        DRI=0.
        XRR=0.
        XRI=0.
        ZRR=0.
        ZRI=0.
        DUN=0.
        RPHA(I)=RPHA(I)/57.3
        TPHA(I)=TPHA(I)/57.3
        REFR=(-1.)*(10.**(RMOD(I)/20.))*COS(RPHA(I))
        REFI=(-1.)*(10.**(RMOD(I)/20.))*SIN(RPHA(I))
        BR=(10.**(TMOD(I)/20.))*COS(TPHA(I))

```

L30

```

BR=(10.*x(TMOD(I)/20.))*COS(TPHA(I))
BI=(10.*x(TMOD(I)/20.))*SIN(TPHA(I))
PHI=FACT*F
CALL CPLEX(BR, BI, COS(PHI), -SIN(PHI), TRAR, TRAI, 1)
VIR=TRAR+REFR
V1I=TRAI+RLFI
V2R=TRAR-REFR
V2I=TRAI-RLFI
CALL CPLEX(VIR, V1I, V2R, V2I, DR, DI, 1)
AR=1.0-DR
AI=-DI
CALL CPLEX(AR, AI, V1R-V2R, V1I-V2I, XR, XI, 2)
CALL CPLEX(XR, XI, XR, XI, BR, BI, 1)
ER=BR-1.0
CALL CPLEX(BR, BI, DUM, DUM, AR, AI, 3)
GR=XR+AR
GI=XI+AI
IF(SQRT(GR**2+GI**2).GT.1.0) GR=XR-AR
IF(SQRT(GR**2+GI**2).GT.1.0) GI=XI-AI
CALL CPLEX(VIR, V1I, GR, GI, AR, AI, 1)
CALL CPLEX(V1R-GR, V1I-GI, 1.0-AR, -AI, ZR, ZI, 2)
CALL CPLEX(1.0+GR, GI, 1.0-GR, -GI, C1R, C1I, 2)
CALL CPLEX(ZR, ZI, DUM, DUM, AR, AI, 4)
C2R=AR*FACB/F
C2I=AI*FACB/F
IFREQ(N)=F
CC1R(N)=C1R
CC1I(N)=C1I
CC2R(M)=C2R
CC2I(M)=C2I
MM=M

```

```

L40      MN=MM
          IF (M-N2) 365,370,370
          CONTINUE
365      N=M+1
          F=F+DEL
          CONTINUE
          CONTINUE
370      CALL SMOTH(CC1R,MM)
          CALL SMOTH(CC1I,MM)
          CALL SMOTH(CC2R,MM)
          CALL SMOTH(CC2I,MM)

          C      COMPUTE MU AND EPSILON
          C
          C
          DO 450 IJ=1,MM
            CIR=CC1R(IJ)
            C1I=CC1I(IJ)
            C2R=CC2R(IJ)
            C2I=CC2I(IJ)
            CALL CPLEX(C1R,C1I,-C2I,C2R,XMR,XMI,1)
            CALL CPLEX(-C2I,C2R,C1R,C1I,EPR,EPI,2)
            XMI=XMI*(-1.0)
            IF(XMI,LT,-1.0) XMI=-1.0
            EPI=EPI*(-1.0)
            IF (EPI,LT,-1.0) EPI=-1.0
            IPR(IJ)=100*EPR
            IEPI(IJ)=100*EPI
            MUR(IJ)=100*XMR
            MUI(IJ)=100*XMI
          450 CONTINUE
              RETURN
              END

          EOF

```

```

L30
FTN4,L
SUBROUTINE CPLEX(A,B,C,D,ANR,ANI,N)
THIS IS A COMPLEX ARITHMETIC ROUTINE
THAT DOES ONE OF FOUR OPERATIONS DEPENDING
ON THE VALUE OF 'N'
N=1: (A+JB)*(C+JD)
N=2: (A+JB)/(C+JD)
N=3: (SQRT(A+JB))
N=4: (LN(A+JB))

GO TO (1,3,4,4),N
1 AR=AXC-BXD
AI=AXD+BXD
ANR=AR
ANI=AI
RETURN
3 DIV=CXC+DXD
AR=(AXC+BXD)/DIV
AI=(BXD-AXD)/DIV
GO TO 2
4 R=SQRT(AXA+BXB)
TH=ATAN2(B,A)
IF(TH.GT.0.0) TH=TH-6.28318
IF(N.GT.3) GO TO 5
R=SQRT(R)
TH=TH/2
7 AR=R*COS(TH)
AI=R*SIN(TH)
GO TO 2
5 AR=ALOG(R)
AI=TH
/

```

```

L30      C      AI=TH
          C      IF(AI.GT.0.0) GO TO 6
          C      GO TO 2
          C      6  AI=AI-6.28318
          C      END
          C      END$
          C      EOF
          C      /

```



```

L40
FTN4,L
      SUBROUTINE LIST(LU,N,IFR,IER,IEI,IMR,IMI,IC)
C
C
C      THIS SUBROUTINE LISTS 30 LINES OF MU/EP
C      DATA, MAKES A HARD COPY, ERASES THE SCREEN
C      AND REPEATS THE PROCESS UNTIL THE N DATA
C      POINTS ARE LISTED.
C
      DIMENSION IFR(1),IMR(1),IMI(1),IER(1),IEI(1),IC(1)
      NEWPG=2
C
C      CALL WAIT(100)
C      CALL MODE(NEWPG)
C      CALL WAIT(200)
      KK=N/30+1
      DO 1 J=1,KK
        WRITE(LU,4) (IC(II),II=1,32)
        DO 2 I=1,30
          K=I+((J-1)*30)
          IF(K.GT.N) GO TO 5
          WRITE(LU,3) K,IFR(K),IER(K),IEI(K),IMR(K),IMI(K)
        CONTINUE
      2  CONTINUE
      5  CONTINUE
C      CALL WAIT(3500)
C      CALL HDOPY
C      CALL WAIT(100)
C      CALL MODE(NEWPG)
C      IF(K.GE.N) RETURN
      1  CONTINUE
      3  FORMAT(15," FRLQ=",I6,5X,"EP=",I6," +J",I6,5X,"MU=",I6," +J",I6)
      4  FORMAT(32A2)
      CALL WAIT (200)
      RETURN
      END
      IEND$

```

EOF

```

L30      PROGRAM PLT(,8)
FTN4,L   DIMENSION IRY1(120),IRY2(120),IRY3(120),IRY4(120),IRY5(120),
          IIRY6(32),IRY7(120),LU(5),IDATA(1024),IPRAM(5)
          DATA IUL/2HPL/
          THIS SUBROUTINE DRIVES THE SPERRY
          PLOT PACKAGE USED TO OUTPUT COMPLEX
          MU-EF GRAPHS VERSUS FREQ.

          THE ABOVE PARAMETERS ARE USED AS
          FOLLOWS.....
          NSP: # OF POINTS TO PLOT
          NN1: FIRST POINT
          NN2: LAST POINT
          IRY1: EPSILON (REAL PART)
          IRY2: EPSILON (IMAG PART)
          IRY3: MU (REAL PART)
          IRY4: MU (IMAG PART)
          IRY5: FREQ (MHZ)
          IRY6: ALPHA-NUM COMMENT LINE
          IRY7: TEMP DATA STORAGE ARRAY

          CALL RHPAR(IPRAM)
          WRITE(6,1000)
          C1000  FORMAT("PROGRAM PLT BEGIN")
          C      READ IDATA ARRAY FROM DISC
          C      C
          C      C
          ISTRK=IPRAM(1)
          CALL EXEC(1,2,IDATA,1024,ISTRK,0)
          LU=IPRAM(5)

```

L30

```

LU=IPRAM(5)
DO 100 I=1,120
  IRY5(I)=IDATA(I)
  IRY1(I)=IDATA(I+120)
  IRY2(I)=IDATA(I+240)
  IRY3(I)=IDATA(I+360)
  IRY4(I)=IDATA(I+480)
100 CONTINUE
NSP=IDATA(601)
NN1=2
NN2=NSP
WRITE(LU,101)
101 FORMAT("PLEASE ENTER STATEMENT ABOUT SAMPLE.")
READ(LU,102) (IRY6(I), I=1,32)
102 FORMAT(32A2)
A=FLOAT(IRY5(1))/1000.
B=FLOAT(IRY5(NSP))/1000.
IXMIN=INT(A)
IXMAX=INT(B)+1
IF((FLOAT(IXMAX)-B).EQ.1.) IXMAX=IXMAX-1
LARGE=0
YMIN=0.
NEWPG=2
NPL=1
10 CONTINUE
CALL WAIT (200)
CALL MODE(NEWPG)
CALL WAIT(200)
C WRITE THE HLADR COMMENT LINE
CALL HEADR(LU,IRY6)
C DRAW THE GRID
/

```

```

L30
C      DRAW THE GRID
C      CALL WAIT(2000)
C      CALL HGRD
C      IF(NP.LEQ.1) CALL YMAXI(IRY1,IRY3,NSP,LARGE)
C      SET FLAG FOR 'REAL PART' GRAPH
C      JJ=1
C      IF(NP.LEQ.1) LG1=LARGE/100
C      CALL PLOT(NSP,LC1,YMIN,JJ,IXMAX,IXMIN)
C      LABEL THE GRAPH
C
C      SAVE THE FREQ IN IRY7
C      DO 1 LLL=1,NSP
C      IRY7(LLL)=IRY5(LLL)
C
C      SCALE EP' AND FREQ TO ABSOLUTE
C      TETRONIX COORDINATES.
C
C      IF(NP.LEQ.1) CALL SCL(LARGE,NSP,IRY1,IRY5)
C      DO 2 LLL=1,NSP
C      IRY5(LLL)=IRY7(LLL)
C      SCALE MU' AND FREQ INTO ABSOLUTE
C      TETRONIX COORDINATES.
C
C      IF(NP.LEQ.1) CALL SCL(LARGE,NSP,IRY3,IRY5)
C      PLOT EP' AS A DASH LINE
C      CALL DLIN(NN1,NN2,IRY5,IRY1)
C      PLOT MU' AS A LINE
C      CALL LIN(NN1,NN2,IRY5,IRY3)
C      CALL HDOPY
C      CALL WAIT(200)

```



```

L30      IF (NPL.EQ.1) CALL SCL(LARGE,NSP,IRY4,IRY5)
C          PLOT EP" AS A DASH LINE
C          CALL DLINE (NN1,NN2,IRY5,IRY2)
C          PLOT MU" AS A LINE
C          CALL LINE (NN1,NN2,IRY5,IRY4)
C          CALL HDCPY
C          CALL MODE(NEWPG)
C          LU=IPRAM(5)
C          NPL=2
C          WRITE(LU,6)
6          FORMAT("ENTER IPL TO REPLOT.")
7          READ(LU,7) IANS
C          FORMAT(A3)
C          CALL WAIT(500)
C          IF (IANS.EQ.IPL) GO TO 10
C          END

```

```

EOF
/ER

```

```

L30
FTN4,L
SUBROUTINE HEADR(LU,IPARM)
C
C      THIS SUBROUTINE PRINTS AN ASCII HEADER STATEMENT
C      OR COMMENT STATEMENT STORED IN THE ARRAY IPARM.
C      IT BELONGS TO THE LOW FREQUENCY PLOT PACKAGE
C
C      DIMENSION IPARM(1)
C      WRITE(LU,20) (IPARM(I),I=1,32)
C      FORMAT(" SAMPLE:",3X,32A2)
C      CALL WAIT(50)
C      RETURN
C      END
C      END$
20
EOF

```

```

L30
FTN4,L
C
C
C
C
      SUBROUTINE SMOTH(DATA,N)
      DIMENSION DATA(1),WORK(120)

      THIS SUBROUTINE PERFORMS A 4TH ORDER DATA SMOOTHING
      OF THE 'N' ELEMENTS OF THE DATA ARRAY.

      FACTR=3./35.
      MAXI=N-1
      DO 10 I=1,MAXI
        WORK(1)=DATA(I+1)-DATA(I)
10    CONTINUE
      DO 20 J=1,3
        TOP=WORK(1)
        MAXI=MAXI-1
        DO 20 I=1,MAXI
          WORK(I)=WORK(I+1)-WORK(I)
20    MAXI=N-2
      DO 30 I=3,MAXI
        DATA(1)=DATA(I)-WORK(I-2)*FACTR
        DATA(1)=DATA(1)+TOP/5.0+WORK(1)*FACTR
        DATA(2)=DATA(2)-TOP*0.4-WORK(1)/7.0
        DATA(N)=DATA(N)-WORK(N-3)/5.0+WORK(N-4)*FACTR
        DATA(N-1)=DATA(N-1)+WORK(N-3)*0.4-WORK(N-4)/7.0
      RETURN
      END
      ENDS$

```

EOF
/


```

L40
FTN4,L
SUBROUTINE HFGRD
C
C THIS PLOTTING SUBROUTINE, WHICH BELONGS
C TO THE (MU-EP) HIGH FREQ PLOTTING
C PACKAGE, PLOTS A GRID ON THE CRT.
C ALL CONSTANTS ARE IN THE TETRONIX
C ABSOLUTE COORDINATES.
C WRITTEN 2-07-79 BY CAM
C
C DRAW THE VERTICAL GRID LINES
C
C DRAW THE LINEAR HORIZONTAL GRID LINES
C
IX1=100
DX=82.90909
DO 25 I=1,12
  IY=75
  IDX=DX*(I-1)
  IX=IX1+IDX
  CALL PLOT(IX,IY,3)
  IY=680
  CALL PLOT(IX,IY,2)
25 CONTINUE
C
IY1=30
IDY=50
DO 100 N=1,13
  IY=IY1+N*IDY
  IX=95
  CALL PLOT(IX,IY,3)
  IX=1012
  CALL PLOT(IX,IY,2)
100 CONTINUE
RETURN
END
END$
COF

```

SUBROUTINE FL_EL(NN,MAX,YMIN,JJ,IXMAX,IXMIN)
DIMENSION LA(20),LY(23),LS(15),LX(20)

THIS SUBROUTINE, WHICH IS PART OF THE
 SPERRY PLOTTING PACKAGE, LABELS THE
 MU AND EF GRAPH THAT IS PLOTTED ON THE
 TETRONIX CRT. THE PARAMETERS PASSED TO
 THE SUBROUTINE ARE USED TO SCALE THE AXIS
 PROPERLY. THE 'JJ' SWITCH SPECIFIES THE
 "REAL" OR "IMAG" PORTIONS OF MU AND
 EPSILON TO BE PLOTTED.

DATA LX/2HF ,2HER,2H Q,2H HG,2H Z,2H ,2H ,2H ,
C 2H ,2H ,2H ,2HER,2H LA,2H ,2HAP,2H TR,2H MI,
C 2HGA/
DATA LY/2H R,2H E,2H L,2H A,2H T,2H I,2H V,2H E,2H ,
12H M,2H U,2H ,2H A,2H N,2H D,2H ,2H E,2H P,2H S,2H I
2,2H L,2H O,2H N/

THE FOLLOWING ROUTINE SCALES THE
VERTICLE AXIS ACCORDING TO THE
LARGEST VALUE OF THE MD OR EP SENT
TO THIS SUBROUTINE, AND THEN ROUNDS
OFF TO THE NEAREST FACTOR OF 5.

NOCT=608
MY=MAX

```

L30      MY=MAX
          MY=1+MY/5
          LIMIT MAX SCALE TO 95 (I.E. 5X19)
          IF(MY.GT.19) MY=19
          NDEC=MY
          YMIN=-1.0*FLOAT(NDEC)
          MY=5*MY
          DO 25 N=1,11,2
            NY=MY
            NY=NY/10
            IF(NY) 10,10,5
            5  CONTINUE
            NOINY=NOCT+NY
            LS(N)=NOINY
            GO TO 15
            10 CONTINUE
            LS(N)=20040B
            15  CONTINUE
            NY1=MY-(NY*10)
            LS(N+1)=NOCT+NY1
            MY=NY-NDEC
            25  CONTINUE
          BEGIN LABELING THE AXIS
          CALL SYMB(500,5,5,1,LX)
          C    LABELS "FREQ(GHZ)"
          DEL=FLOAT((IXMAX-IXMIN)/11.
          AMY1=IXMIN
          AMY2=FLOAT((IXMIN)+(6*DEL)
          AMY3=IXMAX
          CALL SYMB(5,650,23,2,LY)
          C    LABELS "RELATIVE MU AND EP"

```

```

L30
C      LABELS "RELATIVE MU AND EP"
      IF(JJ-1) 60,60,70
60    CONTINUE
      CALL SYMB(480,710,5,1,LX(14))
      LABELS "REAL" PART
      GO TO 75
70    CONTINUE
      CALL SYMB(480,710,2,1,LX(19))
      LABELS "IMAG"
      CALL SYMB(535,710,3,1,LX(16))
      LABELS "PART"
      GO TO 75
75    CONTINUE
      DO 32 J=1,11,5
      IF(J.EQ.1) AMY4=AMY1
      IF(J.EQ.6) AMY4=AMY2
      IF(J.EQ.11) AMY4=AMY3
      DO 31 N=1,5
      FN=FLOAT(N)
      NY1=AMY4*(10.*FN)/1000.
      IF(NY1) 26,26,27
26    IF(N.EQ.1) LA(J+N-1)=20040B
      IF(LA(J+N-1).EQ.20040B) GO TO 28
      IF(N.GT.2) GO TO 30
      IF(LA(J+N-2).EQ.20040B) LA(J+N-1)=20040B
      IF(LA(J+N-2).NE.20040B) GO TO 30
      GO TO 28
27    CONTINUE
      NOINY=NOCT+NY1
      LA(J+N-1)=NOINY
28    CONTINUE

```


L30

```
CALL SYMB(84,50,1,1,LA(2))  
CALL SYMB(97,50,1,1,LA(3))  
CALL SYMB(110,50,1,1,LA(16))  
CALL SYMB(123,50,1,1,LA(4))  
CALL SYMB(136,50,1,1,LA(5))  
CALL SYMB(552,50,1,1,LA(6))  
CALL SYMB(565,50,1,1,LA(7))  
CALL SYMB(578,50,1,1,LA(8))  
CALL SYMB(591,50,1,1,LA(16))  
CALL SYMB(604,50,1,1,LA(9))  
CALL SYMB(617,50,1,1,LA(10))  
CALL SYMB(949,50,1,1,LA(11))  
CALL SYMB(962,50,1,1,LA(12))  
CALL SYMB(975,50,1,1,LA(13))  
CALL SYMB(988,50,1,1,LA(16))  
CALL SYMB(1001,50,1,1,LA(14))  
CALL SYMB(1012,50,1,1,LA(15))  
RETURN  
END
```

EOF

```

L30
FTNA,L SUBROUTINE POINT(IX,IY)
      DIMENSION IO(4)
C
C      THIS SUBROUTINE CHANGES THE TETRONIX CRT TO THE
C      GRAPHICS MODE, AND MOVES WITH A DARK VECTOR TO
C      THE POINT (IX,IY)
      N=IX/32
      IO(3)=N+32
      IO(4)=IX-32*N+64
      N=IY/32
      IO(1)=N+32
      IO(2)=IY-N*32+96
      M=...4
      CALL OUT2(M,IO)
      RETURN
      END

```

```

EOF
/ER

```

```

L30
FTN4,L
      C
      C
      C
      C
      C
      C
      SUBROUTINE DLINE(JXX,JXY,NXPT,NYPT)
      DIMENSION NYPT(1),NXPT(1)

      THIS SUBROUTINE PERFORMS THE SAME
      OPERATION AS SUBROUTINE 'LINE' EXCEPT
      IT PLOTS A DASH LINE INSTEAD.

      CALL MODE(3)
      DO 1 I=JXX,JXY,2
        IF(I.EQ.JXX.AND.JXX.GT.1) CALL PLOT(NXPT(I-1),NYPT(I-1),3)
        CALL PLOT(NXPT(I),NYPT(I),2)
        CALL PLOT(NXPT(I+1),NYPT(I+1),3)
      1 CONTINUE
      RETURN
      END
      EOF

```



```

L30
FTN4,L
SUBROUTINE LINE(JXX,JXY,NXPT,NYPT)
DIMENSION NYPT(1),NXPT(1)

C
C
C
C
C
C
C

      THIS PROGRAM PLOTS THE LINE FOR THE
      MU AND EPSILON CURVES.
      ONLY MINOR CHANGES TO ACCOMODATE
      INDIRECT ADDRESSING DISCERN THIS
      PROGRAM FROM THE RCS 'LINE' SUBROUTINE

      CALL MODE(3)
      DO 1 I=JXX,JXY
        CALL PLOT(NXPT(I),NYPT(I),2)
        CONTINUE
      1 CONTINUE
      RETURN
      END

      EOF

```

```

L30      FTN4,L
          SUBROUTINE PLOT(IX,IY,IPEN)
C
C          THIS SUBROUTINE MOVES FROM TETRONIX CURRENT
C          (X,Y) COORDINATE TO THE COORDINATE (IX,IY)
C          WITH EITHER A LIGHT VECTOR (IPEN=2) OR A
C          DARK VECTOR (IPEN=3)
C
C          N=IABS(IPEN)
C          IF(N=2) 2,2,3
C          C.....IPEN=2, MOVE WITH LINE
C          2      CALL POINT(IX,IY)
C          RETURN
C          C.....IPEN=3, MOVE WITH NO LINE
C          3      CALL MODE(3)
C          CALL POINT(IX,IY)
C          RETURN
C          END
          EOF

```

```

L30
FTN4,L  SUBROUTINE HDOPY
C.....MAKES A HARD COPY FROM EITHER THE A/N OR THE GRAPHICS MODE
C.....TERMINAL REMAINS IN THE MODE PRIOR TO THE HARD COPY COMMAND
        DIMENSION L(2)
        L(1)=27
        L(2)=23
        CALL OUT2(-2,L)
C.....WAIT FOR HARD COPY
        CALL WAIT(4000)
        RETURN
        END
EOF
/

```

```

L40      SUBROUTINE YMAXI(IY1,IY2,N,NBIG)
      FTN4,L
      DIMENSION IY1(1),IY2(1)
      C      THIS SUBROUTINE SEARCHES FROM NL TO NU TO FIND
      C      THE BIGGEST ELEMENT IN THE TWO ARRAYS HY1(N)
      C      AND HY2(N) AND SENDS THIS VALUE BACK TO THE
      C      CALLING PROGRAM THROUGH 'NBIG'
      C      SUBROUTINE MODIFIED 3 APR 79 BY CAM
      C      SUBROUTINE WRITTEN FOR LOW-FREQ PLOTTING PKG.

      NL=4
      NU=N-3
      NBIG=0
      DO 5 L=NL,NU
        IF(IY1(L)-NBIG) 3,3,2
        CONTINUE
        NBIG=IY1(L)
        CONTINUE
      2    CONTINUE
      3    CONTINUE
      5    CONTINUE
      NBIG1=0
      DO 10 L=NL,NU
        IF(IY2(L)-NBIG1) 6,6,7
        CONTINUE
        NBIG1=IY2(L)
        CONTINUE
      6    CONTINUE
      10   CONTINUE
      IF(NBIG-NBIG1) 15,15,20
      15   CONTINUE
      20   NBIG=NBIG1
      CONTINUE
      RETURN
      END
      EOF

```

```

L30 ASMB,R,L,T
    NAM OUT2
    ENT OUT2
    EXT .ENTR
N    NOP
IO    NOP
OUT2  NOP
    JSR .ENTR
    DEF N
    DLF IO
LOC  BSS 1
OUTPT EQU 21B
*
ATTN OCT 120000
    CLF 00
*
    LDA N,I
    STA LOC
    LDA IO,I
    JSR OUTCH
    LSR 8
    SZA
    JSR OUTCH
    ISZ IO
    NOP
    ISZ LOC
    JMP *-8
    STP 0
    JMP OUT2,I
*
    OUTCH NOP
/

```

21B IS THE I/O SLOT OF THE GRAPHICS CRT

```

L30 OUTCH NOP
    LDR ATTN
    OTR OUTPT
    OTA OUTPT
    STC OUTPT,C
    SFS OUTPT
    JMP x-1
    JMP OUTCH,I
    *
    END
    EOF
    /

```

```

L30
FTN4,L
      SUBROUTINE MODE(I)
      DIMENSION IO(4)
      C.....SUBROUTINE TO CHANGE TEKTRONIX MODE
      IF(I-2)1,2,3
      C.....MODE I=1 IS ALPHANUMERIC
      1  IO(1)=31
        M=-1
        CALL OUT2(M,IO)
        RETURN
      C.....MODE I=2 GIVE NEW PAGE
      2  IO(1)=27
        IO(2)=12
        M=-2
        CALL OUT2(M,IO)
        WAIT FOR PAGE ERASE
      C.....CALL WAIT(750)
        RETURN
      C.....MODE I=3 IS GRAPHICS MODE
      3  IO(1)=29
        M=-1
        CALL OUT2(M,IO)
        RETURN
      END
      END$

```

EOF
/

```

L40
FTN4,L  SUBROUTINE SYMB(IX,IY,N,IHV,IO)
        DIMENSION IO(30)

C
C
C
C
C
C
C
C
C.....MOVE TO X,Y; CHANGE MODE
        CALL MODE(3)
        CALL POINT(IX,IY)
        CALL MODE(1)
        IF (IHV-1) 1,1,2
C.....SYMBOLS ALONG HORIZONTAL LINE (IHV=1)
1      M=-N
        CALL OUT2(M,IO)
        RETURN
C.....SYMBOLS ALONG VERTICLE (Y) AXIS (IHV=2)
2      JY=IY
        DO 3 I=1,N
            M=-1
            IT=IO(1)
            CALL OUT2(M,IT)
            CALL MODE(3)
            JY=JY-20
            CALL POINT(IX,JY)
            CALL MODE(1)
            RETURN
3
        END
EOF

```

THIS PROGRAM OUTPUTS A SYMBOL (IN ASCII)
FOR A STRING OF SYMBOLS STORED SEQUEN-
TIALY IN AN ARRAY
TO A LOCATION (IX,IY), POINTING EITHER
HORIZONTALLY OR VERTICALLY DEPENDING
VAULE OF IHV.


```

L30
FTN4,L SUBROUTINE WAIT(N)
C.....WAIT IS A SUBROUTINE THAT DOES NOTHING BUT WASTE TIME
C.....N DETERMINES THE AMOUNT OF TIME TO BE WASTED
DO 1 I=1,N
Y=I
X=SQRT(Y)
RETURN
END
1
EOF
/

```

APPENDIX B

First Test Setup of Frequency Domain Measurement System

The equipment used in the first test setup of the frequency domain measurement system will be described. Then the procedures used to measure fiberglass and two thicknesses of plexiglas will be discussed. Finally, the relative complex μ and epsilon values measured for the fiberglass and two thicknesses of plexiglas will be presented.

Equipment

The equipment used to support this thesis test setup consisted of a frequency synthesizer which served as the signal source, a network analyzer used for making relative decibel amplitude and phase measurements, an anechoic chamber used for the transmission coefficient measurements, a sectoral horn assembly used to make the reflection coefficient measurements, and a Hewlett-Packard 21MX RTE computer used to control the measurement setup. The complete measurement setup is diagrammed in Figure 18.

The power source was a Watkins and Johnson model 1204-1; rapidly tunable over a frequency range of 0.1 - 26 GHz. The following information was taken from the Watkins and Johnson 1204-1 specification sheet. The frequency resolution was 10 kHz from 100 MHz to 249.99 MHz, 100 kHz from 250 MHz to 1.9999 GHz, and 1 MHz from 2 - 26 GHz. The frequency was displayed with a five-digit LED, in GHz, with floating decimal. The frequency accuracy was $\pm 0.00035\%$ for 180 days over a

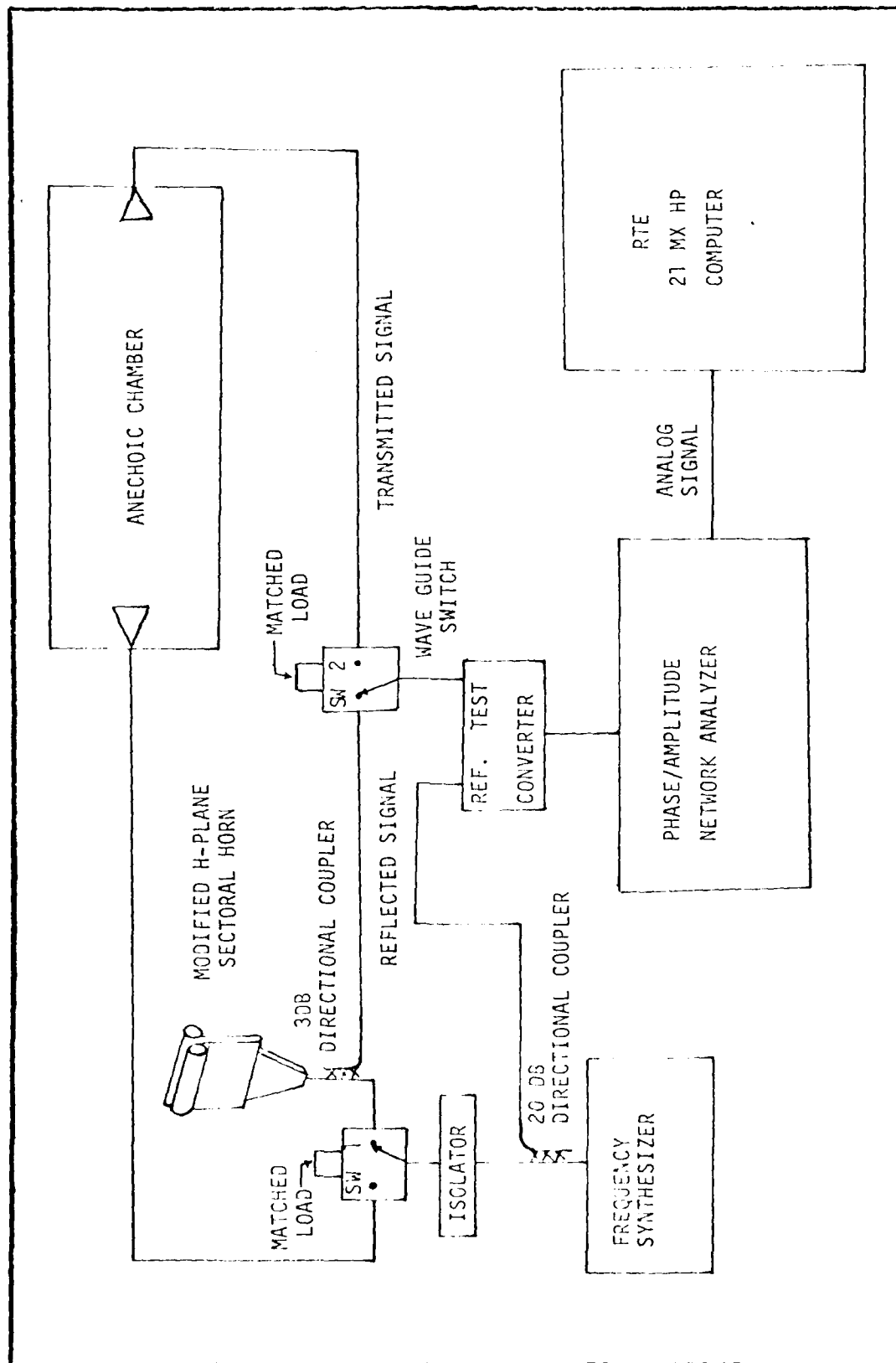


Figure 18. Frequency Domain Measurement Test Setup

0 - 50° C range. A single frequency could be selected on the keyboard with the enter, ENT, button and displayed on the LED. The frequency could be slewed up or down in 1, 10, and 100 MHz steps as selected on the INCREMENT controls. The synthesizer sweeps repetitively upward within the following bands: 0.1 - 1 GHz, 1 - 2 GHz, 2 - 8 GHz, 8 - 13 GHz, 13 - 18 GHz, and 18 - 26 GHz. The ΔF symmetrical sweep about phase-locked center frequency F which was displayed on the LED readout was 0 to +0.1% of F . The synthesizer provides 0 dBm (1 mw) minimum leveled output power. The variations in leveled power for the 0 dB attenuator setting was ± 1 dB over the range of 0.1 - 26 GHz. The output power could be attenuated over a range of 0 to 90 dB in 10 dB steps. The output power accuracy (meter reading plus attenuator setting) was: +0 dB attenuator setting, 0.1 - 18 GHz, ± 1 dB and 18 - 26 GHz, ± 1 dB; 10 dB - 90 dB attenuator setting, ± 2 dB and 18 - 26 GHz, ± 2.5 dB.

The network analyzer was a Hewlett-Packard Model 8410A with a phase-gain indicator. The 8413A phase-gain indicator used a meter display. The 8411A harmonic frequency converter provided RF-to-IF conversion. Measurements were based on the use of two wideband samplers to convert the input frequencies to a constant IF frequency. RF-to-IF conversion took place entirely in the harmonic frequency converter, which converted frequencies over a range of 12.4 - 18 GHz to 20 MHz IF signals. The phase and amplitude of the two RF input signals were maintained in the IF signal. The network analyzer mainframe provided the phase-lock circuitry to maintain the 20 MHz IF frequency while frequency was being swept, took the ratio of the

reference and test channels by use of identical AGC amplifiers, and then converted down to a second IF of 278 kHz. It also had a precision 0 to 69 dB IF attenuator with 10 and 1 dB steps for accurate IF substitution measurements of gain or attenuation.

The frequency domain measurement setup utilized the following piece of equipment during data measurements: a plug-in for the 8410A mainframe, the 8413A phase-gain indicator. It compared the amplitudes of the two IF signals and provided a meter readout of their ratio directly in dB with 0.1 dB resolution. It also compared phase in degrees over a 360° unambiguous range with 0.2° resolution on the meter. Phase difference was presented on the same meter when the appropriate function button was depressed. This plug-in had two analog output ports accessible from the front, one for dB amplitude, 20 mv/dB, and one for phase, 50 mv/degree.

The anechoic chamber was a 9.5 ft x 3 ft x 3 ft upright box structure as shown in Figure 19. The outer structure was made of 2 in x 6 in boards covered with 1/2 inch plywood. The inner structure was 1/2 inch plywood supported by 2 inch x 4 inch boards. The 1/2 inch plywood inside of the chamber was covered with 4 inch thick CV-4 radar absorbing material (RAM). At the middle of the chamber, a 2 inch thick styrofoam square and AN-74 RAM square provided a table top support area for the test sample. An 8 inch square hole was cut in the table top to provide a window for signal transmission. At the top and bottom of the anechoic chamber, there were 3 square inch holes cut to allow access for horn antennae. A hinged door was located at one side of the chamber to allow easy insertion and removal of samples to be tested.

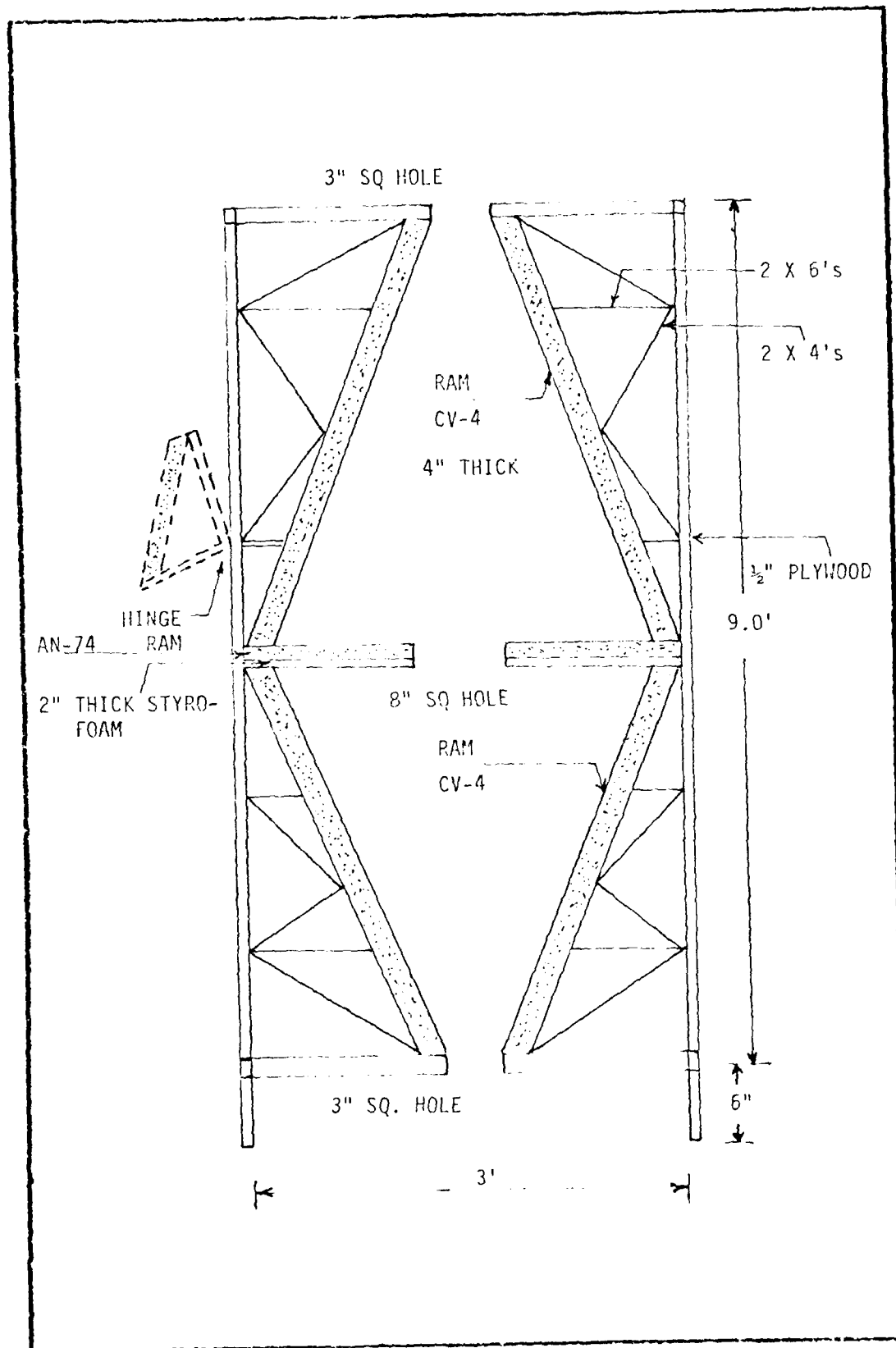


Figure 19. Anechoic Chamber Used in Frequency Domain Measurement Test Setup

An H-plane sectoral horn was designed and built for this project using formulae from Jasik, pages 10-8 and 10-9. An improved free space match was obtained by introducing a set of parallel plates coupled with a set of curved cylinders at the mouth of the horn. The horn is depicted in Figure 20. The theoretically computed phase variations across the aperture were 49.7° at 12.4 GHz to 71.7° at 18 GHz.

The Hewlett-Packard 21MX computer was used to control the data measurement. The frequency synthesizer was commanded to a discrete frequency by the computer and a data measurement was taken through the computer A/D converted, connected to the network analyzer. The disk subsystem and I/O devices were used to store, process, and display the results of a data run. The software used in the computer for the test setup was an earlier version of that given in Appendix A.

Procedures

The procedure followed in measuring the complex mu and epsilon values of a test sample involved the preparation of the sample, initialization of the computer program, setup and measurement of the reflection coefficient values, setup and measurement of the transmission coefficient values, data calculation to obtain mu and epsilon, and data output to present the mu and epsilon values.

In preparing the sample, a one square foot piece of test material was used. From the one square foot piece of material, a small strip 0.8 inches in width was cut from one side. The 0.8 inch wide piece of test material was used in the sectoral horn for reflection

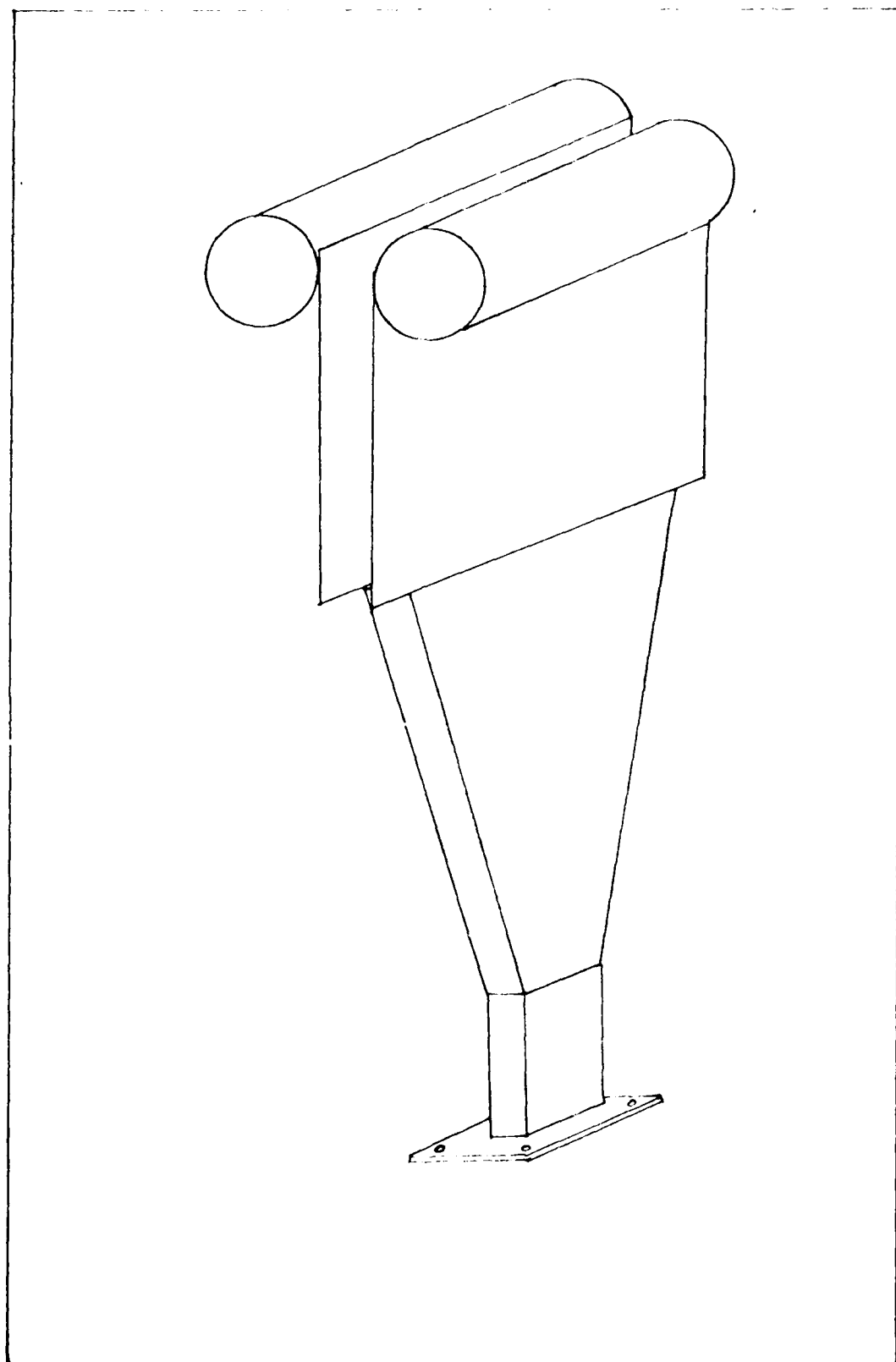


Figure 20. Modified H-Plane Sectoral Horn

coefficient measurements. During reflection coefficient measurements, the sample piece was placed directly on the mouth of the horn where the parallel plates were attached. The larger piece of the sample was placed inside the anechoic chamber during transmission coefficient measurements.

Once the sample pieces were prepared, the computer program was initialized. The operator entered a comment statement that identified the sample. This statement was printed as the heading for the line printer output of the μ and ϵ values. The thickness of the sample was entered next. Then, the start and stop frequencies were entered and the number of discrete frequencies at which measurements occurred were entered. At this point, the operator entered the portion of the program that makes reflection coefficient measurements.

For the reflection coefficient measurements, the sectoral horn was switched into the network by manually setting switch number one (the switch feeding power to the horn) to the right, and switch number two (the switch connected to the test signal port of the converter unit) to the left. The shorting plate was placed on the horn at the location previously described for the sample. The network analyzer gain amplifier was set to 13 dB. The frequency synthesizer power output was set to zero dB. The operator commanded the computer to step the frequency synthesizer across the frequency range to obtain a background reference for the short. Next, the sample was placed in the horn and the operator allowed the computer to step through the frequencies again. The computer determined the difference between the two sets of values and stored these differences as the reflection

coefficients. Now, the operator entered the portion of the program to obtain transmission coefficients.

The large sample piece was used for determining the transmission coefficients. The gain amplifier on the network analyzer was set to 41 dB. The anechoic chamber was switched into the network by placing switch one to the left and switch two to the right. The anechoic chamber was set up first with nothing over the 4 inch square window on the table assembly. The operator allowed the computer to measure the open window across the frequency range for a reference background measurement. Next, the sample was placed flush against the table surface, centered on the 4 inch square window. The first set of values for the sample transmission coefficients was determined and stored in the computer. Next, the sample was offset with two shims that were 0.5 cm thick and a second set of transmission coefficients was measured. The two sets of values were averaged to obtain a single set of values as the transmission coefficients. This procedure was performed to help compensate for the inherent VSWR within the anechoic chamber. At this point, the data needed to compute μ and ϵ had been obtained.

The data calculation to obtain the complex μ and ϵ values was now performed by the computer at the operator's request. The system was ready to output this data as hard copy at the line printer or as plots.

The output could be requested in the form of hard copy. This output gave the frequency in MHz and the μ and ϵ values scaled up by a factor of 100. A second program was loaded into memory at the request of the operator to produce plots.

The plot program was requested from the main program. It required a statement about the sample for use as a title on the plots. The output was produced on the CRT of the computer and automatically copied to a Tektronix hardcopy unit. At the direction of the operator, the main program was reentered and terminated.

Fiberglass Sample

The frequency domain data for the fiberglass sample is given in Figure 21A and 21B. The frequency domain values of relative μ and epsilon between 12 and 18 GHz are compared to the time domain data from Figure 7A and 7B in Table XI.

First Plexiglas Sample

The frequency domain data for the 64 mil plexiglas sample is given in Figure 22A and 22B. The frequency domain data between 12 and 18 GHz is compared to the time domain data from Figure 9A and 9B in Table XII.

Second Plexiglas Sample

The frequency domain data for the 172 mil plexiglas sample is given in Figure 23A and 23B. The frequency domain data between 12 and 18 GHz is compared to the time domain data from Figure 11A and 11B in Table XIII.

SAMPLE #1: FIBERGLASS THICKNESS = 142 MILS.

REAL PART

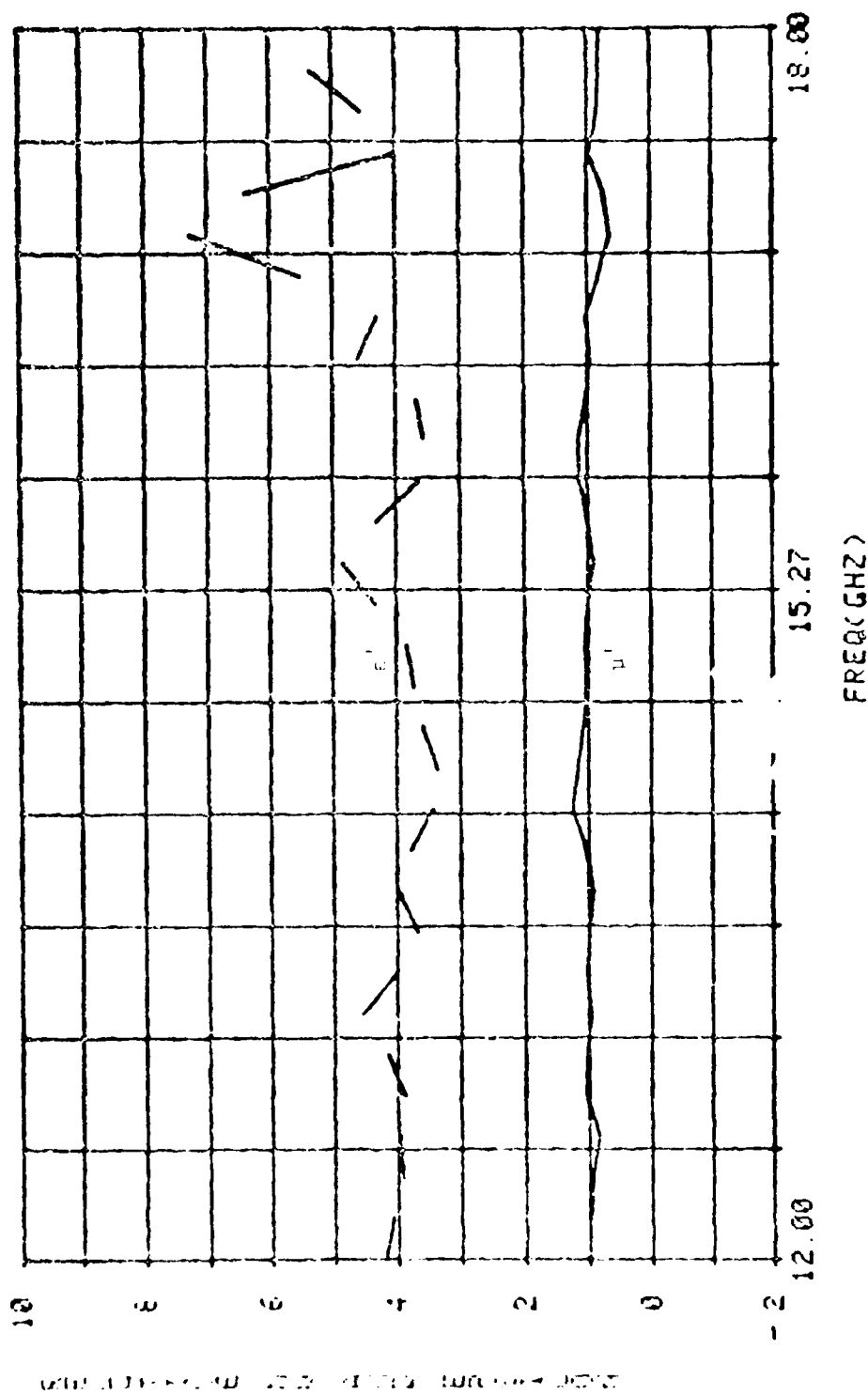


Figure 21A. Frequency Domain (R.ai) Data for 142 mil Fiberglass Sample

SAMPLE 01: FIBERGLASS THICKNESS = 142 MILS.

IMAG PART

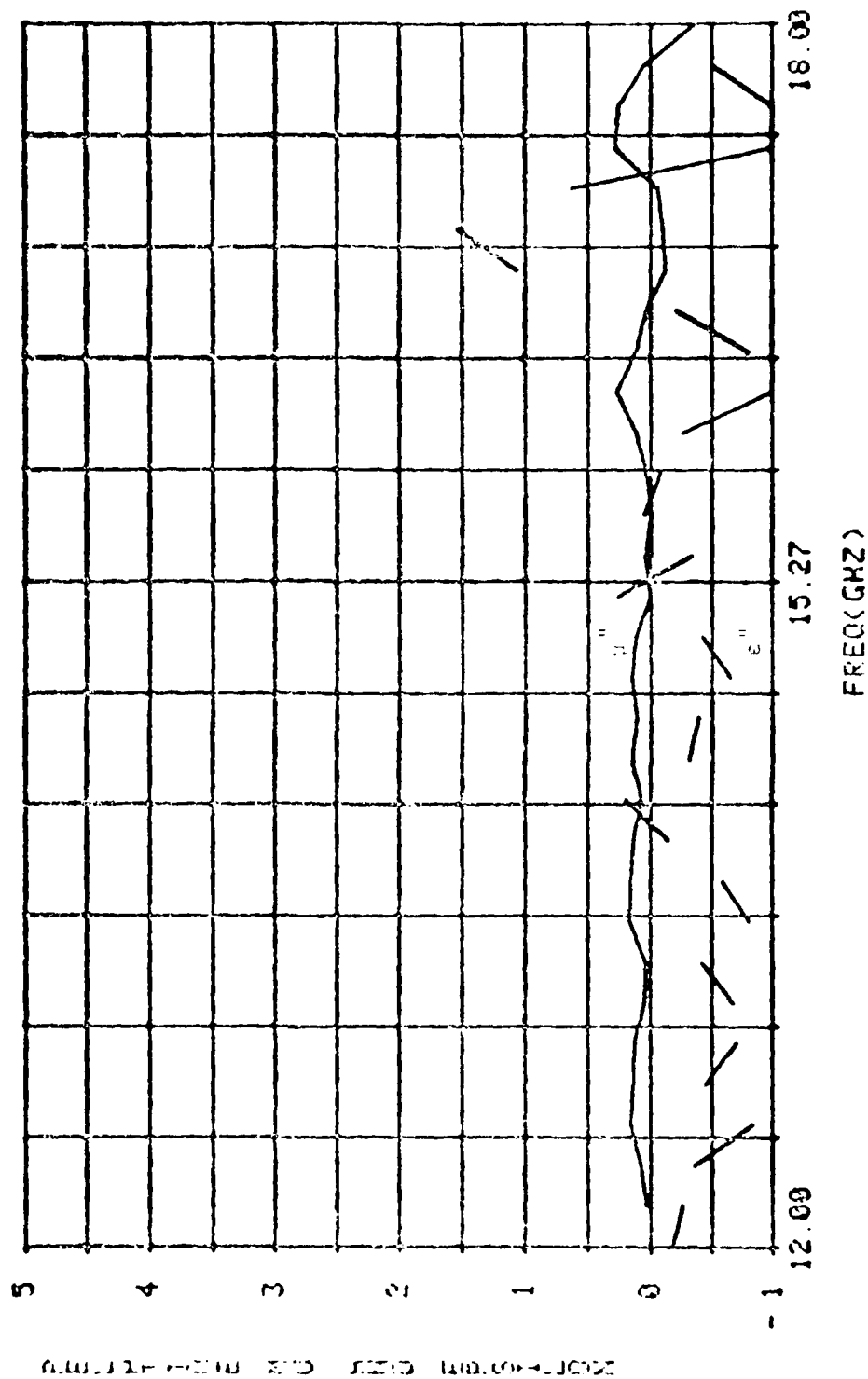


Figure 213. Frequency Domain (Imaginary) Data for 142 mil Fiberglass Sample

TABLE XI

SAMPLE: FIBERGLASS

FREQUENCY DOMAIN SYSTEM

THICKNESS = 134.5 MILS

THICKNESS = 142 MILS

<u>FREQUENCY (GHz)</u>	<u>EPSILON</u>	<u>MU</u>	<u>FREQUENCY (GHz)</u>	<u>EPSILON</u>	<u>MU</u>
12.0	4.36+J.21	.95+J.00	12.0	4.21-J.12	.99+J.00
12.4	4.25+J.25	.97-J.01	12.4	3.93-J.35	.95+J.08
12.8	4.19+J.25	.99-J.01	12.8	3.89-J.44	1.04+J.14
13.2	4.18+J.27	1.00-J.01	13.2	4.54-J.58	.97+J.05
13.6	4.19+J.23	1.00-J.01	13.6	3.68-J.81	.98+J.17
14.0	4.12+J.17	1.00+J.00	14.0	3.78-J.74	1.04+J.14
14.4	4.32+J.06	.96+J.00	14.4	3.37-J.31	1.16+J.15
14.8	4.62-J.09	.90+J.02	14.8	3.72-J.66	1.02+J.15
15.2	4.64+J.02	.89+J.02	15.2	4.35+J.26	1.01+J.00
15.6	4.36+J.01	.92+J.04	15.6	4.32+J.05	1.00-J.01
16.0	4.20-J.01	.94+J.07	16.0	3.54-J.26	1.15+J.12
16.4	4.26+J.67	.98-J.03	16.4	4.60-J.81	.94+J.12
16.8	4.18+J.80	1.00-J.24	16.8	5.53+J.06	.82-J.12
17.2	3.74+J.46	1.16-J.27	17.2	6.40-J.63	.75-J.06
17.6	3.44+J.44	1.30-J.13	17.6	4.54-J.00	.85-J.26
18.0	3.58-J.02	1.24-J.07	18.0	4.63+J2.47	.80-J.35

SAMPLE: #2: PLEXIGLAS THICKNESS = 64 MILS.

REAL PART

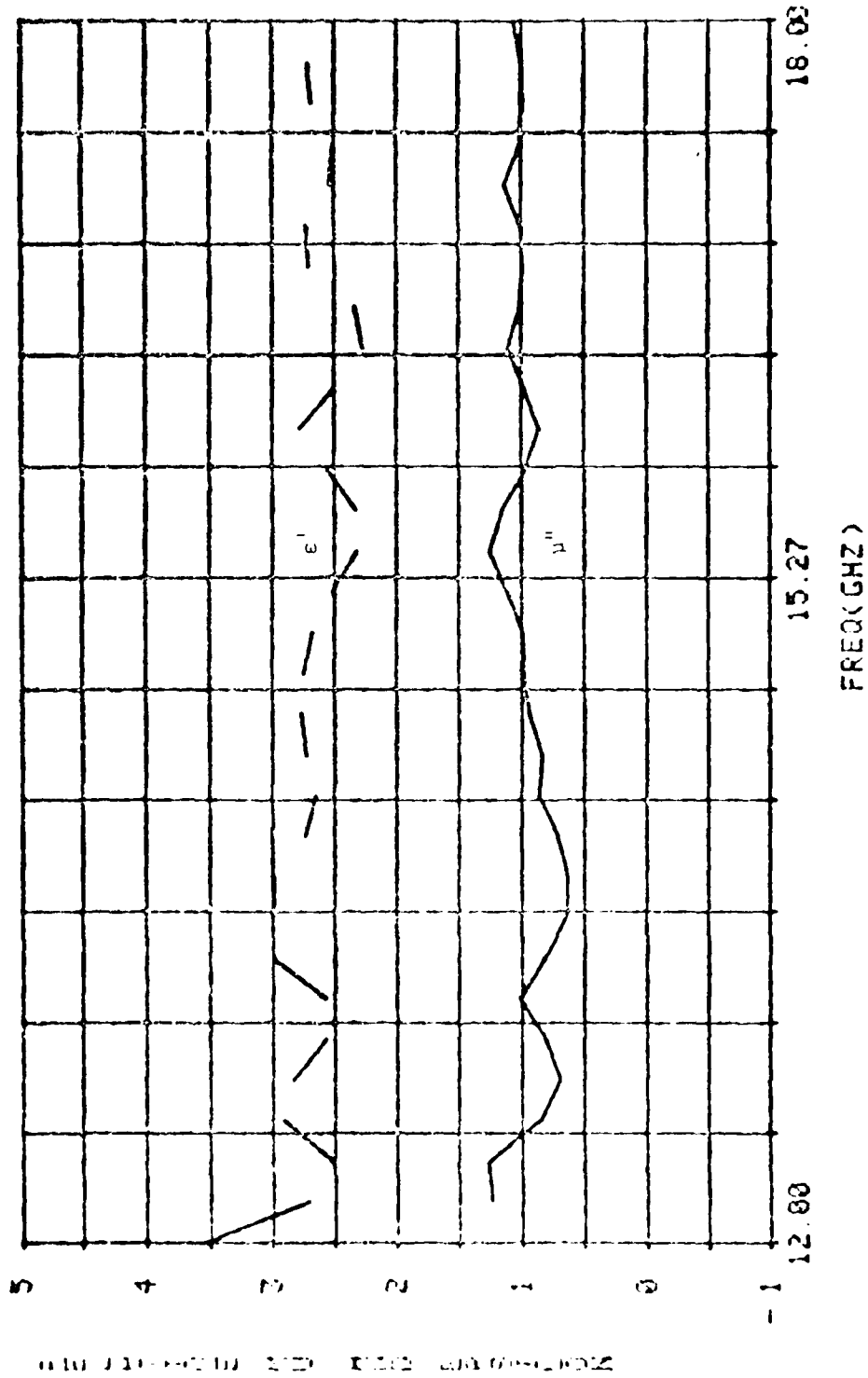


Figure 22A. Frequency Domain (Real) Data for 64 mil Plexiglas Sample

SAMPLE: 02 PLEXIGLAS THICKNESS = 64 MILS.

IMAG PART

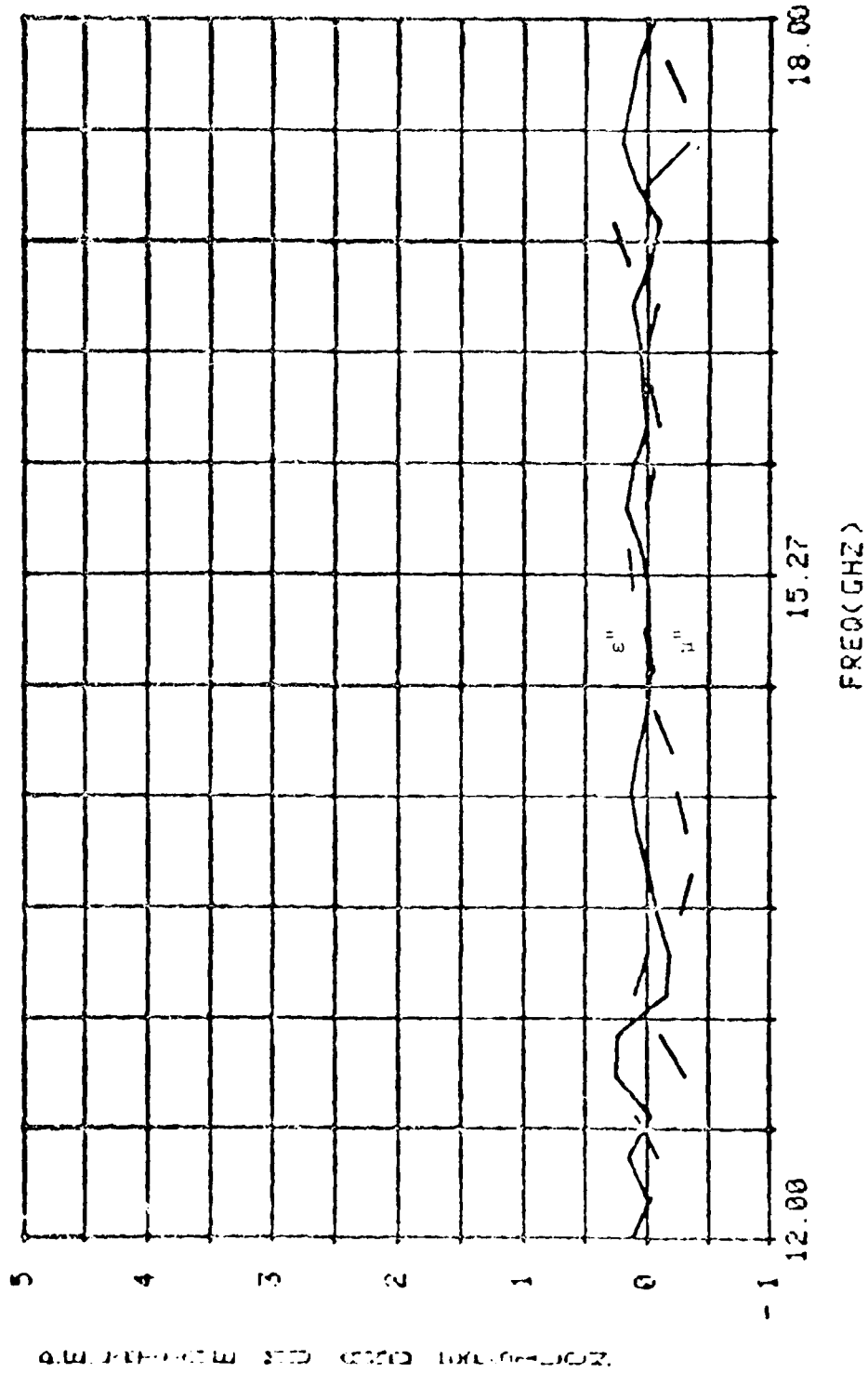


Figure 228. Frequency Domain (Imaginary) Data for 64 mil Plexiglas Sample

TABLE XII

SAMPLE: PLEXIGLAS

FREQUENCY DOMAIN SYSTEM

THICKNESS = 64 MILS

TIME DOMAIN SYSTEM

THICKNESS = 64.5 MILS

<u>FREQUENCY (GHz)</u>	<u>EPSILON</u>	<u>MU</u>	<u>FREQUENCY (GHz)</u>	<u>EPSILON</u>	<u>MU</u>
12.0	2.51+J.09	.99-J.02	12.0	3.53+J.12	.65-J.10
12.4	2.47+J.04	.99-J.02	12.4	2.51-J.09	1.26+J.15
12.8	2.44+J.03	1.02-J.05	12.8	2.84-J.31	.69+J.25
13.2	2.43+J.00	1.05-J.09	13.2	2.57+J.10	1.01-J.16
13.6	2.47+J.06	1.09-J.10	13.6	2.99-J.27	.64-J.08
14.0	2.55+J.06	1.07-J.04	14.0	2.74-J.32	.71+J.08
14.4	2.64+J.14	1.07-J.02	14.4	2.73-J.20	.84+J.08
14.8	2.69+J.14	1.06+J.02	14.8	2.75-J.05	.98-J.03
15.2	2.69+J.24	1.10+J.03	15.2	2.52+J.12	1.11-J.01
15.6	2.58+J.17	1.08+J.07	15.6	2.33+J.01	1.15+J.17
16.0	2.52+J.28	1.15+J.05	16.0	2.78-J.10	.86+J.09
16.4	2.46+J.46	1.28+J.03	16.4	2.27+J.00	1.10+J.06
16.8	2.59+J.75	1.40-J.16	16.8	2.71+J.15	.99-J.02
17.2	2.74+J.70	1.30-J.35	17.2	2.54-J.01	1.13+J.09
17.6	2.75+J.40	1.15-J.33	17.6	2.69-J.30	.99+J.14
18.0	2.56+J.15	1.05-J.17	18.0	2.61+J.12	1.06-J.05

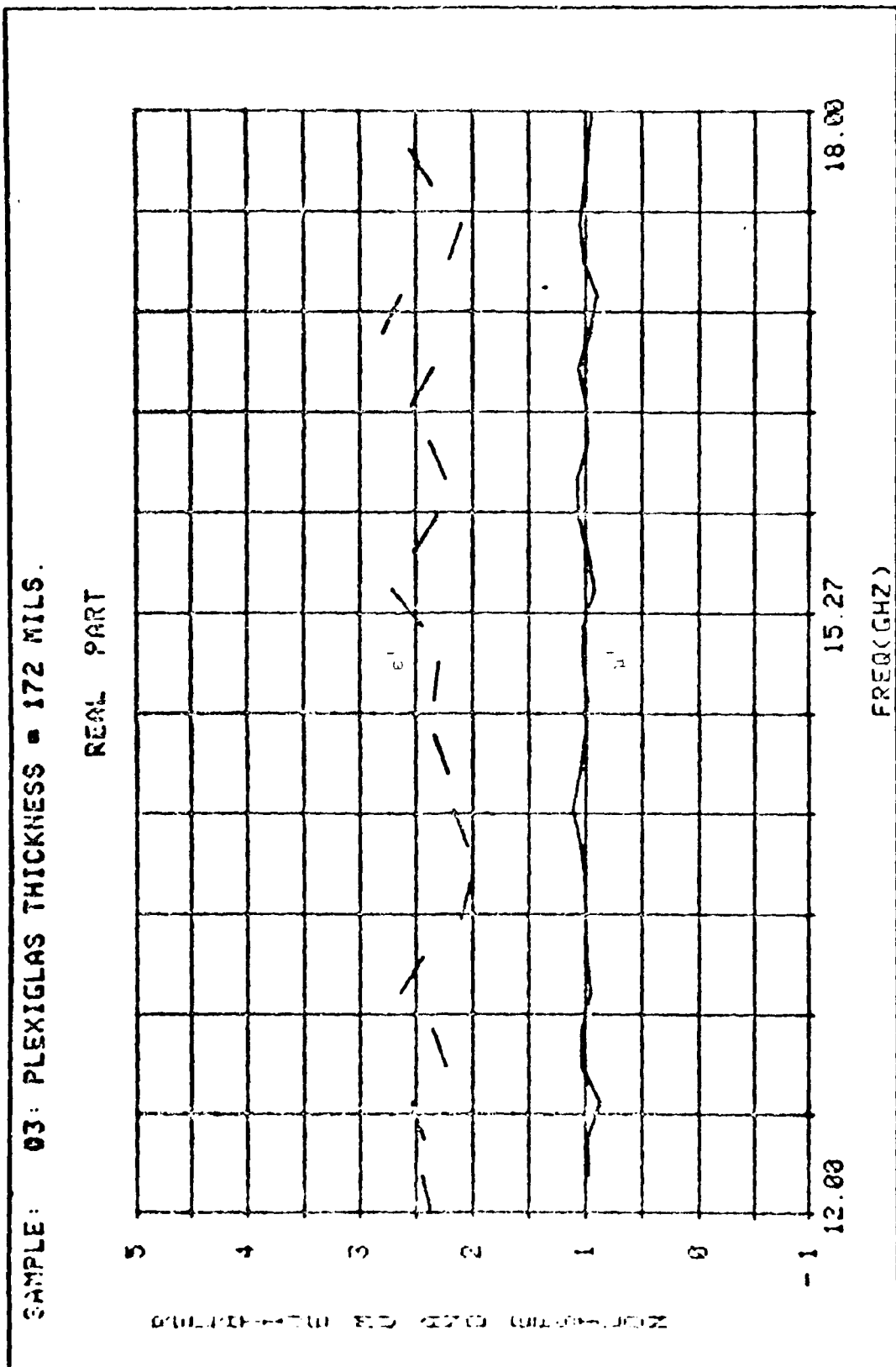


Figure 23A. Frequency Domain (Real) Data for 172 mil Plexiglas Sample

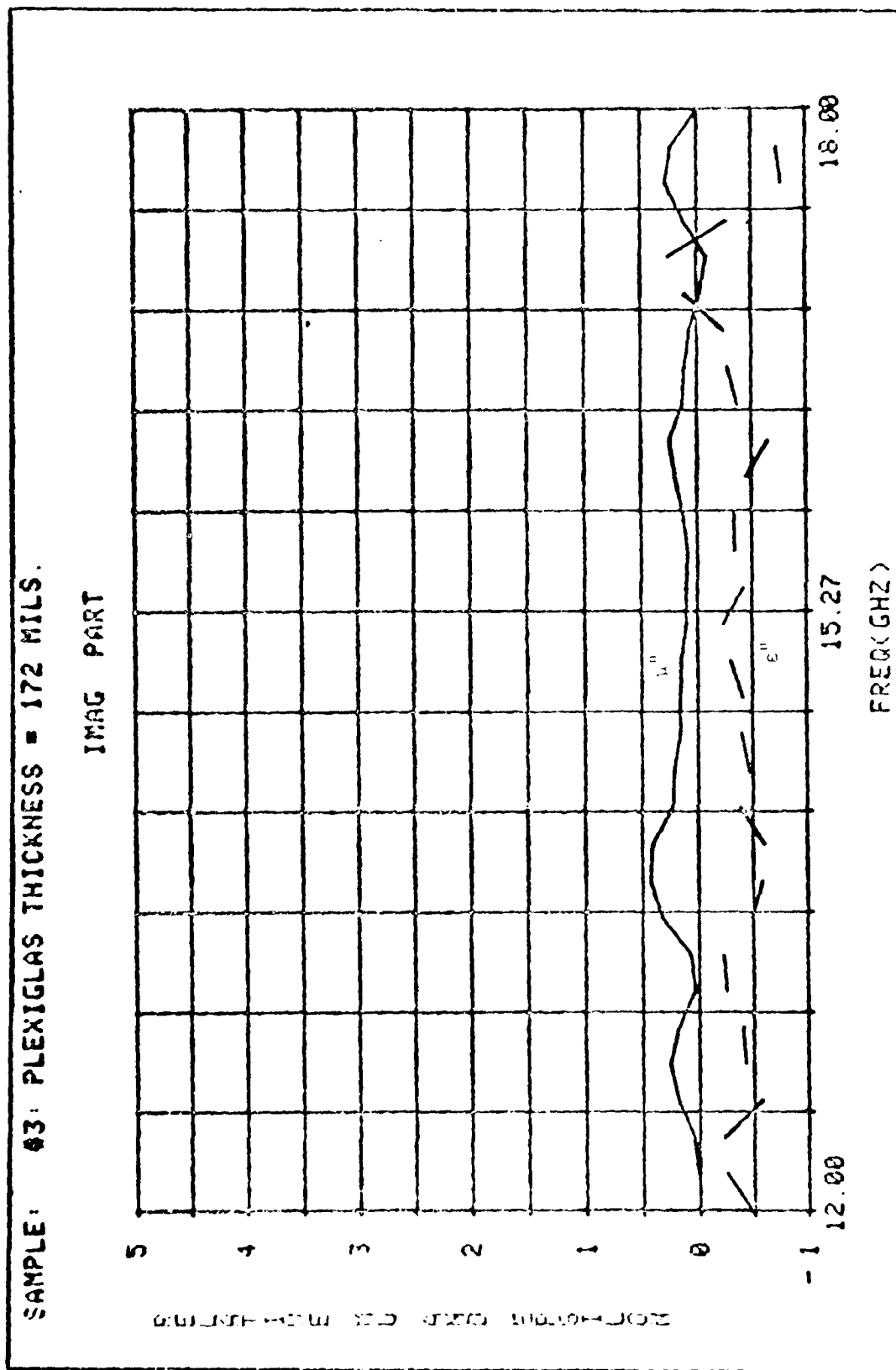


Figure 233. Frequency Domain (Imaginary) Data for 172 mil Plexiglas Sample

TABLE XIII

SAMPLE: PLEXIGLAS

FREQUENCY DOMAIN SYSTEM

THICKNESS = 172 MILS

TIME DOMAIN SYSTEM

THICKNESS = 174 MILS

<u>FREQUENCY (GHz)</u>	<u>EPSILON</u>	<u>MU</u>	<u>FREQUENCY (GHz)</u>	<u>EPSILON</u>	<u>MU</u>
12.0	2.42+J.00	1.00+J.00	12.0	2.37-J.47	.96+J.27
12.4	2.43+J.01	1.00+J.00	12.4	2.43-J.22	.96+J.05
12.8	2.46+J.05	.99-J.03	12.8	2.24-J.43	1.03+J.26
13.2	2.44+J.04	.99-J.05	13.2	2.64-J.25	.95+J.04
13.6	2.49+J.08	.98-J.04	13.6	2.10-J.49	1.00+J.33
14.0	2.55+J.04	.97-J.03	14.0	2.05-J.61	1.04+J.42
14.4	2.58+J.05	.96-J.03	14.4	2.22-J.47	1.05+J.22
14.8	2.54+J.14	.96-J.04	14.8	2.34-J.41	.98+J.16
15.2	2.47+J.17	1.01-J.05	15.2	2.44-J.23	1.02+J.10
15.6	2.32+J.25	1.06-J.09	15.6	2.52-J.34	.98+J.09
16.0	2.39+J.35	1.05-J.16	16.0	2.24-J.45	1.07+J.20
16.4	2.35+J.58	1.00-J.24	16.4	2.55-J.37	.99+J.13
16.8	2.53+J.81	.80-J.26	16.8	2.80-J.24	.96+J.07
17.2	2.39+J.47	.83-J.13	17.2	2.21+J.26	1.02+J.04
17.6	2.48-J.12	.92+J.04	17.6	2.36-J.78	1.01+J.23
18.0	1.87+J.00	1.16+J.08	18.0	2.68-J.06	.94+J.00

VITA

Donald G. Aguirre was born on 12 March 1950 in Holdenville, Oklahoma. He graduated from high school in Holdenville, Oklahoma in 1969 and attended the University of Oklahoma from 1969 to 1971, at which time he enlisted in the Air Force. Through the Airmen Education and Commissioning Program, he attended the California State University in Sacramento, California, from which he received (with honors) the degree of Bachelor of Science in Electrical Engineering in January 1976. Upon graduation, he attended the Officer Training School and received his commission in April 1976. He served as a technical engineer with the 341st Strategic Missile Wing at Malmstrom AFB, Montana, until entering the School of Engineering of the Air Force Institute of Technology in June 1979.

Permanent address: 224 South Oak
Holdenville, Oklahoma
74848

UNCLASSIFIED

SECURITY CLASSIFICATION OF THIS PAGE (When Data Entered)

REPORT DOCUMENTATION PAGE

1. REPORT NUMBER AFIT/GE/EE/90D-8		2. GOVT ACCESSION NO. AD-A100 764		3. HEADQUARTERS REPORT DOCUMENT NUMBER	
4. TITLE (and Subtitle) FREQUENCY DOMAIN MEASUREMENTS OF MICROWAVE ABSORBER DESIGN MATERIALS		5. TYPE OF REPORT & PERIOD COVERED MS Thesis			
7. AUTHOR(s) DONALD G. AGUIRRE Capt USAF		6. PERFORMING ORG. REPORT NUMBER			
9. PERFORMING ORGANIZATION NAME AND ADDRESS Air Force Institute of Technology (AFIT/EN) Wright-Patterson Air Force Base, Ohio 45433		8. CONTRACT OR GRANT NUMBER(s)			
11. CONTROLLING OFFICE NAME AND ADDRESS ATC/AFIT/EN WPAFB Ohio 45433		10. PROGRAM ELEMENT, PROJECT, TASK AREA & WORK UNIT NUMBERS			
14. MONITORING AGENCY NAME & ADDRESS (if different from Controlling Office)		12. REPORT DATE December 1980			
		13. NUMBER OF PAGES			
		15. SECURITY CLASS. (of this report) Unclassified			
		15a. DECLASSIFICATION/DOWNGRADING SCHEDULE			
16. DISTRIBUTION STATEMENT (of this Report) Approved for public release; distribution unlimited.					
17. DISTRIBUTION STATEMENT (of the Abstract entered in Block 20, if different from Report)					
18. SUPPLEMENTARY NOTES Approved for public release; IAW AFR 190-17 16 JUN 1991 Fredric C. Lynch, Major, USAF Director of Public Affairs					
19. KEY WORDS (Continue on reverse side if necessary and identify by block number) Microwave absorber Intrinsic properties Frequency domain Radar absorber					
20. ABSTRACT (Continue on reverse side if necessary and identify by block number) Using frequency domain techniques, a system was developed to measure the complex permittivity and permeability of different materials in the Ku band (12.4 to 18 GHz). A sample of fiberglass, teflon, ICM-40, and two different plexiglas configurations were chosen for this experiment. The newly developed measuring system consisted of a two horizontal-plane sectoral horn and a sample holder assembly. A 9.5 x 0.8 cm piece of the sample material was cut and fitted into the sample holder assembly. The reflection and transmission coefficients for the sample were measured, using a network analyzer and frequency synthesizer.					

DD FORM 1 JAN 73 1473

EDITION OF 1 NOV 65 IS OBSOLETE

UNCLASSIFIED

SECURITY CLASSIFICATION OF THIS PAGE (When Data Entered)

Item 20 (continued)

as the swept frequency signal source. A dedicated computer calculated the complex permittivity and permeability and plotted the output data. The measurements were performed automatically by having the computer control the frequency synthesizer while running the experiment.

The two configurations of plexiglas and the fiberglass sample were tested ten times to obtain a statistical representation of the results. In all cases good repeatability was obtained. The standard deviation of the real part of the permittivity and permeability for the two cases of plexiglas was within $\pm 4\%$ of the mean. The fiberglass had a typical standard deviation within $\pm 7\%$ of the mean for the real part of the permittivity and permeability.

The permittivity and permeability obtained for the selected samples using the frequency domain measurement technique were compared with the results obtained in a previously developed system which used time domain techniques. The data comparison between the two systems was good for teflon, plexiglas, and fiberglass in the frequency range from 12.4 to 16 GHz. Some variations were noted for the FGM-40. Since the results obtained were generally consistent between both techniques, it is claimed that the newly implemented frequency domain system is a viable alternative for the rapid measurement of intrinsic properties in the Ku band.

END

DATE
FILMED

7-18-1

DTIC